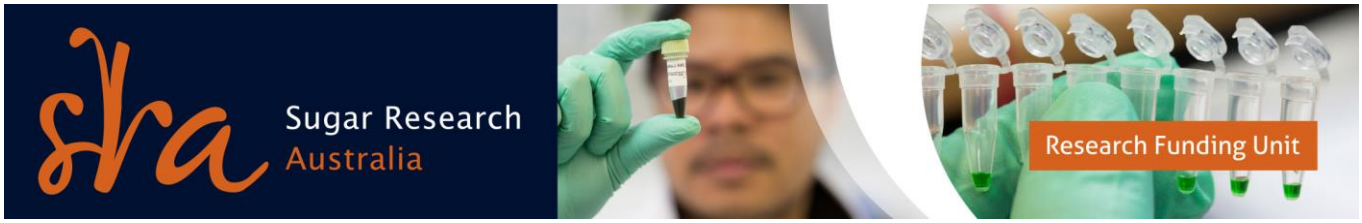

SRA Research Project Final Report

Development of value-added products from sugar cane boiler ash: final report 2011/903

SRA Project Code	**SCU003 (=2011/903)**		
Project Title	**Development of Value-added Products From Sugar Cane Boiler Ash**		
Key Focus Area in SRA Strategic Plan			
Research Organisation(s)	Southern Cross University and Australian Bio Refining Pty Ltd		
Chief Investigator(s)	A/Prof Malcolm Clark, Dr's Neal Lake & Lachlan Yee		
Project Objectives			
Milestone Number			
Milestone Due Date	01/05/2015	**Date submitted**	23/6/2015
Milestone Title	Final Report		
Success in achieving the objectives	X Completely Achieved ☐ Partially Achieved ☐ Not Achieved		
SRA measures of success for Key Focus Area (from SRA Strategic Plan)			

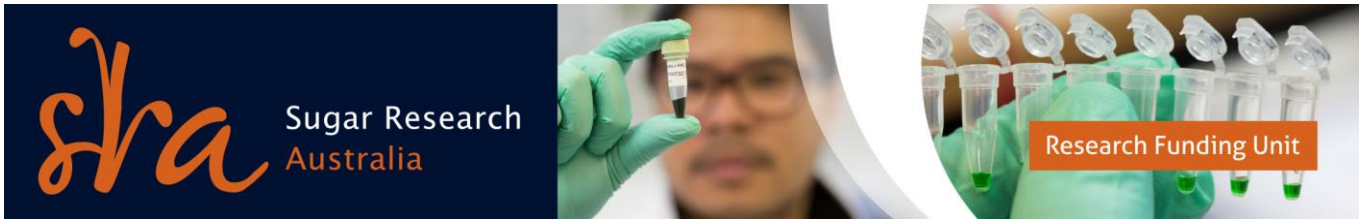

Please cite as: Clark M, Lake N, Yee L. 2015. Development of value-added products from sugarcane boiler ash. Final Report 2011/903. Sugar Research Australia Limited, Brisbane.

PART A

Section 1: Executive Summary

Bagasse fly ash from co-generation plants is often recycled into the sugarcane fields. However, bagasse fly ash contains quartz (naturally accumulated by the cane) that may be re-suspended into respirable-sized particulate by wind erosion and cultivation, where it can cause silicosis. Therefore, the transformation of the bagasse fly ash waste stream into value-added products such as zeolites and or concretes has been investigated. Factorial Design Analysis (neural network development) has been utilised to define the optimal conditions for zeolite manufacture and addition rates to concretes.

Zeolite development shows that the extremely versatile zeolite-X can be manufactured at temperatures that allow the utilisation of waste steam from the sugar mill, under alkaline hydrothermal conditions. The zeolite produced has a very high cation exchange capacity, making it desirable for water treatment, soil addition, and other industrial uses. Moreover, the zeolites developed are self supported providing very high surface areas on relatively large particles, which facilitate the treatments of waste waters by increasing flow rates. Adsorption kinetics of Cu and Zn to zeolite indicates that these are rapid second order kinetics, which coupled with the high exchange capacity, increases the usefulness of the product in water treatment systems.

Concretes developed showed improved strengths, and chemical resistance, particularly to chemicals (sulphate and chloride) and acids. Acid resistance in concrete improves service life of the concrete, particularly to organic acids found in silage and spilled cane juice. Hence the concretes developed have immediate application with sugar mills, where cane-juice often leads to the rapid exposure of concrete aggregate and concrete deterioration.

Economic assessments based on the test results are promising, with a modest capital investment in plant and equipment to process the bagasse fly ash to zeolites. Similarly there is a modest investment to process the ash for use in concrete works close to the mills. This modelling suggests that there could be a return on investment of about 23% for zeolite manufacturing, and 21% on reuse of the bagasse fly ash into concretes. This does not include the cost recovery from dealing with the bagasse fly ash as a product rather than a waste for disposal.

Both of the successful outcomes (zeolites and concretes) provide alternatives to the issue of bagasse ash disposal, which is becoming increasingly restricted. Both outcomes provide new products with increased and improved performance that provide a value added pathway for a sugar mill waste stream. Furthermore, the zeolite production is achievable at temperatures which can utilise the residual steam developed in the cogeneration boilers, to generate further efficiencies from the calorific value of the sugar cane bagasse.

Section 2: Background

Introduction

Sugar cane (*Saccharum officinarum*) is a major crop grown in many parts of the sub-tropical ad tropical growing areas and the production process generates sugar cane bagasse that is widely used in steam and electricity production at the sugar mills (Sales & Lima, 2010). Currently there are four product streams in a cane sugar mill – sugar, bagasse, molasses, and mill mud. Sugar and molasses are saleable products, bagasse is burnt for generation of steam and electricity to operate the plant, and mill mud from sugar clarification is redistributed over cane fields for disposal and nutrient enrichment of the soil. The sugar cane plant

accumulates amorphous silica within cells typically at an average rate of 1.509 % SiO_2 (Hodson et al., 2005), which is on the upper end of silica accumulation in plants. Moreover, the plant acts as a natural filter, such that many trace metals are excluded from accumulation, which is problematic for coal fly ashes. After the burning of bagasse, silica and aluminium oxide are two major elements that accumulate in the bagasse fly ash (Teixeira et al., 2008). The bagasse fly ash recycled into the sugarcane fields contains quartz and some of the quartz could be re-suspended into respirable-sized particulate by wind erosion and cultivation (Le Blond et al., 2010). The human body is not capable of processing the inhaled silica; exposure to crystalline silica particles, which are in the respirable-size range can cause silicosis (Kaewamatawong et al., 2005). Therefore, the transformation of the bagasse fly ash waste stream into value-added products such as zeolites and or concretes have been investigated.

Zeolites are alumino-silicate minerals that have a repeating channel or cage-like structure resulting from the repeating silica tetrahedral and alumina octahedral bonding (Deer et al., 1966). These structures have varying size cages or channels, and have strong ion exchange properties due to the negative charge on the framework from the incomplete tetrahedral structure of alumina. This negative charge is balanced usually by an alkali metal cation loosely held in the cage or channel bonding (Deer et al., 1966). Although zeolites are found naturally and have commercial use as such, zeolite minerals synthesized from aluminium and silicon-containing admixtures has the advantage of the control of cage or channel size, control of crystal size (i.e. higher surface area on smaller crystals), and control of purity.

At higher temperatures (>175°C) more crystalline and compact zeolitic structures develop and often lead to crystallisation of sodalite and cancrinite (Shiraki et al., 2001). Whereas at more moderate temperatures (≈120°C – 160°C) more open zeolites (e.g. Analcime) develop, and at lower temperatures (≈80°C) even more open and poorly crystalline structures (e.g. Zeolite-A) develop (LaRosa et al., 1992; Valtchev et al., 2005). The consequence of decreasing crystallinity is that Cation Exchange Capacity (CEC) tends to increase, and therefore the industrial and environmental applications are likely to increase. According to (Purnomo, 2012) the bagasse fly ash could be a good source of silica for zeolite-A and zeolite–X with high purity production because of its low heavy metals contaminants. It is likely that synthesised zeolites may include products for industrial, environmental and agricultural applications.

Concrete is the most widely used construction material in the world and whilst there is increasing demand for concrete production there is also increasing concern for the environmental impacts of the concrete industry. Concrete is composed of binder, aggregate and water. Ordinary Portland cement (OPC) is the most commonly used binder, with global production estimated to be over 4 billion tonnes (Cembureau, 2015). OPC production is known to release carbon dioxide (CO_2), a greenhouse gas (GHG) in an energy intensive method. In fact, 7% of global CO_2 emissions are due to OPC production (Benhelal et al., 2013). Aggregates, which make up to 80% by weight of concrete are typically a mix of raw finite materials such as sand and basalt rock. Depletion of sand is an environmental concern leading to degradation of the local ecosystems.

The construction industry has implemented many advances in technology to improve the carbon footprint of concrete. Improved efficiency in cement production leads to reduced GHG emissions. Geopolymer technology provides an alternative to OPC systems also leading to GHG reductions. Supplementary cementitious materials from a renewable source can be used to make hybrid geopolymer blended concretes thus reducing the demand for cement production. Waste material incorporation into concrete and mortar as aggregates reduces the demand on raw finite resources.

In addition, supplementary cementitious materials (SCMs) have been successfully used to form geopolymer-blended cements, (hereafter blended cements). Again suitable materials are fine pozzolanic aluminosilicates, a typical example being coal fly ash (CFA). The pozzolanic reaction that occurs within the blended cement concrete produces calcium silicate hydrates (CSH), which are responsible for the strength of concrete. The incorporation of SCMs has been shown to increase not only the strengths of concrete but also the durability and chemical resistance (Mehta, 2004).

In the case where a waste material is not active or only mildly active in terms of the pozzolanic reaction it is often incorporated into concrete and mortars as an inert aggregate material. Depending on the size of the particle, the alternative material may replace either sand or gravel. Typical materials used are recycled materials such as recycled construction wastes, or by-products such as incinerator bottom ash or even organic materials like rice husks (CCCA, 2008).

The aim of this study is to determine the most suitable utilisation for sugarcane bagasse ash (SCBA) within a concrete system. The SCBA that is assessed in this study is that produced by a local co-generation sugar mill, Broadwater Sugar Mill. SCBA is known to be a source of silica and is a fine particulate aluminosilicate and potentially a pozzolan similar to coal fly ash. As a potential pozzolan, SCBA may be a candidate for geopolymerisation in a blended cement system. If determined to have limited pozzolanic activity, the fine particulate nature of SCBA means that it may be suitable as a fine aggregate replacement in concretes and mortars.

A benefit to the sugarcane industry of utilising SCBA in concrete is the potential to generate an income stream from a waste material and also the possibility to alleviate the concerns of waste disposal. SCBA may also provide a superior or at least comparable concrete to traditional concrete thus improving the environmental impact of both the sugarcane and construction industries. It is necessary therefore to study the behaviour of SCBA in concrete systems. SCBA chemical characterisation is investigated in this study, to help determine the extent of the pozzolanic reactivity, by XRD and XRF analysis. Indication of the pozzolanic reactivity allows this study to focus on the most suitable utilisation of SCBA in concrete. This study then investigates the fresh properties of concretes and mortars including consistency, flow and slump. Hardened properties investigated are compressive strength, flexural strength, acid-resistance, and sulphate resistance. Tests performed adhere to the Australian Standards, where possible, to bring relevance of the study to the concrete industry.

Concrete Literature Review

Cement production globally in 2011 was 2.8 billion tonnes which has since risen to over 4 billion tonnes in present times (Armstrong, 2013). The raw materials used to produce OPC are primarily limestone (80%) and one or more of either clay, iron ore, slate, shells or shale (20%) (Ali, Khan, & Hossain, 2008). The limestone provides a source of calcium carbonate ($CaCO_3$) and the remaining 20% of the mix provides a source of silica, alumina and iron oxides, otherwise known as alumino-silicates. The first stage in the production of OPC is the formation of clinker. Which is produced by heating limestone and clay in a kiln to sintering temperatures of about 1450 ˚C – 1500 ˚C. The reaction occurring in the kiln forms calcium silicates and releases CO_2 as is shown in Equation 1.

$$5\ CaCO_3\ + 2\ SiO_2\ \rightarrow ((CaO)_3 \cdot SiO_2) \cdot ((CaO)_2 \cdot SiO_2) + 5CO_2$$

Equation 1

The resultant material is an aggregate that is described as a hydraulic material consisting of 66% calcium silicates (by mass) and the remainder a combination of iron and aluminium oxides (EN 197-1:2011). This material is ground to a very fine powder with an addition of approximately 5% calcium sulphate (gypsum) to retard the setting time of concrete. The final composition of this fine powder (OPC) is predominately calcium silicates and calcium aluminates along with minor amounts of other oxides. The major oxides typically present in OPC are listed in Table 1:

Table 1 Major chemical compounds of ordinary Portland cement

Compound	Chemistry	Cement Chemist Notation	Mass %
Tricalcium Silicate	$(CaO)_3.SiO_2$	C_3S	45-70
Dicalcium Silicate	$(CaO)_2.SiO_2$	C_2S	7-32
Tricalcium Aluminate	$(CaO)_3.Al_2O_3$	C_3A	0-13
Tetracalcium Aluminoferrite	$(CaO)_4.Al_2O_3.Fe_2O_3$	C_4AF	0-18

The formation of concrete is achieved by the hydration of the OPC in the presence of aggregates and can be represented by the following equations (2, & 3):

$$Ca_3SiO_5 + H_2O \rightarrow (CaO) \cdot (SiO_2) \cdot (H_2O)(gel) + Ca(OH)_2$$

Equation 2

Or in abbreviated form:

$$C_3S + H \rightarrow C - S - H + CH$$

Equation 3

Where; H represents water (H_2O), or hydroxide (OH^-). It can be seen that C_3S is primarily responsible for the binding properties of the OPC; however C_2S also contributes to the cementitious properties.

The embodied energy imparted to produce OPC due to the manufacturing process is significant. It is estimated that OPC production accounts for 2% of primary energy consumption and 5% of industrial energy consumption globally (Chen & Juenger, 2011). The high embodied-energy in concrete is also in part due to the high kiln temperatures reached during clinker formation. The production of 1 tonne of OPC releases approximately 1 tonne of the greenhouse gas (GHG), CO_2, into the environment mostly from the direct reaction in the kiln, but also from the transport and heating requirements involved during production (Benhelal, Zahedi, Shamsaei, & Bahadori, 2013).

In light of the potential for global warming and climate change, the release of GHG into the environment is a major concern. There have been many initiatives by the cement industry to reduce the environmental impact of cement production. Some of these measures involve more efficient kiln operating conditions and also carbon sequestration. Incorporation of recycled pozzolan materials or SCMs like fly ash, to replace up to 65% of the OPC to form blended cement (AS 3972-2010) is another commonly employed strategy. In fact it is estimated that blended cements are the most widely used cements in modern applications (Schneider et al., 2011). Substitution of OPC by waste products is aimed at reducing the costs associated with obtaining and treating raw resources, whilst still producing quality concrete products complying with regulatory standards. The incorporation of a waste material also combats the challenges associated with disposal of the waste.

It is well known that incorporation of a pozzolan material as a supplementary cementitious material can also improve the properties of OPC concrete. The benefits of incorporating pozzolans into modern day OPC concrete have been reported to be increased durability, higher resistance to sulphate attack by decreased permeability, increased workability, and increased late compressive strength. Suitable SCMs are siliceous, or

siliceous and aluminous materials which are not naturally cementitious, but will with moisture react with calcium hydroxide ($Ca(OH)_2$) to form cementitious compounds (International, 2014). The reaction is summarised in Equation 4:

$$Ca(OH)_2 + H_4SiO_4 \rightarrow Ca^{2+} + H_2SiO_4\ 2 \cdot H_2O$$

Equation 4

This pozzolanic reaction, occurs within the concrete matrix where the SCM is able to react with free $Ca(OH)_2$ (lime) , that is formed as a product of the cement hydration reaction. The product of the pozzolanic reaction is calcium silicate hydrates (CSH), which are responsible for the characteristic strength and durability of concrete. Another benefit of the pozzolanic reaction is that it consumes lime. Excess lime in concrete can lead to spalling, fine cracking and degradation at later stages in the concretes lifetime due to what is known as the alkali silica reaction (ASR). The reduction in lime has also been reported to improve the acid resistance of OPC concretes (Zivica, & Bajza, 2002). Incorporation of a pozzolan to prevent ASR and improve durability is now common practice (Obla, 2008). A material may be classed as a pozzolan if its Strength Activity Index (SAI) or sometime referred to as the Pozzolanic Index (PI) is at least 75% (International, 2012), which is determined by comparing the compressive strength developments between a concrete supplemented with the potential pozzolan and a control concrete (Australia, 1995; International, 2013).

Coal fly ash (CFA) is the most commonly utilised waste material in blended cements. The generalised make-up of all CFA is a typical aluminosilicate, containing silicon, aluminium, iron and calcium oxides with minor amounts of other oxides and carbon. Standards regulating the incorporation of CFA into OPC classify CFA into 2 classes, F and C, based on the oxide content and LOI (ASTM C618; AS 3582.1). The main difference between class F and C is the calcium oxide content, class C possessing the higher amount. The minimum amount of SiO_2 + Al_2O_3 + Fe_2O_3 for ASTM class F fly ash is 70% by weight and class C requires at least 50% by weight.
Table 2 outlines the differences in composition typically found between the two CFA classes (McCarthy, et al., 1989):

Table 2 Typical chemical composition of class F and C coal fly ash to comply with ASTM C618

Oxide	Class F Mass%	Class C Mass%
SiO_2	52.5	36.9
Al_2O_3	22.8	17.6
Fe_2O_3	7.5	6.2
CaO	4.9	25.2
MgO	1.3	5.1
SO_3	0.6	2.9
Na_2O	1.0	1.7
LOI*	2.6	0.33

*LOI = Loss on ignition

CFA consists primarily of amorphous or glassy, round particles, although some crystalline content is usually present. This is due to the CFA being cooled rapidly after removal from the flue gases, which retards the growth of a crystalline structure. The amorphous nature of the CFA results in an aluminosilicate material that possesses pozzolanic activity making it suitable for addition to OPC to form hybrid geopolymer blended concretes (Davidovits, 2013).

In sugar production, sugarcane stalks are crushed to a fibrous pulp or 'bagasse' to extract the sucrose rich juice. Residual bagasse is often used as fuel to generate electricity and/or to produce steam for use in the mill.

The unburnt fraction remaining is the SCBA, which is predominately silica with minor amounts of aluminium, iron oxides and other oxides, however variations occur due to growing conditions, burn temperatures, collection point and source (Table 3). Although variations are apparent, SCBA in most cases falls into the category of a class F fly ash.

Table 3 Chemical composition and LOI of sugarcane bagasse ash by %mass from varied sources.

Reference	SiO_2	Al_2O_3	Fe_2O_3	CaO	MgO	SO_3	Na_2O	K_2O	LOI
(Akram, Memon, & Obaid, 2009)	62	6.7	5.8	6.2	3.0	0.7	3.2	6.9	2.6
(Chusilp, Jaturapitakkul, & Kiattikomol, 2009)	54	5.7	3.5	15	1.4	0.0	…	…	19.0
(Cordeiro, 2011)	78	8.6	3.6	2.2	1.7	…	0.1	3.5	0.42
(Frias, Villar, & Savastano, 2011)	67	9.5	10	1.4	0.9	0.1	0.2	3.2	4.3
(Janjaturaphan & Wansom, 2010)	76	5.3	2.2	3.9	1.2	0.2	1.0	3.1	6.6
(Montakarntiwong, Chusilp, Tangchirapat, & Jaturapitakkul, 2013)	77	…	0.38	9.0	7.5	…	3.2	2.4	…
(Sales & Lima, 2010)	88	2.3	5.1	0.6	0.4	<0.1	0.1	1.3	0.35

It is estimated that 1 tonne of sugarcane provides over 6kg of SCBA (Fairbairn et al., 2010), and Australia's annual SCBA production is potentially over 230 thousand tonnes (CANEGROWERS, 2013). SCBA has limited nutritional value, but has been traditionally returned to the growing fields mixed with mill mud (dirt and solids washed from the cane, and clarified from the cane juice) as a form of fertiliser and convenient disposal method. Given environmental concerns this practice is diminishing in favour of value added utilisations. Utilisations include use as an adsorbent (Rehab & El Anany, 2013; Srivastava, et al, 2006), glass-ceramic material production (Teixeira et al., 2014), and zeolite production (Moisés, et al. 2013). The majority of the research however has focused on SCBA incorporation into concrete and cements as either a cementitious replacement (Akram et al., 2009; Chusilp et al., 2009c; G. C. Cordeiro, 2011; Fairbairn et al., 2010; Frias et al., 2011; Janjaturaphan & Wansom, 2010; Montakarntiwong et al., 2013) or as an aggregate replacement (Modani & Vyawahare, 2013; Sales & Lima, 2010). One major advantage to incorporation of SCBA into concrete is the potential to utilise high volumes of SCBA.

There are varied reports on SCBA pozzolanic potential ranging from excellent (Payá et al., 2002) to limited (Martirena Hernández et al., 1998). Previous studies indicate that a replacement of OPC by SCBA at 20% by OPC weight can increase the compressive strengths of concrete (Akram et al., 2009; Chusilp et al., 2009c) or at least produce equivalent strength (Ganesan et al., 2007), however others report that 20% SCBA reduced 28 day compressive strength and that a 5% replacement was optimal (Maldonado-Bandala et al., 2011). Mortars produced with a 10% replacement with SCBA for binder showed a pozzolanic index above the required 75% (Janjaturaphan & Wansom, 2010) and also improved sulphate resistance (Chusilp et al., 2009a). A replacement level as high as 30% however, has also been reported to develop greater compressive strength in mortars (Chusilp et al., 2009a). Other studies indicate that where SCBA as-received showed poor strength development in concrete, that various pre-treatments to the SCBA could improve the pozzolanic activity (Cordeiro, 2011; Cordeiro et al., 2009; Cordeiro et al., 2004). Studies also show that where pozzolanic activity is low the material can still benefit concrete through filler effects by replacing sand instead of binder (Sales & Lima, 2010). The filler effects are due to the ash particles packing together closely, resulting in a dense microstructure, which also contributes to the strength of the concrete (Manz, 1998). The dense packing reduces the pore size of the concrete enhancing the resistance to water, chloride and air permeability.

Zeolites Literature Review

Zeolites belong to the framework aluminosilicates with open 3-dimensional structures composed of corner-sharing TO_4 tetrahedra, where T is usually Al or Si (Figure 1; Deer et al., 1966). Zeolite's open tetrahedral

framework allows ion exchange and reversible dehydration (Smith, 1984). Silicates, the parent group of zeolites, are rock-forming minerals that are classified into categories such as ortho-, chain-, sheet- and framework-silicates. The analcite and zeolites groups are among the framework silicates; other groups are feldspar, sodalite, cancrinite and silica minerals where quartz belongs (Deer et al., 1966). The framework silicates, also referred to as tectosilicates, are composed of interconnected tetrahedrons forming an intricate tridimensional framework. Quartz (SiO_2) is formed from only silicon and oxygen; however the aluminium ion can easily substitute for the silicon ion in the tetrahedrons. In other subclasses of silicates this occurs to a limited extent but in the tecto-silicates, it is a major basis of the varying structures (International Zeolite Association, 2005). Therefore, a number of different structures could have the same chemical formula (McCusker & Baerlocher, 2007). While the tetrahedron is nearly the same with an aluminium at its centre, substitution of some of the Si with Al leads to negative charge (-5) instead of the normal negative four (-4) balanced by cations usually within the pore structure. The cation in the pore structure can be exchanged by another metal; ion exchange is an important property of zeolites (Chester & Derouane, 2010).

The basic zeolite corner-sharing tetrahedral units form secondary building units (SBU's) that are geometric arrangements of those tetrahedra (Dyer, 1988) (Smith, 1984) (Baerlocher et al., 2007) and can be arranged into larger structures. The SBU can be simple arrangement of tetrahedra in four, six, eight, ten or more complex membered ring (Chester & Derouane, 2010) and the wide variety of zeolites is due to the large number of ways in which the SBU's can be linked (Georgiev et al., 2009). If more than one SBU is possible, for a given framework types, all are listed (Currao, 2007). The framework contains open cavities, these micro-porous cavities referred to as channels or cages are large enough and vary from 0.3 to 20 Å. They allow other molecules that do not belong to the zeolite crystal to reside or pass through the micro-pores of the zeolite crystal.

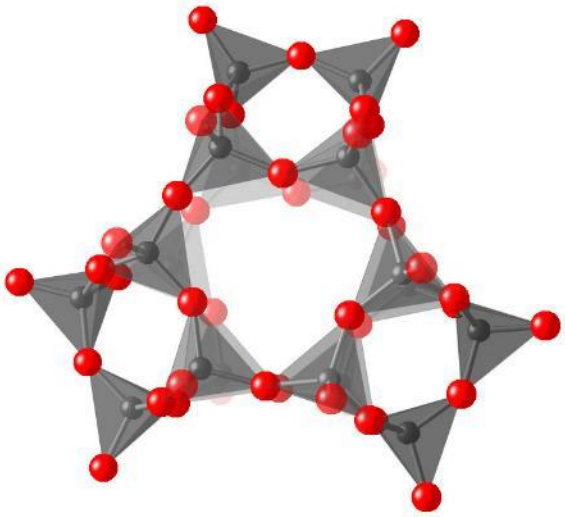

Figure 1 A zeolite structure built from corner-sharing tetrahedral units with grey Si or Al at the centre and oxygen in red (Wells et al., 2011).

The strength of the ion exchange properties due to the negative charge on the framework, from the incomplete tetrahedral structure of alumina, depends upon the framework and cations. The main feature of a zeolite structure is its framework type that describes the arrangement of the cages, the dimensionality of the channel system and the approximate size of the pore openings (McCusker & Baerlocher, 2007). Although the tetrahedral structure forms the basis of a framework of linked building blocks, the oxygen-silicon-oxygen bond angle defines the tetrahedral nature of the structure (Roy et al., 1999).

The use of organic structure directing agents in zeolite syntheses has dramatically extended the number of zeolite structure types during the past decades (Pophale et al., 2013) and a treatment approach could lead to zeolite structure stabilization by post-synthetic isomorphic substitution of Al for Ge (Gao et al., 2009). Zeolites are expressed according to the following formula: $Mx/n\ [(AlO_2)x(SiO_2)y] \cdot wH_2O$, where M is a cation with n valence, w is the number of water molecules per unit cell, x and y are the total number of tetrahedra per unit cell (Georgiev et al., 2009). The International Zeolite Association (IZA) maintains databases on natural zeolites and rules for the presentation of experimental data. The International Centre for Diffraction Data® (ICDD®) collects and publishes powder diffraction data for the identification of crystalline materials including zeolites. IZA and (ICDD®) rules and databases are of relevance to any new type of zeolite synthetised in the experimental work of this study.

Zeolites nomenclature and framework

A method for the systematic description of zeolites can equally be applied to natural zeolites as well as synthetic zeolites. Full information provided by an overall unique formula should include briefly cation exchange, isomorphic replacement and structural types (Barrer, 1979). According to the recommended nomenclature for zeolite minerals: report of the subcommittee on zeolites of the international mineralogical association, zeolite species are not to be distinguished solely on the ratio Si:Al (Coombs, 1998). Frameworks, considered corner-sharing network of tetrahedral-coordinated atoms, form distinctive structures (Currao et al., 2007). Structures containing an interrupted framework of tetrahedra are accepted where other zeolitic properties prevail, and complete substitution by elements other than Si and Al is allowed (Baerlocher et al., 2007).

Common building blocks of zeolite structures consist of 3, 4, 5 and 6 membered rings. The structures are arranged such that they form larger rings that represent the molecular pores (Chester & Derouane, 2010). The wide variety of possible zeolite structures is due to the large number of ways in which the SBU can be linked to form various polyhedral; these polyhedra create networks of regular channels and cavities. One such polyhedron is the truncated octahedron, better known as the sodalite cage; each sodalite cage consists of 24 linked tetrahedral, which are further linked to form different zeolites with distinct framework topologies. The number of unique frameworks exceeds 200, The IUPAC (International Union of Pure and Applied Chemistry) Commission on Zeolite Nomenclature, 1978, recommended a three letter coding for each framework (Baerlocher et al., 2007).

Each framework has a code, in the case of Zeolite-A, for example, it is LTA and has a corresponding abbreviated name, “Linde Type A” and a full name: “Zeolite-A(Linde Division, Union Carbide)”. A typical crystal chemical formula for zeolite-A would be $Na_{12}(H_2O)_{27}|[Al_{12}Si_{12}O_{48}]–$ LTA (McCusker et al., 2003). While the Zeolite type categories are silicates and phosphates, the framework type groups are silicates, phosphates, and both silicates and phosphates. The framework density, FD, that is the number of T-Atoms divided by $1000A^3$, distinguishes zeolites from zeolite-like materials. Non-zeolitic framework structure: FD = 20-21 while zeolite frameworks FD = 12.1 -20.6 (Baerlocher et al., 2007).

Different materials with the same framework structure can exhibit widely different chemical properties and families of minerals are classified by partial structural similarities such as framework and subfamilies are based on specific similarities. In a supergroup the structural arrangement remains unchanged, while groups are composed of iso-structural phase. A subgroup is based on chemistry such as sulphides or oxides. Related structures are based on structural distortion of the group structure. Unnamed zeolites have a 3 letters

framework code based on topologically distinct tetrahedral TO_4 where T= Si, Al, P, Ga and others (International Zeolite Association, 2005).

Natural zeolites

The Swedish mineralogist Axel Fredrik Cronstedt observed, in 1756, that upon rapidly heating the natural material stilbite it produced large amounts of steam; the name zeolite is a reference to the two Greek words “ζέω” = "boil" and “λίθος” = "stone" (Flanigen, 1991). Geologists considered the zeolite minerals to occur as fairly large crystals in the cavities of basalts and other traprock formations (Mumpton, 1999). Natural Zeolites form where volcanic rocks and ash layers react with alkaline groundwater; under natural conditions, zeolites form under low temperature geothermal conditions often from the alteration of volcanic ashes (Deer et al., 1966).

Natural zeolites such as natrolite are high in Na, thomsonites contain more Ca than Na, philipsites contain Ca, Na and K while chabasites contain only Ca cations and faujasites contain double as much Na to Ca. Several other natural zeolites contain a variety of Na, Ca and K and a variety of Al:Si ratios (Deer et al., 1966). Natural zeolite can be modified, for example, clinoptilolite zeolite has been modified for its NH_4+ retention capacity (Jha & Hayashi, 2009). The zeolites can be subdivided into a number of sub groups based on their structures:

1. Natrolite includes: natrolite, mesolite, scolecite, thomsonite, gonnardite and edingtonite, it is a fundamental chain-like unit.
2. Harmotone includes: harmotone, philipsite, gismondine and garronite, the chains are linked laterally containing four fold and eight fold rings.
3. Chabasite includes: chabasite, gmelinite, levyne and erionite, in this structure exist single or double six-fold rings of tetrahedral.
4. Faujasite tetrahedra form cubo-octahedral cage-like units joined to give a pseudo-cubic symmetry.
5. Modernite includes: modernite and dachiardite containing five-fold rings of tetrahedra that can be linked in various ways.
6. Heulandite includes heulandite, stilbite, epistilbite, ferrierite and brewsterite (Deer et al., 1966).

Synthetic zeolites

Zeolite synthesis originated with Richard Barrer and Robert Milton, in the late 1940s, the discovery of synthetic zeolites A, X and Y by Milton and Breck (Breck et al., 1956) in the late 1940's to early 1950's led to their introduction as a new class of industrial adsorbents in 1954, when a final structure of zeolite-A and -X have been determined, In 1959 they were introduced as hydrocarbon conversion catalysts (Flanigen, 1991). Zeolites are used as ion exchangers as well (Dyer, 1988; Juan et al., 2002) and the micro-porous alumino-phosphate and metallo-silicates were added to the molecular sieves (Flanigen, 1991). The d-spacing or the planar distance within a crystal, is an indication of the compactness or porosity of the zeolite, when the pore size is less than 20 Å it is defined as micr-oporous (McCusker et al., 2003). Barrer investigated the conversion of known mineral phases under the action of strong salt solutions at high temperatures (170–270 C°). The products, species P and Q displayed unique characteristics as synthetic zeolite with no natural correspondent (Cundy & Cox, 2005). Many synthetic zeolites have no natural counterparts and in some cases Al and Si have been replaced wholly or in part by other elements such as Ga or Ge (Shin et al., 2010). A heavier element replacement produces more definite information on subtitutional disorders (Goldsmith, 1950).

Synthetic zeolites can be prepared from a variety of sources such as coal ash (Prasad et al., 2012) (Ahmaruzzaman, 2010) or bagasse fly ash (B. Shah et al., 2011) (Purnomo et al., 2012) (Affandi et al., 2009) or rice husk ash (Wajima et al., 2009) (Furukawa, 2010). In a series of experiments to produce zeolite-A, bagasse fly ash was added to 2-5 N alkaline solution, and heated for dissolving at 90-120°C, meta-aluminate was added to obtain crystallisation at 90-100°C for 2-3 hours (Furukawa, 2010); this is a very short crystallisation time but required the addition of extra compounds. In a different method silica was extracted as sodium silicate from bagasse ash using NaOH solution, sodium silicate was then reacted with HCl to produce silica gel. High-purity silica xero-gels were obtained by acid treatment, ion exchange treatment, and washing with de-mineralized water (Affandi et al., 2009). Zeolite-X has been prepared using pure materials like silica powder, aluminium hydroxide, sodium hydroxide and distilled water to prepare zeolite-X under hydrothermal condition at atmospheric pressure (Htay, 2012). SiO_2 and Al_2O_3 from fly ash and co-disposal were synthetised into faujasite, sodalite, and zeolite-A zeolitic material (Somerset, 2005). Organized assemblies using templates represent a viable design strategy for developing crystalline micro and meso-porous inorganic frameworks (Lin et al., 2013).

T-atoms other than Si and Al such as Ga and Ge could replace the silica, cations that balance the charge of the anionic framework are loosely associated with the framework oxygens, and the remaining pore volume is filled with water molecules. The tetrahedral framework allows ion exchange and reversible dehydration. The non-framework cations are generally exchangeable and the water molecules removable. In synthetic zeolites several element Organic species (cationic or neutral) could be found in the pores (IZA). A large number of synthetic zeolites nowadays available have no corresponding natural zeolite (Thompson, 1998) such as zeolite-A.

Zeolite-A

Zeolite-A was the first zeolite to be successfully synthesized in the laboratory (Flanigen, 1991) and, even after half a century it is still one of the most widely used industrial adsorbents. The remarkable relationship between the crystal structure and the macroscopic adsorptive properties was first recognized by (Breck et al., 1956). Zeolite-A is constructed from sodalite cages connected by 4-MR (membered ring) leading to a cubic structure and three orthogonal 8-MR pores with a diameter of 4.1 Å with an SiO_2:Al_2O_3 ratio of 2 (Chester & Derouane, 2010) (Baerlocher et al., 2007). The tree-dimensional pore system and molecules of zeolite-A may diffuse in all three directions in space by moving across the 8-ring windows that connect the cavities (Figures 1 and 2). A typical crystal formula for zeolite-A would be $|Na_{12}(H_2O)_{27}|\ Al_{12}Si_{12}O_{48}|-LTA$ (McCusker et al., 2003), the formula clearly shows an Al:Si ratio of 1:1 (Figure 2).

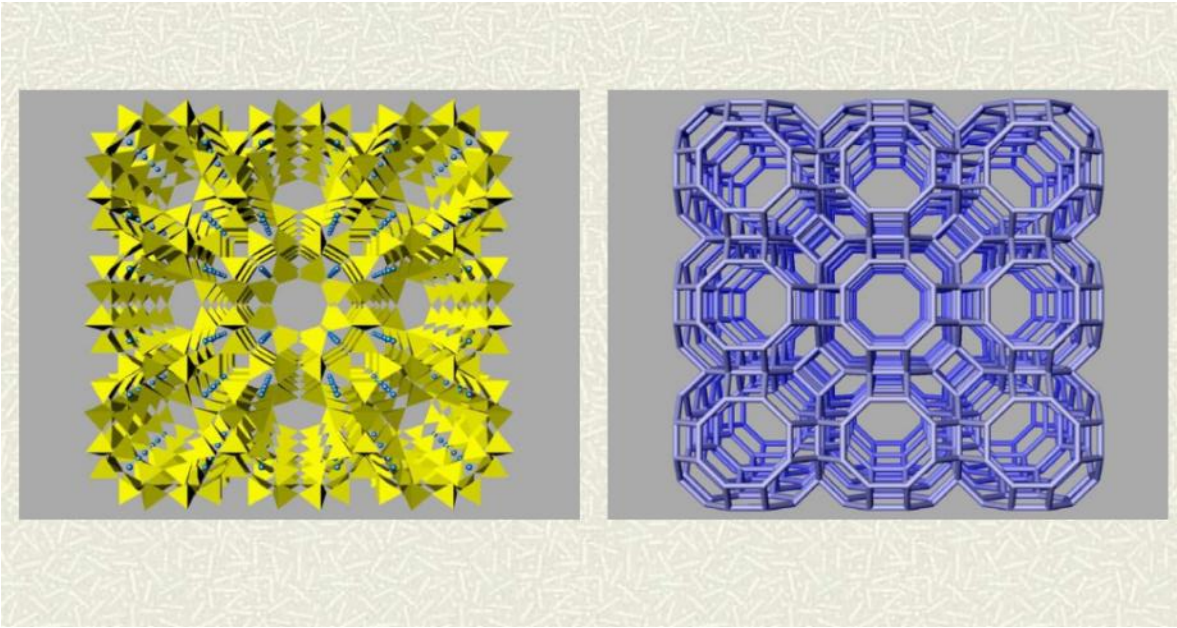

Figure 2: LTA Structure and Framework showing octahedral sodalite cages separated by additional linkages (Baerlocher et al., 2007)

Zeolite-A has properties important for surfactants: significantly higher rate of Ca^{2+} exchange (Vučelić, 1994), due to the high affinity for heavy metals, zeolite-A behaves as an environmental cleaner (Vučelić, 1994). SiO_2 and Al_2O_3, as feedstock for zeolite synthesis, can be successfully converted into faujasite, sodalite, and zeolite-A zeolitic material (Somerset et al., 2005). The synthesis of zeolite-A has reached 83% using clear alkaline silicate and aluminate solution at room temperature from organic-template-free precursors (Valtchev et al., 2005). Single Zeolite-A crystals nucleated in amorphous gel particles of 40 to 80 nm within 3 days at room temperature and embedded in gel that was consumed during further crystal growth. Heating to 80 C˚ resulted in substantial growth of zeolite-A crystals (Mintova et al., 1999).

Zeolite-X

Zeolite-X synthetised by Linde's laboratories has the structure of natural faujasite, that is based on sodalite cages connected through 6-MR channels and a central 12-MR pore (Figure 3) of 7.4 Å, it was used originally in cracking catalyst (Chester & Derouane, 2010). Some of the properties of the natural mineral faujasite are found to be very similar to those of the synthetic analogues with the same $SiO_2/A1_2O_3$ molar ratio (Stamires, 1973). The formula of a single crystal of dehydrated zeolite zeolite−X is $Na_{92}Si_{100}Al_{92}O_{384}$ (Zhu & Seff, 1999), it is of an Al:Si ratio slightly higher than zeolite-A. Zeolite-X has been synthetised from bagasse fly ash (Purnomo et al., 2012).

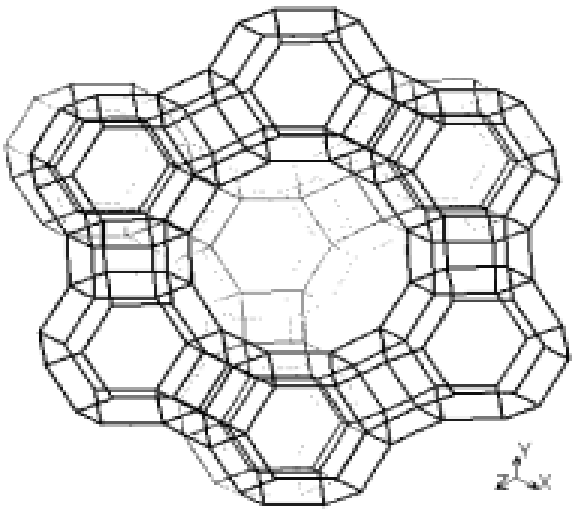

Figure 3: Zeolite-X framework showing a similar structure to zeolite-A but with a corner sodalite octahedral cage missing from 1 corner (Baerlocher et al., 2007).

Sugar cane and bagasse

The sugar cane plant (*Saccharum officinarum*) of the Poaceae family is an important perennial cane grass grown widely in the tropical and subtropical areas of the world; it produces sugar and molasses beside the bagasse fibrous leftover after juicing and the mill mud, the residual fibrous mass from the sugarcane juice (FAO). The Sugarcane plant is known to absorb more Si than any other mineral nutrient, accumulating approximately 380 kg ha^{-1} of Si, in a 12 months old crop (Savant et al., 1999). Application of silicate materials increased the levels of Si, P, Ca, and Cu and reduced the levels of N, K, Mg, Fe, Mn, and Zn in the sugar cane leaf (Elawad et al., 1982). Sugarcane leaves contain mostly amorphous silica, up to 1.8 wt% crystallising to cristobalite or quartz during harvesting as burning registered up to 1056 degrees C, which is sufficient for metastable cristobalite formation (Le Blond et al., 2010). However, Clark et al., (2012) suggest that localised bagasse burn temperatures may be in excess of 1550°C because the presence of β-quartz skipping the β-cristobalite phase transition and moving directly to melt with α-quartz rather than the expected α-cristobalite.

Paper Pulp has been prepared from bagasse (Eklund & Seaquist, 1972) that has also been used as partial Portland cement replacement (Cordeiro et al., 2008). High yields of pulp, suitable for paper manufacturing were obtained (Funk, 1975) and sugar cane bagasse fibres were modified to improve their adhesion with polystyrene matrix (Garcia-Hernandez et al., 2004) and cooking bagasse and other fibres with lime-based products improved the quality of fibreboard (Madan, 1981). Bagasse when compressed mainly with stearic acid, zinc oxide is an environmentally safe oil absorbing material (Brown & Ludwick, 2004), bagasse has also been used for removal of heavy metals by an adsorption process and as an absorbent for the removal of chromium and nickel from an aqueous solution (Rao et al., 2002). However, large quantities of bagasse are burnt at the sugar mill processing plants however the fly ash (Figure 4) in general has found several applications.

Fly ash and its applications

Coal fly ash (CFA) has several usages similar to bagasse fly ash such as dyes removal (Gupta et al., 1998) (Rachakornkij et al., 2004) and pyridine-removal (Lataye, 2006). CFA is used in construction and as a low-cost adsorbent for the removal of organic compounds, flue gas and metals, light weight aggregate, mine back-fill, road sub-base, and zeolite synthesis (Ahmaruzzaman, 2010).

In many sugar cane growing areas of the world, bagasse is one of the important biomass sources, used as a fuel in the sugar industry and large quantities of fly ash create a serious disposal problem (Batra et al., 2008). In Mauritius, commercial scale cogeneration of power from bagasse is continuous in some factories (Deepchand, 2001). The disposal of the fly ash in NSW, Australia, by mixing in the soil is to be changed (Gorta, 2006). While the high un-burnt carbon content has a contamination potential (Batra et al., 2008). Silica in the form of quartz of varying size crystals have been related to silicosis (OSHA, 2002; Kaewamatawong et al., 2005). Quartz and cristobalite in bagasse ash recycled onto the fields could be re-suspended into respirable-sized particulate and may present an occupational health hazard (Le Blond et al., 2010).

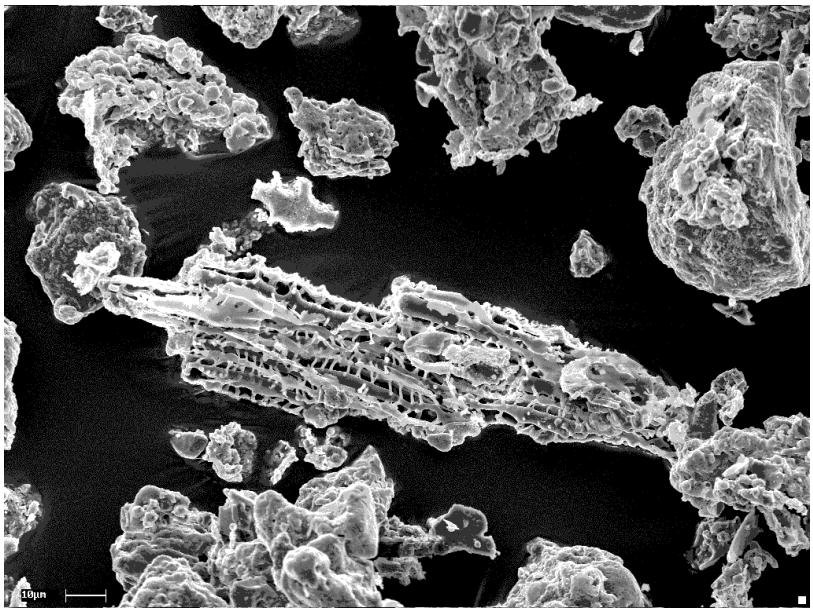

Figure 4: Bagasse fuel, from a sugar mill factory at Harwood, NSW, partial melting fly ash (irregular shapes) and phytolith with preserved inner articulations

Bagasse ash is an effective adsorbent for the removal of phenol and nitrophenol (Gupta et al., 1998). Bagasse fly ash contains carbon (Batra et al., 2008), if a method could be found to clean the carbon, several industrial, environmental and agricultural applications could be considered (Querol et al., 2002). Applications such as ion exchange, molecular sieves, and adsorbents are among many other usages (Flanigen, 1991; Pine et al., 1984; Wajima et al., 2007), zeolites are used as detergent builders as well (Shelke et al., 2011; Sherman, 1999). Coal fly ash (CFA) has been used to produce zeolite but (CFA) contains large quantities of impurities such as heavy metals and metals in general (Ahmaruzzaman, 2010). Converting fly ash into zeolites not only alleviates the disposal problem but also converts a waste material into a marketable commodity (Ahmaruzzaman, 2010). Bagasse fly ash contains iron, calcium, magnesium, and potassium oxides as minor components beside the major components, silicon and aluminium oxides (Teixeira et al., 2008). The heavy metals are present in negligible amounts and silica is the main element (Cordeiro et al., 2008; Purnomo et al., 2012). Although bagasse fly ash and ash in general have certain usages, however, solving the disposal problem through synthesis of zeolites from these waste materials has wider applications.

Applications of zeolites

Zeolite is versatile and has many existing and potential uses in the chemical industry. The utility of zeolites arises from the number of the many distinct zeolite frameworks and the fact that different materials with the same framework structure can exhibit widely different chemical properties (IZA-SC). Synthetic zeolite have large internal pore volumes, molecular-size pores, regularity of crystal structures, and the diverse framework chemical compositions allow "tailoring" of structure and properties, highly active and selective catalysts as well as adsorbents (Sherman, 1999).

Zeolites as molecular sieves

Crystals used as molecular sieve have very small holes of precise and uniform size, these holes are small enough to block large molecules and allow small molecules to pass through. Synthetic zeolites are used mainly as catalysts in hydrocarbon processing and ion exchangers for water softening as well as molecular sieves for gas adsorption (Dyer, 1988) and gas separation (Aoki et al., 2000b). In a study on the ethane exclusion and ethylene adsorption on silver-exchanged zeolite-A, it was found that it is dependent on the pore size of the adsorbent (Aguado et al., 2012). Ion exchange to remove copper from an aqueous solution using zeolite, copper was preferred to the zeolite alkali metal ion (Keane, 1998). Molecules smaller than the zeolite pore diameter are adsorbed whilst excluding larger molecules (Dyer, 1988) (Ijima 1986). The crystallization process produces the required sodium alumino silicate structure. The formed zeolite crystals can be ion exchanged to adjust the pore size. Zeolites may be also used to adsorb water molecules from gas streams or to trap SO_2 and NH_3 from low-water gaseous emissions (Querol et al., 2002).

Cracking, catalytic and environmental applications

Selective catalysts reduce undesirable by-products and increases selectivity of hydrocarbon cracking on Y-Zeolite-based catalysts (Yaluris et al., 1994). Natural minerals such as chabazites and clinoptilolite, when acidified, have the ability to catalyse the cracking of bitumen in the Canadian oil sand and adsorbing a large fraction of the undesirable compounds (Junaid et al., 2009). The transformation of reactants into products depends on how the processed molecules fit the active site and form and guide the identification of zeolite structures (Smit & Maesen, 2008). Hydrophobic zeolites made from fly ash have applications in oil spill management (Adebajo et al., 2003) and in storage of molecules since zeolites belong to a most prominent class of nano-porous materials which have been considered as potential sorbents for hydrogen storage. The adsorption of hydrogen molecules on MFI, MOR and LTA zeolites, which encompass a range of different pore structure and chemical composition, has been simulated (Xiu Liu, 2012). Zeolite-Beta was grown in microgravity to produce higher-quality catalysts and absorbents crystals with higher selectivity compared to terrestrial/controls (Akata et al., 2004).

Detergent builders-phosphate replacement

When zeolites are used as a detergent builder, they are usually in a sodium ion form, and serve as water softeners by exchanging sodium for calcium (ZEODET, 2007). Synthetic zeolites are replacing phosphate compounds in laundry detergent powders (Hui & Chao, 2006; Shelke et al., 2011; Vučelić, 1994). Current world production of synthetic zeolites is estimated to be about 1.4 million metric tons per year 80 % of synthetic zeolite is used in the detergent industry (Virta, 2008). For the detergent industry where zeolites are routinely used as water softeners, less crystalline zeolites are preferred (e.g. zeolite-A) because of the high exchange capacity to remove water hardening elements such as Ca and Mg. The results of zeolite 4A tests on calcium binding capacity showed similarity to the commercial detergent in removing calcium ions during the washing cycle (Hui & Chao, 2006). This study has the potential of producing zeolite-A for detergent applications once, the bagasse fly ash or the produced zeolite, is purified.

Ion exchange processes

Synthetic zeolite-A can be used as an efficient ion exchange material for the removal of zinc and cadmium ions from industrial and radioactive wastewaters (El-Kamash et al., 2005). The removal of nickel and copper from aqueous solution by batch ion exchange with solid Y zeolites showed that the extent of transition metal removal is dependent strongly on the nature of the out-going alkali metal (Keane, 1998). The removal of fission products from mixed solvents using zeolite was studied by (Dyer & Aggarwal, 1997) for radioactive

fission products (Cs, Sr). Zeolite is also used in synthesis that is to hold a molecule in place for a reaction (Chen & Garwood, 1978).

The cation exchange capacity of zeolite-Y ranges between 400 and 450 meqr100 g (Rayalu et al., 2000). The cation exchange capacity up to 250 meq/100 g and ammonium adsorption capacity of 22.93 mg NH_4 +/g indicate that the fly ash zeolite may be potentially useful to reduce heavy metals and other pollutants from contaminated environments (Prasad et al., 2012). According to Ismael (2009), low-silica zeolites with Al/Si ratio of 1:1, such as zeolite- A, zeolite P and zeolite X, exhibit the highest ion exchange capacity. The consequence of decreasing crystallinity (Javier, 2002) is that CEC tends to increase, and the industrial and environmental applications tend to increase.

Zeolitic products having up to 3 meq g^{-1} may be easily obtained from high-glass (CFA) by direct conversion (Querol et al., 2002). Foletto (2009) studied the formation of Zeolite-A and the zeolitic materials from rice-husk ash using NaOH, both presented high capacity of cation exchange, in the range of 5-6 meq/g. In an investigation of the removal efficiency of ammonium (NH_4^+) ion from aqueous solution, natural zeolite was found suitable for the removal of NH_4^+ ions in wastewater treatments and agricultural purposes to in terms of sustainability of environmental quality (Saltalı et al., 2007). The zeolitic material may be also used for the uptake of ammonium from polluted waters but high concentrations of other cations may considerably reduce the ammonium absorption efficiencies due to ion competition (Querol et al., 2002). Both the pure and the impure zeolitic material have a high potential for application in wastewater (Moreno et al., 2002). The potential use as a 'once through' cation exchanger of a zeolitic material (NaP1) synthesised from fly ash has been evaluated (Juan et al., 2002). Na-P1 could simultaneously remove NH_4+ and PO_4^{-3} from the solution between pH 4 and 9 (Wajima et al., 2007). The results of the treatment of the acid mine drainage with the prepared fly ash zeolites showed that the concentrations of Ni, Zn, Cd, and Hg were decreased as the zeolite dosages of the fly ash (Somerset, 2005). Shoumkova (2011) and (Querol et al., 1999) studied filtering ammonia from municipal wastewater. The bagasse and fly ash have been used as potential adsorbents before zeolitisation to remove chromium and nickel from aqueous solution (Rao et al., 2003). The removal and recovery of heavy metal cations from drinking and wastewater have also been investigated. (Ismail, 2009) work is on Water removal of heavy metals, zeolite is an efficient adsorbent for the hydrophobic fraction from wastewater treatment plants effluents Membrane with crystalline pores (Aoki et al., 2000a).

In car catalytic converters for filtering car exhaust, zeolites are used as micro-sieves for adsorbing any pollutants. The sorption removal of zinc and cadmium ions from aqueous solutions using synthetic zeolite-A can be used as an efficient ion exchange material (El-Kamash et al., 2005). Mercury has been removed from industrial effluents using the clinoptilolite zeolite group (Chojnacki et al., 2004). Similarly in studies on removal of phenol from wastewater, (BFA) was converted into zeolitic materials and the sorption capacity of synthetic zeolitic products was significantly increased after alkaline hydrothermal treatment (Bhavna Shah et al., 2011). However bagasse fly ash converted into zeolitic material and showed enhanced capacities for the sorption of 2-chlorophenol and can be utilized as a low cost sorbent for treatment of phenolic waste-water (B. Shah et al., 2011). Gupta (1998) characterized a zeolitic product used for the removal of some phenols. In other application measuring trace organic vapors, a zeolite thin film-coated long period fibre-grating sensor was developed for direct measurement of trace organic vapors (Zhang et al., 2009).

Agricultural and other usages

Zeolites are used as fertilizer or fertilizer enhancer (Fansuri, 2008) and soil additives for supplying plant available micronutrients that are not freely water soluble and high CEC results were achieved by (Harja, 2012).

In a feed supplements experiments zeolite- A tended to improve Zn utilization in chicks fed inadequate Zn (Watkins & Southern, 1993), when dietary calcium was deficient or marginal, zeolite-A improved calcium utilization (Leach et al., 1990), vitamins and other elements have been added to zeolite used in feed (Papaioannou, 2002). Zeolites can be chemically modified by inorganic salts or organic surfactants, which are adsorbed on the surface and lead to the generation of positively charged surfactant micelles, and which enables the zeolite to bind also anions, like arsenates or chromate, (Karmen et al., 2013). Fluoride removal from aqueous solutions using various modified zeolites have been studied particularly since high fluoride concentrations in groundwater, up to more than 30 mg/L, occur widely (Mohapatra et al., 2009).

Zeolites formation

There is a need to understand zeolite formation under conditions including the amount and kind of silica monomers and polymers present in solution and their behaviour (Hawkins, 1981). Since zeolites are crystalline it is important to understand how synthetic zeolite continues to grow after nucleation. Consequently, it is necessary to understand the nucleation process.

Nucleation

Zeolite synthesis proceeds via nucleation, which is a "consequence of local fluctuations, small in extent but considerable in degree of departure from the mean for the solution, followed by spontaneous growth of nuclei exceeding a critical size" (Barrer, 1989). Many pre-crystallization processes are active, leading to nucleation, followed by rapid crystallization (Vučelić, 1994). Nucleation is the formation of new crystalline entity from a solution where the atoms or molecules of a reactant phase rearrange into a cluster of the product phase large enough as to have the ability to grow irreversibly to a macroscopically larger size (Cubillas & Anderson, 2010). Primary nucleation is characterized as being driven by the solution itself, either strictly within the solution, as in homogeneous nucleation, or catalysed by extraneous material in the solution, as in heterogeneous nucleation. Silver oxide can be used in alkaline solutions in zeolite synthesis and can act as effective heterogeneous nuclei for the crystallization (Hamidi et al., 2012).

Analysis of three different crystallizing systems showed that the rate of homogeneous nucleation is extremely low under the given synthesis conditions, so the other nucleation processes must be considered relevant for the formation of primary zeolite particles (Bronić & Subotić, 1995). Heterogeneous nucleation is anticipated in the presence of amorphous gel in most zeolite synthesis systems; secondary nucleation is catalysed by the presence of parent crystals of the same phase, and occurs with lower activation energy than primary nucleation (Thompson, 1998). At the liquid phase super-saturation with "aluminosilicate ions" directs the nucleation (Subotić et al., 1980). In hydrothermal zeolite systems it is more difficult to identify super-saturation because of the mix present in the aluminosilicate solution, and because the relative concentrations of these in a batch system change as the crystallization proceeds (Thompson, 1998). Building micro-porous structures starts at controlling nucleation kinetics (Ng et al., 2012). Itani established by high-resolution transmission electron microscopy that the nucleation of zeolite occurs in the solid, nuclei are released to the liquid to start crystallisation (Itani et al., 2009). Pre-crystallization processes are active and nucleation is followed by rapid crystallization. The most active species are complexes of aluminium, if these complexes are exposed to non-equilibrium conditions or outside stresses, modified zeolite-A can be obtained (Vučelić, 1994). At 100 °C, the nucleation period of zeolite-Y was determined to be about 6.5 days, which extended over almost the whole period of crystal growth. The crystallization kinetics of colloidal zeolite Y differed from those for another clear solution, colloidal zeolite system, where the nucleation and crystal growth were found to occur as separate processes (Li et al., 2002).

Nucleation can be affected by other procedures, like aging of the synthesis medium, seeding, and selective crystallization poisoning (Di Renzo, 1998). Aging at room temperature has a pronounced effect on crystallisation (Valtchev et al., 2005). Nucleation could be manipulated with so-called proto-zeolitic nano-clusters that can be assembled into hexagonal, and foam-like framework structures under a variety of assembly conditions (Y. Liu & Pinnavaia, 2002).

Crystallisation

Crystals are solid materials in which atoms are regularly arranged with respect to one another. This regularity of arrangement can be described in terms of symmetry of elements. These elements determine the symmetry of the physical properties of a crystal (Kelly & Knowles, 2012). After nucleation crystallisation occurs, however nucleation and crystallisation can overlap. The dissolution followed by nucleation could be still ongoing while the crystallisation is occurring (Thompson, 1998). Aqueous silica activity, cations concentrations and pH determine which zeolite will form (Chipera & Apps, 2001). Intermediate addition of potassium into the crystallising media results in the selective formation of zeolite-X in the hydrogel phase (Iwama et al., 2010). One of the oldest theories in crystal formation is the Ostwald ripening; Ostwald proposed that the solid first formed on crystallisation of a melt (Threlfall, 2003). According to the (International Union of Pure and Applied Chemistry, 2012) Ostwald ripening is the dissolution of small crystals or sol particles and the re-deposition of the dissolved species on the surfaces of larger crystals or sol particles. The Ostwald rule states that in general it is not the most stable but the least stable polymorph that crystallises first, the basis of this rational is the "irreversible thermodynamics, structural relationships, or a combined consideration of statistical thermodynamics and structural variation with temperature" (Threlfall, 2003). Alternatively, a theory not completely proven on the reversed crystal growth states that aggregation of nanoparticles may dominate in the early stages of crystal growth, followed by surface crystallization, and then extension from surface to core of the disordered aggregates (Zhou, 2010). The reversed crystal growth discovery is based on the extension to the core of the disordered aggregates from the surface (Zhou, 2010).

Control of crystal size

Zeolite crystals appear to grow rather slowly compared to ionic or molecular crystals because of the construction a three-dimensional lattice (Cundy & Cox, 2005). The size of zeolite crystals can be controlled by a proper choice of crystallization conditions (Di Renzo, 1998). Crystals up to 340 µm have been synthesized from gels (Warzywoda, 1999). High crystallinity needs high temperature (Sanhuesa, 2004), the high crystallinity was obtained rapidly when SiO_2:Al_2O_3 ratio, NaOH concentration and temperature were high (Wajima et al., 2009). However, according to (Kohoutková, 2006) particle size decreases with increasing molarity. The increased alkalinity of the synthesis gel was found to be the one that caused a decrease in the final particle size (Chaves et al., 2012). However the benefits from higher surface area on smaller crystals negative charge is balanced usually by an alkali metal cation loosely held in the cage or channel bonding (Deer et al., 1966). The high-resolution transmission electron microscopy (HRTEM) study revealed that a thin layer of amorphous material covers the zeolite particles acting as a binder between individual zeolite crystals (Valtchev et al., 2005). The size of zeolite crystals can be controlled by modifying the nucleation frequency by the addition of silver-based promoters that provide a number of additional seeds proportional to the amount of silver oxide precursors introduced in the synthesis systems (Hamidi et al., 2012).

Large quantities of NaOH are expelled initially from the gel into the solution, which restricts extensive polymerization and leads to formation of small aluminosilicate particles with open pore structure (Itani et al., 2009). The onset of crystallization is controlled by a critical mass of produced viable nuclei and a diffusion that brings the gel to a homogeneous composition close to the zeolite stoichiometry before the crystallization

starts (Itani et al., 2009). Increasing $Na_2O:Al_2O_3$ ratio in the reaction mixture decreases the polycrystalline cluster of the faujasites (Chaves et al., 2012), Moreno (2012) used $Na_2O:SiO_2$ molar ratio of 1:3 to produce zeolite-A.

2.8.4. Factors interactions in zeolites formation

When all factors are more or less the same except for one it is possible to see the effect of that factor without much analysis, however it is rarely the case. Zeolite synthesis is the result of the interaction of several factors but mainly the Al:Si ratio, temperature, molarity, solid to liquid ratio, reaction time and the presence of other element, coming from the fly ash, in the reaction mix as well as other factors, such as pressure, that are of lesser influence.

Aluminium: Silica Al:Si ratio and silica extraction

According to Lowenstein law the Al:Si ratio is 1 at its lower limit since two adjacent AlO_4 tetrahedra will be repulsed by the negative charge. As the Al:Si ratio of the framework increases, the hydrothermal stability as well as the hydrophobicity increases. In a study by (Mokaya, 2000) on aluminium relevance to stability, a material with an Al:Si of 1:23 exhibited intermediate stability. The influence of Al content on the hydrothermal stability is explained with respect to the position occupied by the framework Al within the pore walls, and it is suggested that Al incorporated on the surface or near the surface region of the pore walls provides the greatest protection (Mokaya, 2000).

It is important to adjust the Al:Si ratio in the reaction mixture prior to crystallisation of the end zeolite product. An Si:Al molar ratio of 1.8 was a critical ratio to prepare pure zeolite-X (Purnomo et al., 2012). The Al:Si ratio of the starting materials was of special importance in that zeolites formed with Al:Si ratios similar to or smaller than that of the parent materials. The formation of zeolites with a Al:Si ratio different from the starting material suggest that mass transport with respect to silica and aluminium is also necessary (Wirsching, 1981).

The occurrence of easily soluble silica phases in the original fly ash and a high reactive surface area were found to be the major parameters influencing silica extraction at a $SiO_2:Al_2O_3$ of 2 (Moreno et al., 2002). Although the overall Si/Al ratio does not change significantly during synthesis the final Si:Al ratio of zeolite-Y is controlled by the availability of Si (Christidis, 2008). It has been found that by using initial SiO_2/Al_2O_3 ratio at 2.9 and fixed K_2O/Na_2O ratio at 0.09, it is Possible to avoid co-crystallization of zeolite-A and zeolite-X (Ismail 2009).

At $Al_2O_3:SiO_2$ ratios of 0.4 to 0.5 and an $H_2O:SiO_2$ below 100 with high sodium content co-formation of zeolite-A as well as a small amount of a solid with *d* spacing of about 15 Å was observed (Valtchev et al., 2005). "Some decisive factors favouring silica extraction are: high bulk silica, high silica and low alumina in the glass matrix; when aluminium bearing phases are dissolved the dissolution of zeolites occurs immediately capturing silica in the solids" (Moreno et al., 2002).

Further studies are needed, for low-silica or aluminium rich zeolite with sufficient aluminium to bring the Al:Si fly ash ratio to 1:1. Bagasse fly ash contains about 14 % Al_2O_3 and about 70% SiO_2 (Clark et al., 2012). The silica to aluminium ratio in the bagasse fly ash is almost 5. Any further studies will need to test not only the adjustment of the Al:Si to 1:1 but also the Al:Si 2:1 and Al:Si 1:2, these ratios would cover a range of Al:Si ratio that in combination with other factors might provide sufficient experimental data in a matrix of related experiments.

Temperature

In a study at 104°C during dissolution single phase NaP1 zeolite was obtained at 2M NaOH, but crystallization occurred at 80°C. Conditions favourable for dissolution of fly ash are not favourable for crystallisation of zeolites with larger pores (Walek et al., 2008). H_2O-rich zeolites formed transitorily at higher temperatures (Wirsching, 1981) and in a stirred batch reactor, NaOH solution at molarity nearing 6 M was used to dissolve silicate from rice husk at 80°C and formed higher crystalinity zeolite-A within 48 hours when SiO_2:Al_2O_3 of 1.7–2.8 was at its highest end (Wajima et al., 2009).

A low zeolitisation temperature results in higher purity and smaller particles; however the low treatment temperature required longer curing time (Purnomo et al., 2012). Single-phase zeolite 4A samples in pure form with a high crystallinity were synthesized by applying step-change of synthesis temperature during hydrothermal treatment of coal fly ash (Hui & Chao, 2006). Zeolite-A nanoparticles were synthesized under room-temperature conditions, the composition of the initial system allowed the crystallization to be accomplished within 3 days, individual zeolite, but not well formed, crystals were in the range of 100-300 nm. Well-faceted cubic crystals averaging about 400-500 nm appeared within 10 days (Valtchev et al., 2005). At low temperature in the initial step, K-chabazite was the major zeolite product and K-phillipsite was the major product at high initial step temperature and long crystallization (Fansuri, 2009). Highly saturated solutions form nano-crystals that precipitate into polymers at a later growth stage both at the liquid–solid interface and within the amorphous mass, of idiomorphic crystals of A-type and X-type zeolites (Belviso et al., 2012). Step-change of synthesis temperature during hydrothermal treatment plays an important role in reducing the overall synthesis time while maintaining a high degree of crystallinity for the samples (Hui & Chao, 2006).

The temperature of crystallisation, according to this review, is generally about 100 C, this range of temperature needs to be tested in further work particularly that the silica in the bagasse is mostly quartz and temperature along with molarity could increase the dissolution, however an increase in temperature could produce undesirable zeolite. Further studies are needed to determine suitable temperatures for bagasse fly ash as a source of silica particularly that the temperature along with the molarity seems to determine the transformation into the zeolite types in coal fly ash.

Fly ash to liquid ratio

The solid to liquid ratio seems to have an impact on solubility and SiO_2 availability when it was changed from sample:NaOH ratio of 1:10 and 100 °C in comparison with to 1:30 and 200 °C, while keeping Al concentration low, even at short reaction time (Bui Hoang Bac et al., 2010). Rapid crystallisation at room temperature was observed at H_2O:SiO_2 ratios between 120 and 150. When this ratio is below 100, with high sodium content, formation of both zeolite-A and hydroxyl-sodalite was observed (Valtchev et al., 2005). In a different study using slag and aluminium sludge, hydrothermal treatments followed alkaline fusion and crystallized in sodium hydroxide at 90 degrees C for 1-9h with different H_2O:SiO_2 ratios, higher H_2O:SiO_2 ratio increased the rate of crystallization (Anuwattana & Khummongkol, 2009). 4g/L fly ash increased significantly the dissolution while solid:liquid ratio of 50-150 g/L was largely limited because of surface formation of zeolite on partially dissolved fly ash resulting in low crystallinity zeolite-like material (Walek et al., 2008).

Alkali Molarity

Zeolite formation results from the interaction of multiple factors but one factor can be highlighted such as in the following study where a hydrothermal activation at a solid to liquid ratio of 1:5 of coal fly ash with NaOH at 100 °C and an SiO_2:Al_2O_3 varying between 1.82 and 2.33, NaP1 zeolite was formed at 2M in 24 hours. However Chabasite formed at 3M (Prasad et al., 2012). The increased molarity affected the zeolite type formed, at a

much lower molarity of 0.1 M NaOH and KOH solution at 60-150 degrees produced phillipsite, merlinoite, analcime and zeolite Na-Pl (Querol et al., 1995).

In a different set of experiments pure-form zeolite-A was synthesized at 100 °C from BFA, a mixture phases of zeolites A and X were obtained at the condition of 3.33 M NaOH solution during various crystallization times. Shorter crystallization time of zeolite-A at higher NaOH concentration provided narrower particle size distribution (Wang et al., 2008), NaOH concentration increase can be an essential factor to improved zeolitic materials synthesis but reduces the yield of SiO_2 extraction (Bui Hoang Bac et al., 2010).

In any further study NaOH molarity ranging from 3 to 5 M, as middle ground, might need to be tested for dissolution and crystallisation. The factors are interrelated and the effectiveness of molarity can only be measured when all other conditions are the same however a suitable statistical analysis like the factorial design will provide a multifactor response for each combination of factors.

Reaction time and aging

Porosity explains the need for low temperature pre-ageing during the synthesis of materials such as zeolites A and X (Pope, 1998) particularly in early stages of formation, the silicate material is amorphous (Auerbach, 2005), within 96 hours the formation of zeolite-A is preferred to zeolite-X, but for longer incubation times the X-type become progressively more abundant. The prolongation of the synthesis time up to 10 days led to formation of larger well-faceted cubic crystals averaging about 400-500 nm in size (Valtchev et al., 2005). Time of reaction shifts zeolite type formation (Hawkins, 1981). Faujasites nanocrystals with high micro-porosity and external area were obtained by including an aging step at high alkalinity (Chaves et al., 2012) while long time at about 200 degrees favours analcime but 100 degrees was not enough to form analcime even after 24 hours (Novotna et al., 2003). However, room temperature was enough to produce zeolite-A nanoparticles within 3 days from a very reactive organic template-free gel system (Valtchev et al., 2005). Varying temperature, time and alkali/fly ash rates yielded up to 140 g of SiO_2 per kg using a single step process, thermal pre-treatments may yield up to 210 g kg^{-1} (Moreno et al., 2002). Two days of aging at room temperature and 6 days of curing at 80°C resulted in zeolite-Y and –P type formation (LaRosa et al., 1992). Further studies are needed to determine suitable reaction time for the production of zeolites from bagasse fly ash. The temperature range is wide but it seems that the reaction time needs to be in days not hours or weeks.

The presence of alkali Mg, Ca, K and Fe

Adding seed crystals to a crystallization system has typically resulted in increased crystallization rates (Thompson, 1998). “Hydrated potassium ion has a function to assemble aluminosilicate precursors to form LSX by a strong salting-out effect; otherwise, sodium ion assembles the same building units into zeolite A. Intermediate addition of potassium ion into crystallizing media controls the final precipitating crystalline phase kinetically” (Iwama et al., 2010). The presence of metals or elements: Mg (and possibly Ca) plays a fundamental role in determining the formation of zeolite crystals (Belviso et al., 2012). Calcium is a factor in the type of zeolite formed, the importance of the calcium activity of the reacting solution and the influence of the open system increased as alterations proceeded (Wirsching, 1981). Small conversion values of samples with different Fe content did not affect the zeolite crystallization (Basaldella et al., 1998).

The bagasse fly ash contains several elements such as Mg, Ca and Fe, and they could act as structure directing agent (SDA), which makes it less likely to predict the outcome of the reaction in the presence of those elements particularly in the case of the bagasse fly ash where some elements are 2-3 %. It might be beneficial

in any further study to experiment with some kind of filtering of single elements before the use of the fly ash in the zeolitisation experiments.

Section 3: Outputs and Achievement of Project Objectives

Materials characterization and selection

The sugarcane bagasse ash used in this project was collected from the Broadwater Sugar Mill Co-Generation Plant in November, 2013. The material was dried in an oven at 105˚C until constant weight was achieved and then stored in airtight containers until required. The SCBA was black in color. The chemical composition of the oven dried SCBA was determined by X-ray florescence analysis (XRF) using a PANalytical Epsilon 3 X-ray Fluorescence (XRF) Analyser. Concentrations were calculated against Omnian standards in Panalytical Epsilon 3 Software; as no matrix corrections were applied, the data should be considered semi-quantitative. Carbon and nitrogen concentrations were measured on a LECO 2000 CNS Analyser. The sample was bound with wax (9:1) and pressed as a pellet for 30 seconds at 20 tonnes pressure. The results are summarized in Table 4. It can be readily seen that the major constituents of the material are primarily Silica (SiO_2) and Alumina (AL_2O_3) thus confirming the material as an aluminosilicate. Relative density was determined in accordance with AS3583.5 (Methods of test for supplementary cementitious materials for use with Portland cement. Method 5: Determination of relative density) and is also shown in Table 4 and it can be seen that SCBA is a lightweight material.

The cement used in this project was a general-purpose ordinary Portland cement (GP) manufactured by 'Sunstate Cement' and complying with AS 3972 (2010) General-purpose and blended cements, Standards Australia, SAI Global Limited, Sydney, Australia. The chemical composition was determined by XRF in the same manner as described for SCBA and are also shown in Table 4. Specific gravity was determined as per AS3583.5 (1991) and is given in Table 4. (Methods of test for supplementary cementitious materials for use with Portland cement, Method 5: Determination of relative density).

Table 4 Specific gravity and chemical composition of SCBA and OPC General Purpose Cement as determined by XRF analysis

%wt	SCBA	GP Portland Cement
SiO_2	78.498	19.189
Al_2O_3	7.273	3.489
Fe_2O_3	3.847	2.490
CaO	1.280	58.161
MgO	1.281	0.770
SO_3	1.553	4.343
Na_2O	0.697	<0.001
K_2O	1.414	0.331
COH	1.328	10.498
LECO Carbon	7.150	0.670
LECO Nitrogen	0.090	0.030
Relative Density	2.54	3.15

The mineralogical properties of the SCBA provide insight into the amorphous content of the ash, which if present indicates pozzolanic activity. The mineralogy was determined using X-ray diffraction (XRD) analysis. Samples were milled to a powder (<10µm) prior to XRD scanning by a Bruker D4 Endeavor XRD with a Lynxeye position sensitive detector. Cobalt radiation was used at 40 kV and 40 mA over a range of 5˚ and 80˚ 2θ, with a step size of 0.03572˚ 2θ and 1.65 sec./step. The results of the analysis (Figure) show a strong quartz peak and a broad hump that is characteristic of amorphous minerals. The amorphous hump is shallow here and is

indicative of semi amorphous minerals. This semi amorphous indicator coupled with the strong crystalline quartz peak means that it is likely that there is limited pozzolanic activity in the SCBA.

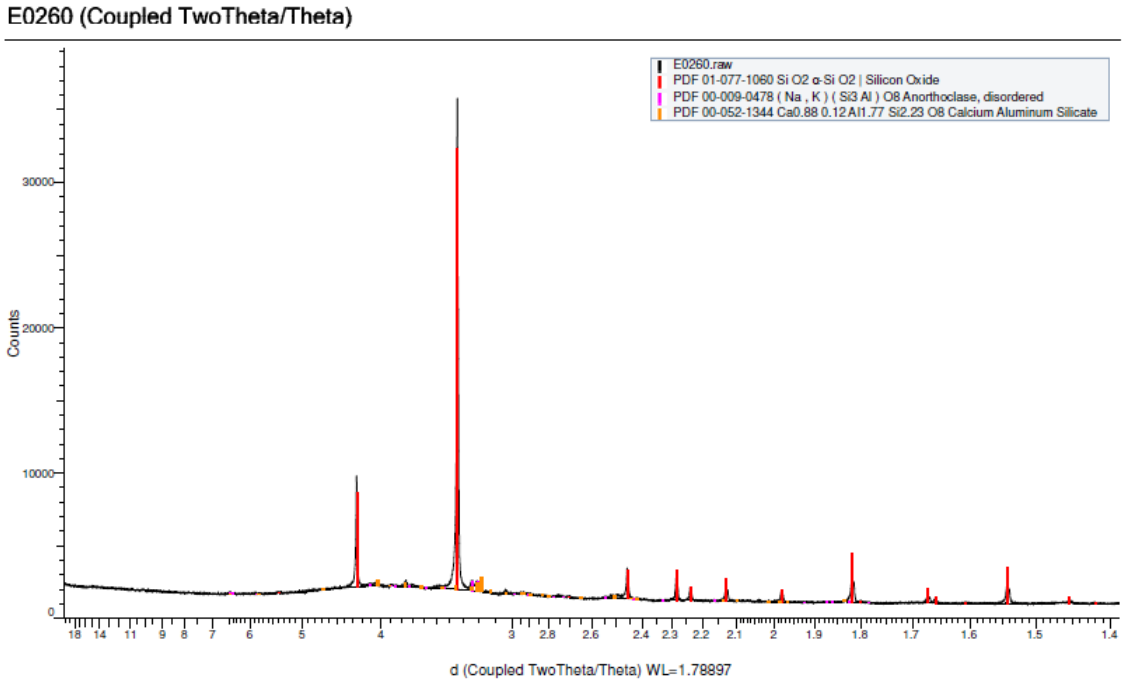

***Figure** 5 XRD Patterns of SCBA, XRD scan shows only a low amorphous hump between 6 and 2.8 Å d-spacing indication only a small fraction of amorphous materials, especially silica.*

The sand used in concrete mixes was double washed kiln dried natural river sand. The particle size distribution was determined in accordance with AS1141.11.1 (2009, Methods for sampling and testing aggregates, Method 11.1: Particle size distribution – Sieving method) and found to comply with AS2758.1. The fineness modulus was determined by sieve analysis in accordance with (AS1141.11.1). Both are shown in Table 5. The particle density and the water absorption were determined and are shown in Table 6. (AS1141.5 – 2000 Methods of sampling and testing aggregates – Particle density and water absorption of fine aggregates.)

***Table** 5 Sieve analysis and fineness modulus of natural river sand.*

Sieve Size (mm)	Cumulative % retained
2.36	0
1.18	0.06
0.60	6.58
0.30	73.85
0.15	100.00
Fineness Modulus	1.80

Table 6 Particle density and water absorption of fine and coarse aggregates

Particle density basis (t/m³)	River sand	10 mm basalt	20 mm basalt
Dry	2.6	2.55	2.56
Saturated surface dry	2.6	2.62	2.62
Apparent particle density	2.6	2.73	2.74
Water absorption (%wt)	1.2	2.6	2.7

The sand used in mortar mixes was CEN Standard Sand EN 196-1 (ISO Standard Sand ISO 679: 2009) which is prepackaged in 1350g sealed bags, manufactured by 'Normensand' and is a naturally rounded sand high in quartz.

The coarse aggregate used in concrete mixes was a 1:1 blend of 10mm nominal and 20mm nominal crushed basalt of angular shape. The size grading was determined by sieve analysis (AS1141.11.1) and complies with the limits set out for single size aggregates in AS2758.1 and is shown in Table 7. All coarse aggregates used in concrete mixes were oven dried at 105˚C for 24 hours and stored in airtight containers until required. The particle density and water absorption of the aggregates were determined (AS1141.6.1 (2000) Methods for sampling and testing aggregates – Particle density and water absorption of coarse aggregate – weighing in water method) and are summarized in Table 6.

Table 7 Sieve analysis and fineness modulus of coarse aggregate

Sieve Size (mm)	Cumulative % retained	
	10 mm Aggregate	20 mm Aggregate
37.5	--	0.0
26.5	--	0.0
19	--	8.2
13.2	0.0	59.8
9.5	24.1	95.7
6.7	89.0	100.0
4.75	100.0	100.0
2.36	100.0	--
0.75	100.0	--
Fineness Modulus	3.13	8.6

The water absorption of the aggregates has the effect of reducing the available water for reaction with the cement. This factor is taken into account when determining the water content of concrete mixes.

The superplasticizer used in concrete mixes was a product called Sika Viscocrete® 20HE sourced from Sika Australia. It is a third generation superplasticizer, which work through steric hindrance, and was designed for the production of concrete, which have a high water demand. The water used in all concrete tests was potable tap water and in mortar tests ultra-pure water was used.

Mix Designs

Mortar mixes were designed where the GP cement binder was partially replaced by SCBA at 0, 5, 10, 15, & 20% by weight, thus focusing on the potential pozzolanic properties of SCBA. The mortar mixes for all mortar tests (pozzolanic activity, acid resistance, sulphate resistance) were determined in accordance with AS3583.6, 1995: Determination of the relative water requirement and relative strength. The amount of total binder and CEN Standard Sand was kept constant at 450±2 g and 1350±5 g respectively, however the water content varied as necessary to maintain a standard consistency (AS2701.7) as determined by the flow table test. The mix proportions and designations are shown in Table 8.

Table 8 Mortar mix proportions

Mix Designation	GP Cement (g)	SCBA (g)	CEN Standard Sand (g)	Water (g)
MControl	450.0	0	1350	225
M5	427.5	22.5	1350	235
M10	405.0	45.0	1350	243
M15	382.5	67.5	1350	256
M20	360	90.0	1350	268

The concrete control mix was designed utilizing the ACI method (American Concrete Institute 211.1-81). The parameters of the concrete were based on the manufacture of a normal weight concrete with the use of nominal size 20 mm crushed basalt aggregate and a target compressive strength of 40 mega-pascals (MPa) with a target workability of 80±10 mm slump. The estimated parameters of the control concrete design as per ACI method are shown in Table 9.

Table 9 ACI Method concrete design parameters

Parameter	Value (Kg/m^3)
Water	200
Binder	469.10
Coarse aggregate content (Kg/m^3)	1190 – 1284.5
Fine aggregate content	450 – 550
Slump	50 – 100 (mm)
Target average 28 day strength	40 (MPa)
Specified 28 day strength	25 (MPa)

Trials of the ACI designed mix resulted in the final control concrete mix. The test mixes for concrete focused on the use of the SCBA as filler where the control sand was partially replaced by SCBA at 5, 10, 15, & 20% by weight of the GP cement. The concrete testing occurred in two stages. In both stage 1 and 2 the water content was kept constant however in stage 2 superplasticizer was added by weight percentage of the GP cement and SCBA, to maintain the same workability as the control. The control and test mixes and designations for stage 1 are shown in Table 10. The stage 2 concrete mixes are the same as stage 1 except the superplasticizer amounts were adjusted by trial and are summarized in Table 11. The water/binder ratio of 0.45 was based on the achievement of the target slump in the control however after adjustments for the water absorption of the aggregates (Table 6) in the control the W/B is reduced to 0.30.

Table 10 Concrete mix proportions stage 1

SCBA Content	0 %	5 %	10 %	15 %	20 %
Mix Designation	CC	CF5	CF10	CF15	CF20
Cement (Kg/m^3)	469	469	469	469	469
Total Water (Kg/m^3)	210	210	210	210	210
Water/Binder (W/B)	0.45	0.45	0.45	0.45	0.45
Adjusted W/B	0.30	0.30	0.30	0.30	0.30
SCBA (Kg/m^3)	0	23	47	70	94
Sand (Kg/m^3)	464	441	417	394	370
Aggregate (Kg/m^3)	1198	1198	1198	1198	1198

Table 11 Stage 2 Concrete Superplasticizer (% of GP Cement and SCBA)

SCBA Content	0 %	5 %	10 %	15 %	20 %
Mix Designation	CC	SPF5	SPF10	SPF15	SPF20
Superplasticizer %	0	0.28	0.35	0.40	0.55

Manufacturing and Curing of Specimens

Mortars were mixed on an automatic bench mounted mixer 'Auto-Mortar Mixer' complying with AS2350.12 (2006, Methods of testing Portland, blended and masonry cements, Method 12: Preparation of a standard mortar and moulding of specimens). The cement was weighed and added to the stainless steel mixer bowl. For test mortars, the SCBA was weighed and added to the cement in the bowl and then stirred until homogenized. The water required was determined by mass and added to the mixer bowl followed immediately by mixing on low speed (140 r/min) for 30 s. The CEN standard sand was then added over the next 30 s followed by increasing the mixing speed to high (285 r/min) for a further 30 s. The mix was then allowed to rest for 90 s followed by another 60 s of mixing on high speed.

The moulding of specimens occurred immediately after mixing (AS2350.12). Mortar specimens for the relative strength tests were 40 mm x 40 mm x 160 mm prisms. Mortar specimens for the sulfuric acid resistance test were 50 mm cubes and sulphate resistance test specimens were 40 mm x 15 mm x 150 mm prisms. All specimens were cured in accordance with Australian Standards (AS2350.11 2006; AS2350.14, 2006) where the moulds were placed in a controlled environment room with the temperature maintained at 23±2 ˚C and the relative humidity kept at 90% for 24 hrs. Sulphate test specimens were maintained in the environment room for a total of 48 hours. Specimens were then demoulded and placed in lime-saturated water maintained at 23±2 ˚C until the time of testing.

Concrete was mixed in a 70L drum 'Creteangle®' concrete mixer. Batch mixing was performed by mass. The procedure set out in AS1012.2-1994 Methods of testing concrete, Method 2: Preparation of concrete mixes in the laboratory. The oven dried coarse aggregate was first added to the drum mixer followed by the natural sand. As the test was focusing on the filler effects of SCBA, it was added at the same time as the sand. Enough of the mix water was added at this stage to wet the SCBA and, fine and coarse aggregates. Where superplasticizer was used it was first added to the mix water and stirred for 30 s. Cement was then added to the mixer after a period of 30s of mixing. Mixing then commenced for 2 min in which time the remaining mix water was added. The concrete mix was then allowed to rest for 2 min followed by further mixing for 2 minutes. At this time the slump was then measured and if correct the slump sample was returned to the drum and the batch mixed for a further 2 minutes.

The moulding of the concrete specimens occurred within 20 minutes after mixing for tests on the hardened properties of concrete. Compressive strength specimens were cast into 100 mm x 200 mm cylindrical moulds and kept covered in the laboratory for 24 hours at 23±2 ˚C for the initial curing period, after which time the specimens were demoulded and placed into the curing tank in lime saturated water maintained at 23±2 ˚C (Figure). Flexural strength test specimens were cast into beam moulds 100 mm x 100 mm x 350 mm. These beams were then kept in the moulds for a further 24 hours but placed into the curing tank. All specimens were then kept in the curing tank until the time of testing .

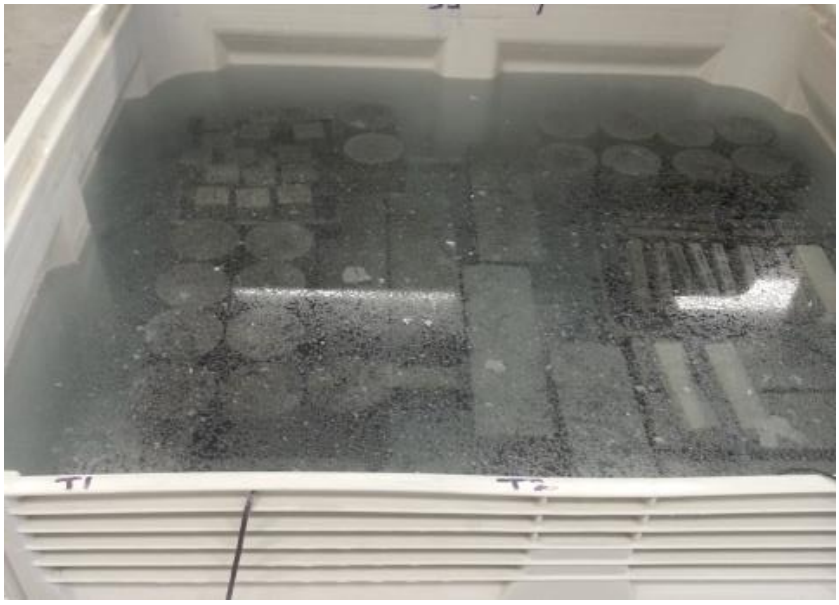

Figure 6 Concrete and mortar specimens in the lime saturated curing tank.

Concrete Testing regime and Methodology

Mortar Flow test

Relative water requirements of test mortars were determined by the flow table test. The flow table used in the tests was an automatic table that dropped the table 25 times in 15 s through a height of 12 mm (AS2701). Fresh mortar mix was cast into the conical mould centered on the flow table (Figure 7). The mould was lifted off and the table allowed to drop thus spreading the mortar into a flattened pat (Figure 8). The initial diameter of the moulded mortar (D_1) and the final diameter (D_2) of the mortar were used to calculate the flow (F) as a percentage (Equation 5).

$$F = \frac{D_1 - D_2}{D_1} \; x \; 100$$

Equation 5

Where F = flow, in percent, D2 = the average of 4 determinations of the diameter after flowing, (mm) and D1 = the internal diameter of the base of the mould, (mm). The target flow for standard consistency of blended cement mortars was 110±5 %. The relative water requirement was then calculated using equation

$$RW = \frac{m_t}{m_c} \; x \; 100$$

Equation 6

Where

RW = relative water requirement (%)

mt = water in test mortar (g)
mc = water in control mortar (g)

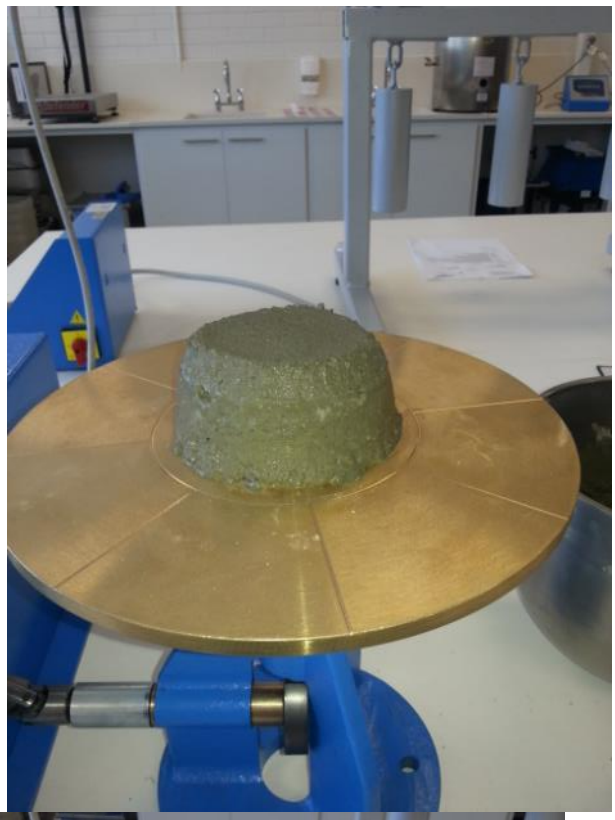

Figure 7 Flow table test. Mortar sample before flow.

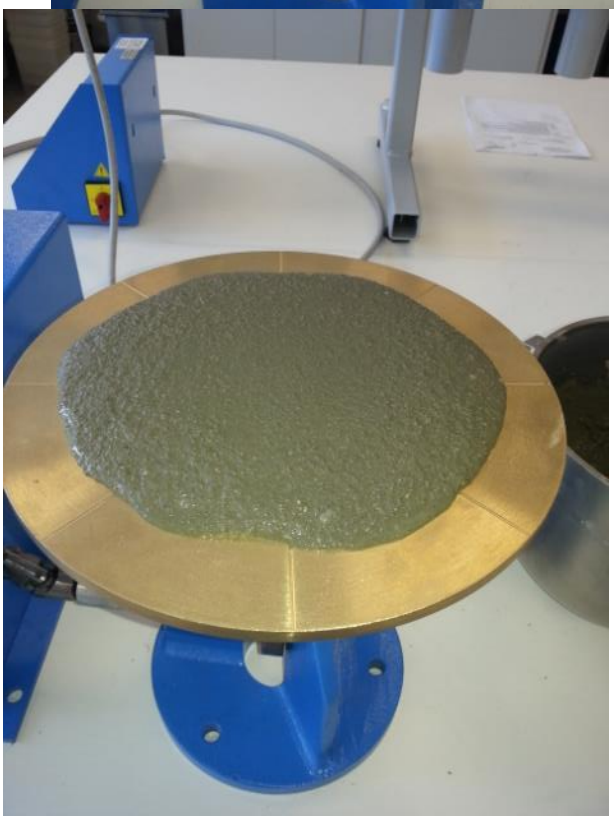

Figure 8 Flow table test. Mortar sample after flowing.

Pozzolanic Activity

For the determination of the pozzolanic index the relative strength of test mortars were tested at age 28 days. One compressive strength test consisted of 3 specimens with a strength determination at each end of the prism (Figure 9) resulting in an average strength based on the 6 strengths readings obtained. The relative strength was then calculated using:

$$(R_{28}) = \frac{T_{28}}{C_{28}}\ x\ 100$$

Equation 7

Where

T_{28} = the mean compressive strength of the test mortars at 28 days and,
C_{28} = the mean compressive strength of the control mortars at 28 days.

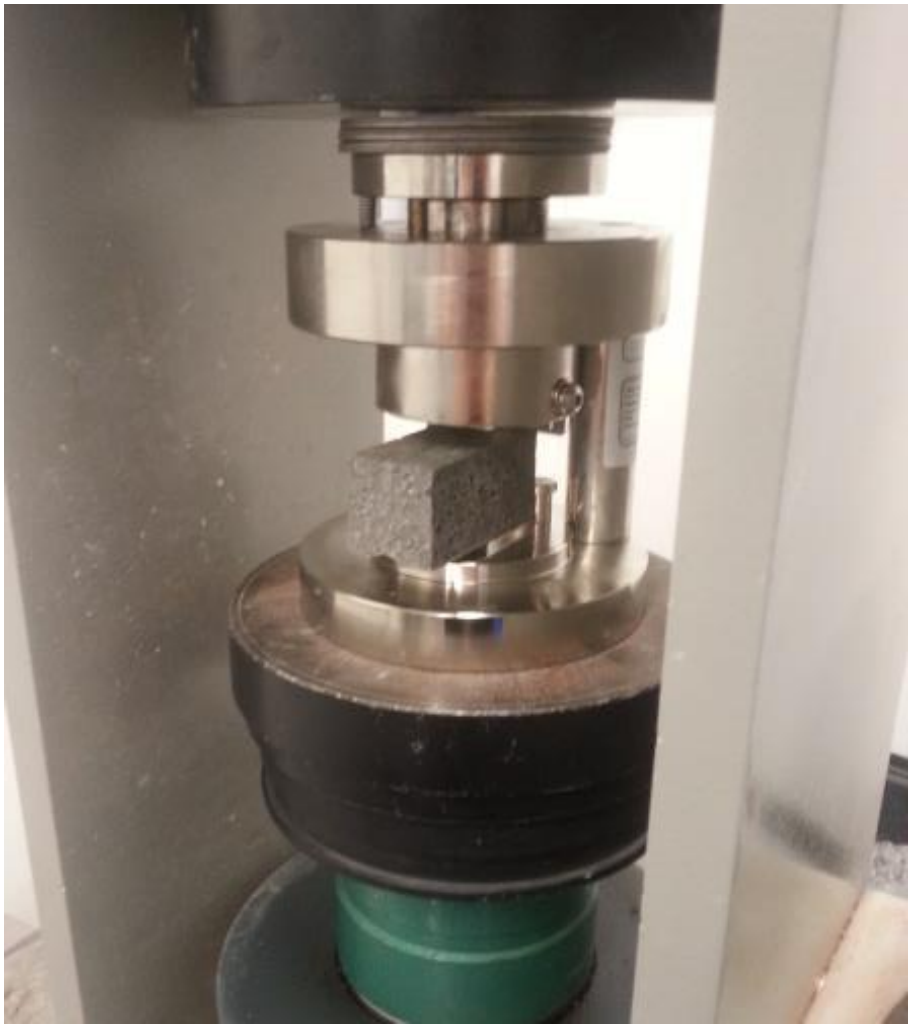

***Figure** 9 Mortar bar in compression jig.*

Sulphuric Acid Test

A total of 60 cube specimens were prepared, 6 of each of the 5 mortar mixes. Three specimens of each mix were treated as controls and were placed into lime-saturated water for the duration of the test. The remaining 6 specimens of each mortar mix were placed into a 1% sulphuric acid solution at age 7 days. The cube specimens were weighed in a saturated surface dry (SSD) condition before immersion. The solution to solid volume ratio was 4:1. The solution was refreshed every 2 weeks. Specimens were tested visually for signs of acid attack and for weight change at 2-week intervals. Specimens were first treated for weight change

measurements by immersion in ultra-pure water for 4 hours and then weighed in a saturated surface dry condition. The average compressive strengths of 3 specimens after 28 days and of 3 specimens at 90 days of exposure to the acid solution were determined and compared to control specimens of the same age. This test is ongoing.

Sulphate Exposure Test

The durability of test mortars in sulphate solution were evaluated based on the change in length of mortar bars exposed to a sulphate solution. Control, M10 and M20 specimens were tested. Each test comprised of 3 bars that were placed in 0.352 M sodium sulphate (Na_2SO_4) solution in a liquid to specimen volume ration of 4:1, at age 7 days. The bar lengths were measured at age 7 days before immersion in the Na_2SO_4 solution and every 2 weeks for a total period of 16 weeks. The solution was refreshed at 2-week intervals. This test is still ongoing.

Concrete Workability

The workability of fresh concrete mixes was determined in accordance with AS1012.3.1 (Method 3.1: Determination of properties related to the consistency of concrete – Slump test.). Concrete was scooped from the mixer into the slump cone in approximately 3 layers until full and tamped with a rod 25 times for each layer. The cone (300 mm (height) x 200 mm x 100 mm) was then lifted away in a vertical direction allowing the concrete mix to slump. The slump was then measured (mm) from the original height of the cone to the new height of the concrete mix.

Compressive Strength

A single determination of the compressive strength was considered to be the average of the compressive strengths of 3, 100 mm x 200 mm cylinders from the same batch of concrete. The compressive strength was determined at age 7, 14, 28, and 56 days for all mixes. The compression-testing machine was a 'Controls' unit complying with AS2193. Specimens were capped with a rubber capping system and placed in the machine (Figure 9). Force was applied to the specimen at a rate of 20±2 MPa/min until failure of the sample. The compressive strength was recorded in MPa.

Flexural Strength

A single determination of the flexural strength was considered to be the average of the flexural strength of 2 beam specimens. The flexural strength was determined at age 7, 28 and 90 days. The beams were placed in the compression test machine into a flexure beam jig. The load was set to 167 kN/s and applied until failure. The flexural strength was then calculated as set out in AS1012.11 (2000, Methods of testing concrete, Method 11: Determination of the modulus of rupture.) and shown in Equation 8:

$$f_{cf} = \frac{PL\,(1000)}{BD^2}$$

Equation 8

Where

f_{cf} = modulus of rupture or flexural strength (MPa)
P = maximum applied force (kN)
L = span length (mm)
B = average width of specimen at the section of failure (mm)
D = average depth of specimen at the section of failure (mm)

Zeolites synthesis conditions

Factorial design

In this study factorial design was used for screening types of crystal formed in relation to the factors. In each complete replication of an experiment, all possible combinations of the levels of the factors were explored. When a change in one factor causes change in effect it is called main effect. Factors are set at high and low levels with a medium centre point level. Coding reduces the range of each factor to a common scale, generally -1 to +1, regardless of its relative magnitude.

3.2.Zeolites Formation, characterisation by (XRD) and optimisation

Five factors were considered in this experimental work, they are temperature, molarity of the sodium hydroxide solution, Time of reaction, solid to liquid ratio (amount of fly ash added to the sodium hydroxide solution) and Aluminium to silica (Al:Si) ratio. The 5 factors were replicated three times, except for the centre point that was replicated more than 3 times as needed for the robustness of the statistical analysis (Anderson & Whitcomb). (Table 1) was established to determine the statistical probability of an optimum design based on the analysis of determined measures, such as silica reduction, zeolite type, zeolite functionality, the conditions of formation for the most desirable materials is determined with subsequent optimisation matrix.

Three batches of bagasse fly ash from the Harwood plant were homogenised to provide sufficient uniform material to conduct all the zeolitisation experiments, and to provide a representative average of bagasse fly ash. Moisture content was determined on a 50 g subsample, dried at 60°C for 24 hours yields moisture content is 37.5%. Homogenisation of the fly ash was done with the mixing of a number of samples with similar parameters in a rotary mixing tub for 48 hours. The mixing is to breakdown larger particles of the fly ash into smaller parts with more surface area exposed to the solution during chemical reactions.

Hydrothermal zeolitatisation was performed in 65 mL Teflon bottles housed within a sealed high tensile steel pressure vessel; pressure vessels are capable of withstanding 300°C and 40 atmospheres of pressure before seals rupture. The fly ash was added to a constant volume (20 mL) of predetermined concentration of NaOH (Table 12). Three replicates of each mixture were made to account for in sample variability. Pressure vessels were then randomly placed within the oven for the predetermined time and allowed to cool down to room temperature (23°C) before vessels were opened and contents were transferred to a centrifuge tube and spun at 4500 rpm for ten minutes, and the excess liquid decanted and saved for further analysis. Solids were then washed with 25 mL of Milli-Q water, shaken for 15 seconds by hand and then for 30 seconds on vortex mixer at 2200 RPM, before being centrifuged again at 4500 rpm for ten minutes, and supernatants decanted.

Results from the factorial design showed that after by 72 hr that the reactions had come to an end and that the solid to liquid ratio had no influence on the yield. The analysis also showed that temperature of maximum yield was possibly less than the minimum value used in Table 12. Hence from the analysis of Table 12 a second more refined factorial design was based around the predicted optimum yield, of temperature of 70 ± 5°C, an Al:Si ratio of 0.6± 0.05, and an alkali molarity of 5 ± 0.5 M (Table 13).

Table 12. Factorial design with 5 factors to account for the Al limitation of the raw fly ash in 1:1 zeolite-X and zeolite-A formations

Temperature °C	Molarity of NaOH	Time Hrs	Solid:Liquid Ratio	Al:Si Ratio	Factorial Design Coding
75	5	72	1/3	1/5	-1,1,1,-1,-1

105	5	24	1/3	1/5	1,1,-1,-1,-1
75	3	24	1/5	2	-1,-1,-1,1,1
105	3	72	1/5	1/5	1,-1,1,1,-1
105	5	72	1/5	1/5	1,1,1,1,-1
105	5	24	1/5	2	1,1,-1,1,1
75	3	24	1/3	1/5	-1,-1,-1,-1,-1
105	3	24	1/3	1/5	1,-1,-1,-1,-1
105	5	72	1/3	1/5	1,1,1,-1,-1
105	5	72	1/3	2	1,1,1,-1,1
75	5	24	1/5	1/5	-1,1,-1,1,-1
75	5	24	1/3	1/5	-1,1,-1,-1,-1
105	3	24	1/5	2	1,-1,-1,1,1
75	3	72	1/5	2	-1,-1,1,1,1
105	5	24	1/3	2	1,1,-1,-1,1
75	3	72	1/5	1/5	-1,-1,1,1,-1
75	5	72	1/5	1/5	-1,1,1,1,-1
105	3	24	1/3	2	1,-1,-1,-1,1
75	5	24	1/3	2	-1,1,-1,-1,1
75	3	72	1/3	2	-1,-1,1,-1,1
75	5	24	1/5	2	-1,1,-1,1,1
75	5	72	1/3	2	-1,1,1,-1,1
105	3	24	1/5	1/5	1,-1,-1,1,-1
105	3	72	1/3	1/5	1,-1,1,-1,-1
105	3	72	1/3	2	1,-1,1,-1,1
105	5	72	1/5	2	1,1,1,1,1
105	5	24	1/5	1/5	1,1,-1,1,-1
105	3	72	1/5	2	1,-1,1,1,1
75	3	72	1/3	1/5	-1,-1,1,-1,-1
75	5	72	1/5	2	-1,1,1,1,1
75	3	24	1/5	1/5	-1,-1,-1,1,-1
75	3	24	1/3	2	-1,-1,-1,-1,1
90	4	48	1/4	1	0,0,0,0,0

Solids from each experimental sample were split in two, with one subsample for visualisation by SEM and the other for XRD analysis. XRD materials were prepared for analysis by micronizing. A 7 ml aliquot of MilliQ water was added to solid samples, micronised for five minutes in a McCrone Micronising Mill as a wet paste. Wet grinding is safer for handling the sample and results in the right size fineness for analysis with X-ray diffraction. XRD analysis identified any formed zeolite and semi-quantification, using the area calculation method, determined the conversion rate of the new materials.

The data were analysed using Design-Expert™ factorial design software for optimisation of zeolite production. A new matrix is built, if needed, for refining the optimisation, the experimental will be re-run based on narrower maximal and minimal levels and the data re-analysed for final optimisation.

Table 13. Factorial design with 3 factors to account for the Al limitation of the raw fly ash in 1:1 zeolite-X and zeolite-A formations at 72 hrs digestion

Temperature °C	Molarity of NaOH	Al:Si Ratio	Factorial Design Coding

65	4.5	0.55	-1,-1,-1
75	4.5	0.55	1,-1,-1
75	5.5	0.55	1,1,-1
65	5.5	0.55	-1,1,-1
75	4.5	0.65	1,-1,1
65	4.5	0.65	-1,-1,1
75	5.5	0.65	1,1,1
65	5.5	0.65	-1,1,1
70	5	0.6	0,0,0

Scanning Electron Microscope (SEM)

This study uses high-energy electrons EVOLS 15 (SEM) to generate a variety of signals at the surface of solid specimens in order to assess the morphology or the external shape of the aggregate of zeolite crystal that appears as an entity under the microscope. SEM allows high-resolution visualisation of materials. The morphology indicates the size of the crystals and dimensions and how well formed. Variation in the crystalline structure and orientation of the examined materials, determined by diffracted backscattered electrons, could also be detected. Chemical composition is also determined for a number of elements.

Surface Area Determinations

A Micromeritics 3Flex was used to determine the zeolite-composite porosity using nitrogen porosimetry (N_2; bath temperature: 77.3 K; equilibration interval: 40 seconds) to give BET and Langmuir surface areas. Hence a series of equilibrations were conducted to determine the zeolite-composite's adsorption capacity as per the linearized Langmuir isotherm equation {Gök, 2008 #484}:

$$1/q_e = (1/q_m.K_L) \,.\, (1/C_e) + (1/q_m)$$

Equation 9

where; C_e is the equilibrium concentration (mg/L), q_e is the amount removed to the solid (mg/g), q_m is the maximum saturation capacity at the isotherm pH (mg/g) and K_L can be determined from the intercept in a plot of $1/C_e$ against$1/q_e$.

Kinetic Determinations

Time batch exchange experiments for Cu, Zn and a mixed Cu/Zn solutions were run at 2, 4, 6, 8, 24, 48, 96, 192 and 384 hours with nine initial concentrations (C_0) made from 1M Cu and Zn stocks of analytical lab grade copper nitrate and zinc nitrate (Table 14). The combined copper and zinc concentrations were of comparable amounts to the total metal concentrations as in single metal adsorption.

Table 14. Initial concentrations (C_0) of copper only, zinc only and mixed copper and zinc solutions.

Solution	Concentration (C_0) (mg/L)							
Cu only	9.4	18.8	38.0	78.3	149.1	221.7	313.4	402.3
Zn only	9.0	18.4	36.3	73.9	146.4	210.4	300.5	414.2
Cu in Cu/Zn	3.1	5.8	12.0	24.5	51.3	100.3	154.7	217.7
Zn in Cu/Zn	3.1	5.9	11.8	23.5	48.8	95.5	152.4	202.2

All adsorption experiments were conducted in 50 mL polypropylene centrifuge tubes with a loading of 1 g of SCBA zeolite-composite and 40 mL of sorption fluid (25g/L). Solutions were maintained 3 times a day to the target pH 5, (the isoelectric point (IEP)) by adding small quantities of 4M HNO_3 or NaOH. The pH was monitored using TPS 901-PH pH electrode calibrated daily using a 2-point calibration in pH 4 and pH 7 buffer solutions. At the scheduled time 3 replicate tubes for each concentration were centrifuged at 3500 rpm for 10 minutes to settle solids and decant liquids. Control tubes of different metal solutions without adsorbent were conducted to determine the adsorption to the polypropylene tubes.

After decanting all metal concentrations were adjusted to pH <1 with a drop of conc. HNO_3, filtered to 0.22µm, before analysis on a Environmental Aanalysis Labortory's (EAL) Perkin Elmer NexION 300D Inductively Coupled Plasma - Mass Spectrometry (ICPMS) that uses a Universal Cell in KED (Kinetic Energy Discrimination) mode to reduce polyatomic interferences. The EAL is full accredited by the National Association of Testing Authorities, Australia (NATA) using the accredited method W32 Salts and Metals by ICPMS, which references to method 3125 in APHA (2012). Experimental QA/QC for ICP-MS analyses were estimated by submitting blanks and standard solutions of known concentration at a rate of 1/20 for blanks, and 1/20 for standard solutions. The adsorption capacity of the SCBA zeolite-composite adsorbent (mg of each metal per g of adsorbent) was determined by calculating the mass (mg) of each metal adsorbed and dividing it by the weight (g) of the adsorbent for each different initial concentration (mg/L). The equilibrium sorption capacity (q_e, mg/g) {Arias, 2009 #487} and the removal ratio (R, %) {Wu, 2006 #421} for metal were determined using equations:

$$q_e = (C_0-C_e) * V / m$$

Equation 10

and

$$R= (C_0-C_e)/C_0* 100\%$$

Equation 11

where; C_0 is the initial metal concentration (mg/L); C_e is the concentration (mg/L) of the metal at equilibrium time; m is the mass (g/L) of the adsorbent and V is the volume (L) of the metal solution.

Kinetic models

Linearized forms of the pseudo-first-order or Lagergren kinetic model (1); a pseudo-second-order PSO model (2); and the Elovich model (3) were used to assess the removal of copper or zinc from the solution. In addition, the Weber and Morris linearized intra-particle diffusion model (4) determined the thickness of the diffusion layer C and the K_{id} (mg/g . $hour^{1/2}$) intra-particle diffusion.

Concrete Results and Discussion

Carbon Content

The black color of the ash is likely due to the presence of carbon. The LECO Carbon analysis reports the carbon content as 7.15% mass, which indicates the presence of a carbon rich feedstock like woodchips or inadequate combustion (Paya et al., 2002; Cordeiro 2009). The requirements for a fly ash to be added to concrete in Australia is that the combustible material (loss on ignition, LOI) be less than 6% (AS3583.3). This SCBA falls just outside this range however it has been shown that SCBA with high LOI (8.16%) can still form blended cements concretes with satisfactory compressive strengths (Chuslip et al., 2009).

Amorphous content

The XRD analysis results Figure , which show the shallow broad hump indicative of amorphous content, and the strong peak, which correlates to quartz content, indicate that there is limited pozzolanic activity. Combustion conditions influence the crystalline content due to phase changes occurring at increasing temperatures. Uncontrolled burning and high temperatures (over 800 ˚C) contribute to high crystalline phases in SCBA (Cordeiro, 2009; Clark et al., 2012). It has been suggested that the ideal temperature for high amorphous content is 600 ˚C (Cordeiro, 2009).

Relative Strength and Water Requirement of Mortars with SCBA.

The flows of the test mortars were acceptable when they were within 3 units of the control mortar, which is 107 % and is shown in Table 12.

Table 12 Flows and relative water requirement of test mortars

Mortar mix	SCBA (wt %)	Flow %
MControl	0	107
M5	5	108
M10	10	108
M15	15	105
M20	20	109

The relative water requirements increased with increasing SCBA as is depicted in Figure .

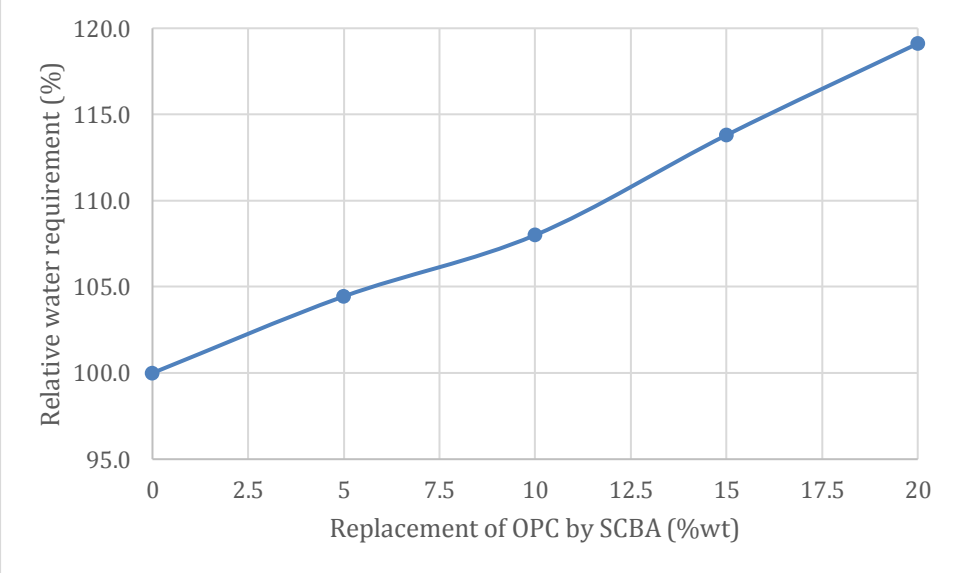

Figure 10 Relative water requirement of test mortars containing 0, 5, 10, 15 & 20% SCBA

The average compressive strength of mortars decreased as the SCBA content increased, however it can be seen there was no change in the average strength between 10 % and 15 % SCBA (Figure).

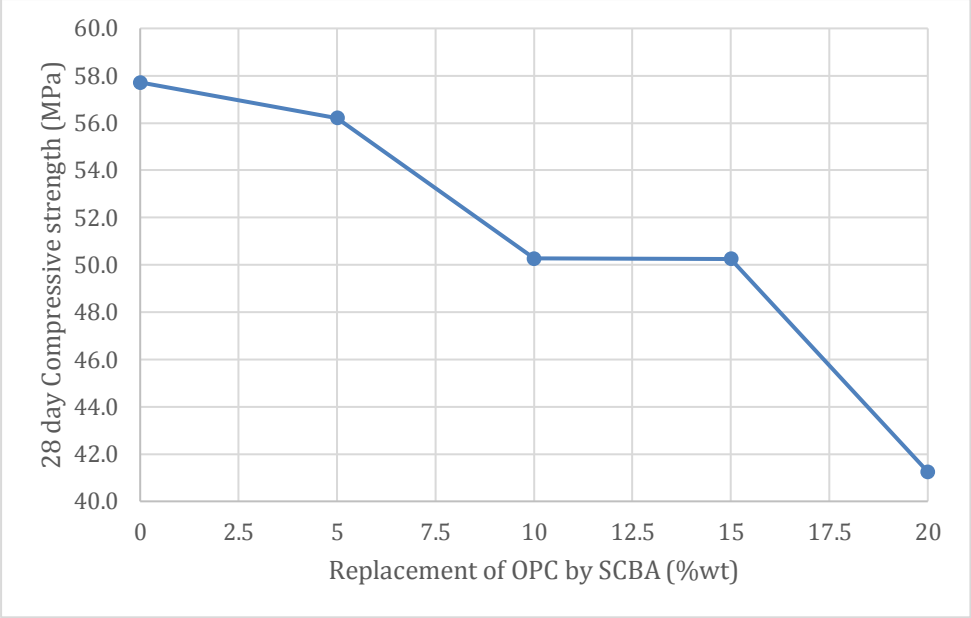

Figure 11 The 28 day compressive strengths of mortar bars with SCBA replacing OPC at 0, 5, 10, 15, & 20%.

The relative strength of the test mortars at 28 days thus also decreased with increasing SCBA as is shown in Table 13.

Table 13 Pozzolanic Index (via Equation 7*) of test mortars with SCBA replacing OPC at 0, 5, 10, 15 & 20% (wt).*

SCBA content (% wt)	Pozzolanic Index (%)
0	100
5	97
10	87
15	87
20	72

The minimum pozzolanic index or relative strength required to classify as a pozzolan is 75% (AS3582.1 – 1998; AS3583.6 – 1995; ASTM C618 – 05, 2005). Our results show that for mixes M5, M10, & M15 the pozzolanic indexes are all above 75%, however M20 is 72%, falling below the required relative strength. This would seem to indicate that the SCBA contribution to strength development is not solely from pozzolanic reactivity but from a pore filler effect. However it should be noted that it is widely accepted that increased water in concrete and mortar will result in reduced strengths. The increase seen here in relative water requirements indicates that the loss of strength cannot be attributed solely to the addition of SCBA and that there is some pozzolanic effect is occurring. The results of the relative strength and relative water test do seem to suggest that while the SCBA has a limited pozzolanic activity it can still benefit mortar and concrete through the filler effect by replacing fine sand.

Sulphuric Acid Test

The weight of the test mortars showed an average slight initial increase in at 14 days and 28 days, whereas the control mortar showed an average slight decrease in weight at both 14 and 28 days. At both 14 and 28 days the visual observations show that the control mortar looks the most susceptible to acid attack with more exposed aggregate Figure 122. The remaining specimens show signs of salt buildup on the surface.

Weight gain in samples (Table 17) may be explained by the formation of gypsum or ettringite, which are both expansive products. The formation occurs in a 2-step reaction in which gypsum is first formed by the reaction

of lime and H_2SO_4. The gypsum then reacts with any aqueous C_3A (from the cement) to form ettringite. However the weight gain in the mortars is minimal and may be due to greater moisture contents or from the problems associated with achieving an identical saturated condition at each test age.

Table 14 Weight change of mortars exposed to sulphuric acid solution

	Average weight change of mortars (%)				
Exposure Time (days)	MControl	M5	M10	M15	M20
14	-1.1	+0.8	+0.5	+0.6	+0.6
28	-1.9	+0.2	+0.2	+0.1	+0.6

Note: - indicates weight loss; + indicates weight gain

MControl	M5	M10	M15	M20

No Acid exposure

14 days H_2SO_4 exposure

28 days H_2SO_4 exposure

Figure 12 Images of mortars with 0, 5, 10, 15, & 20% SCBA content exposed to H_2SO_4 solution at 0 (top), 14 (middle), and 28 (bottom) days.

The visual inspection shows a general increase in resistance to acid attack in test mortars with increasing SCBA content (Figure 12). The 28 day mortars MControl, M5 and M10 all have gravel showing through, particularly MControl. M15 and M20 look fairly smooth and intact. At 28 days of immersion in acid solution the mortars were crushed to determine the compressive strengths. The compressive strengths were compared to

reference mortars of the same age and the same mix but with no acid exposure. The results (Figure) show that where no SCBA was present, as in MControl, the loss in strength was greatest at over 50% loss. There was a general decrease in the loss of strength as the SCBA content increased and in fact at 20% SCBA there was an actual increase in strength by 2%. This minimal increase is the results of averages and helps to confirm that the incorporation of SCBA will increase the sulphuric acid resistance in concretes and mortars.

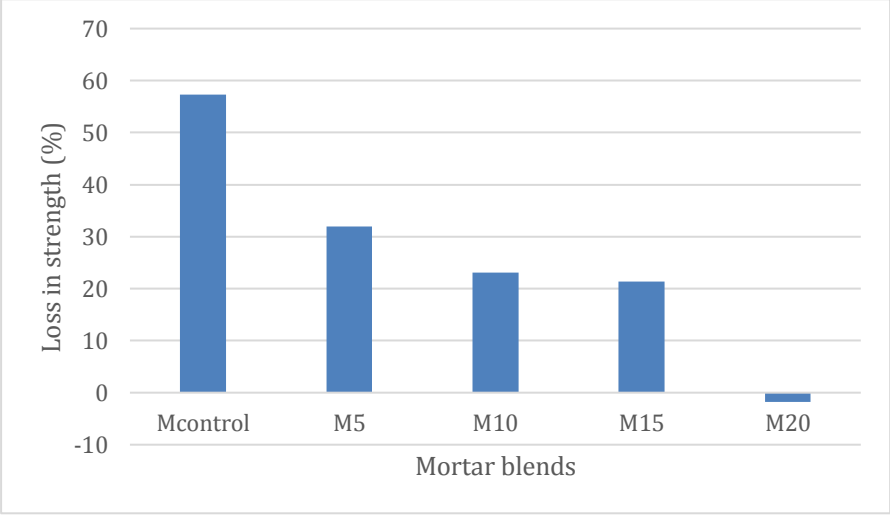

Figure 13. Loss in 28 day compressive strength of test mortars compared to test mortars not exposed to acid.

In comparison of the test mortars exposed to sulphuric acid to the Mcontrol not exposed to acid the loss of strength is still greatest in the mortar with no SCBA content. The strength loss of the blended mortars was the least in M10, however all blends showed a similar amount of strength loss at around 24- 30% (Figure).

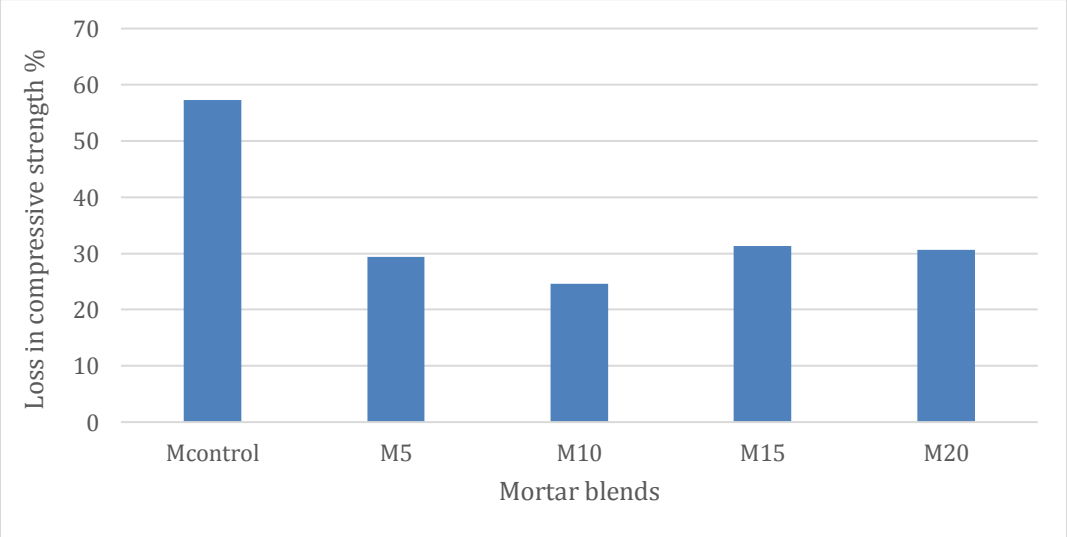

Figure 14 Strength of Test Mortars After 28 days Exposure to Acid Compared to Control Mortar with No Acid Exposure

The results of the sulfuric acid test show much promise for the incorporation of SCBA in concretes for areas that are exposed to acidic conditions and that as little as 5% replacement levels can greatly improve the acid resistance of concretes and mortars

Sulphate Resistance

Sulphate is known to attack concrete whereby the sulphate interacts with available lime in the concrete matrix and forms the expansive products ettringite and gypsum leading to swelling, cracking and spalling. A pozzolan can effectively mop up the free lime and thus potentially increase the resistance to sulphate attack. Previous studies incorporating SCBA have shown that strength loss and weight loss have been reduced compared to the reference mortar when exposed to sodium sulphate solution (Shafiq et al., 2014). The requirements for a cement to be classified as a moderate sulphate resistant cement according to ASTM C 1157-10, Standard Performance Specification for Hydraulic Cement, is that the expansion be less than 0.10% at 6 months. For a high sulphate resistant cement the code requires that the expansion be less than 0.05% at 6 months.

This ongoing test shows (Table 15) that at 2 weeks of exposure to sulphate solution that the average expansion is minimal for both M10 and M20. The mortars showed no signs of deformation or warping from this exposure time (Figure 15). However, further test results are required pending exposure time to fully characterize the sulphate resistance of SCBA in mortars.

Table 15. Expansion (%) in Mortars with SCBA replacing OPC exposed to sulphate solution for 14 days.

	Control	M10	M20
% Expansion	0.009	0.014	0.029

Figure 15. Mortars with 20% (top) 10% (middle) and 0 %(bottom) SCBA replacing OPC exposed to sulphate solution at 2weeks.

Concrete workability

The slump of concrete mixes decreased as SCBA increased where superplasticizer was not added and the total water remained constant at 210 Kg/m^3 as shown in Figure 1. At 5 % replacement the slump was within the ACI design parameters of between 50mm and 100mm however not within the target range of the control. The slump reduced to zero for additions of SCBA at 15% and 20% rendering the concrete unworkable. The 20% mixture was partially dry and mixing was not uniform. Increase in water demand has been reported previously and is likely due to high surface area and porous nature of the fine particles (Sales & Lima, 2010; Chuslip, 2009).

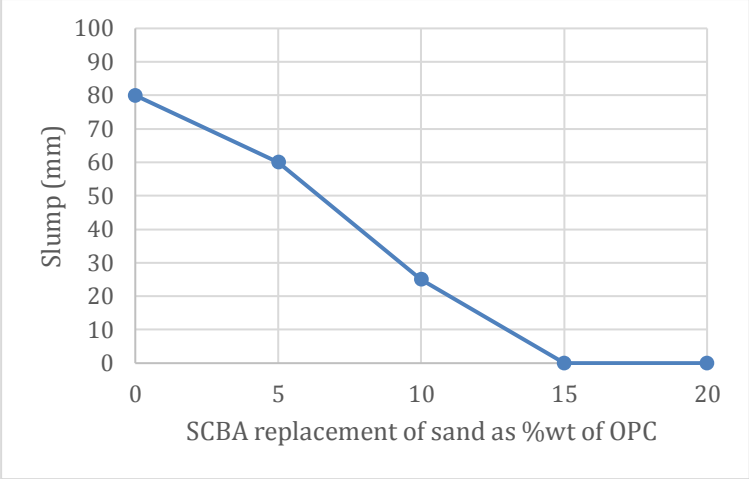

Figure 1 Slump of concrete mixes with a fixed water content and increasing SCBA content

The superplasticizer content required to maintain a slump of 80±10 mm, also increased as the SCBA content increased Figure 2. The addition of superplasticizer had a dramatic effect on the workability of the fresh blended concretes. Typical dosages of third generation superplasticizers are within 0.1 to 1% by mass of the binder. The superplasticizers used in the SCBA blended cements ranged from 0.28 to 0.55% of the weight of the binder and SCBA combined. In terms of just the SCBA the superplasticizer content ranged from 3 – 6%. The results of using the superplasticizer show that the desired workability is obtainable however the dosage range is greater for SCBA than just OPC binders again most likely due to the large surface area and porosity of the SCBA particles.

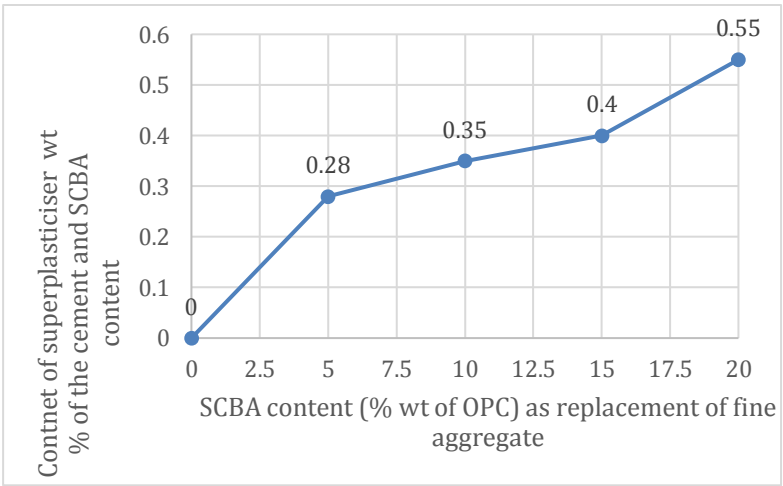

Figure 2. The Superplasticizer content required to maintain 80 ± 10 mm slump in concrete incorporating SCBA

Concrete Compressive Strength

The compressive strengths of 100 mm x 200 mm cylinders made with increasing amounts of SCBA show an increase in strength for all mixes with increasing age. The SCBA supplemented concretes show increased strength compared to the control concrete at each age except for the 7 day CF15 mix which is only less by .2 MPa. The CF5 and CF10 show the most consistent and best strengths and the 56 day CF10 obtained the highest strength overall at 65.4 MPa Figure 3. All of the mixes using SCBA as sand replacement were above the target strength of 40 MPa. These results are positive for the incorporation of SCBA in concrete. It would seem that in the absence of superplasticizer the ideal replacement level is 5%.

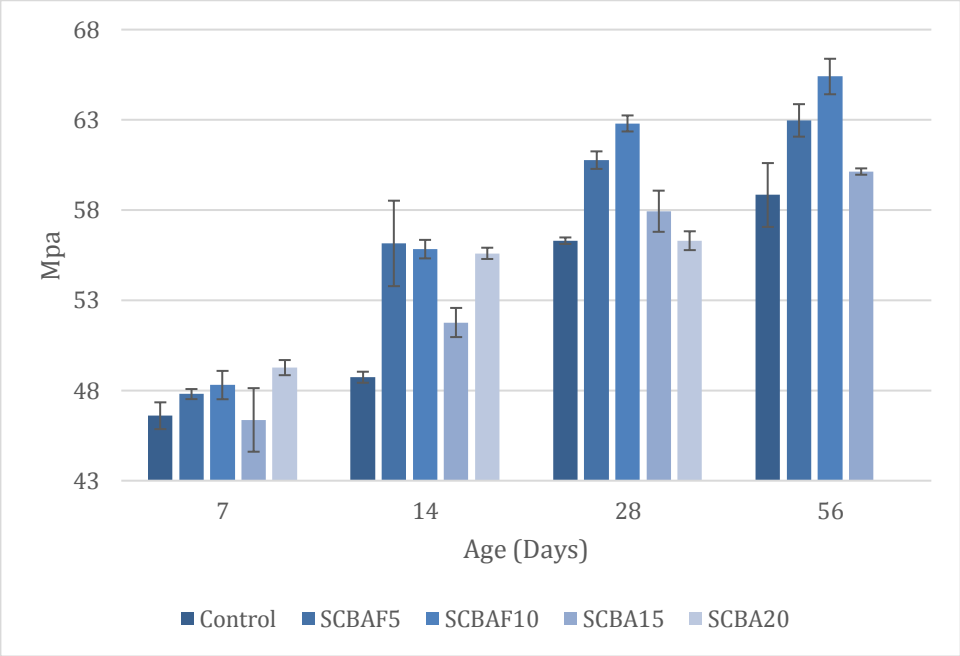

Figure 3 Compressive Strengths of Concrete Cylinders with SCBA Replacing Sand (%wt OPC)

The compressive strength of concrete supplemented with SCBA and superplasticizer show the best 7 and 14 day strengths being achieved with the 20% SCBA mix, SPF20 (Figure 4). The best 28 day strength was achieved by the control concrete which was marginally higher than the compressive strength of the SPF20 test concrete. However, all mixes increased in strength with increasing age as is expected in concretes.

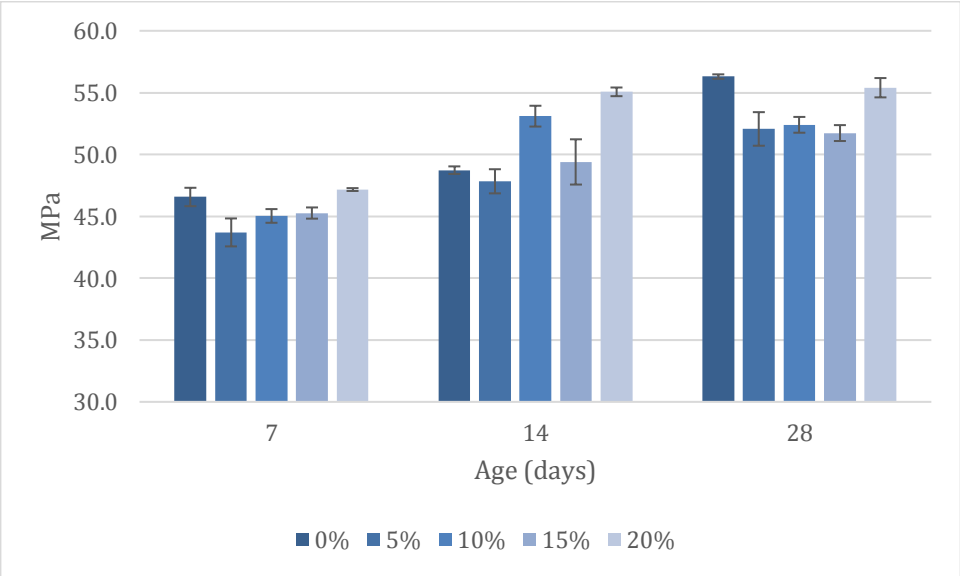

Figure 4 Compressive Strengths of Concrete Cylinders with SCBA and Superplasticizer

At 28 day strength, the concrete with superplasticizer shows a slight decrease of about 9 MPa at all ages in the compressive strength compared to the concrete of the same age but without superplasticizer Figure 20, , except for the 20% SCBA concretes whose strengths were 56 MPa (CF20) and 55 MPa (SPF20). However, the concretes with superplasticizer all achieved strengths above the target 40 MPa and with the same workability of the control. This implies that the optimal replacement level may be as much as 20% when superplasticizer

is incorporated. The slight loss in strength due to superplasticizer is a tradeoff for the increase in workability and is well documented.

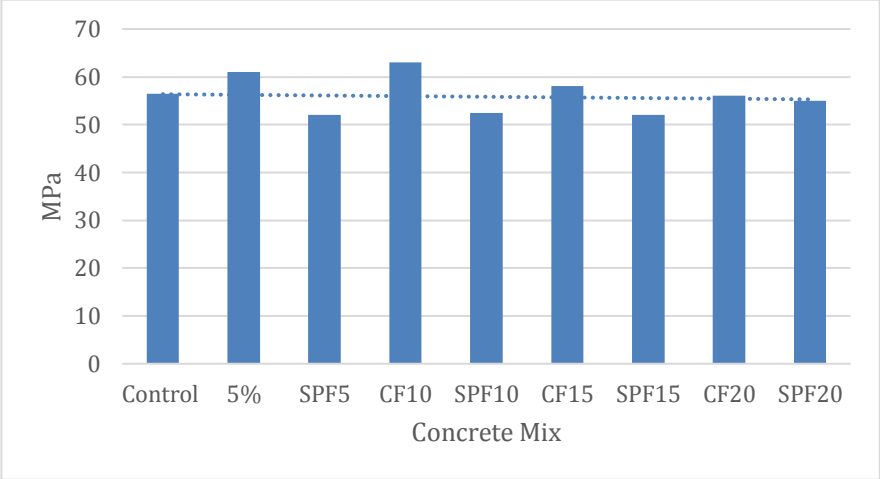

Figure 20, 28-Day Compressive Strength of Concrete Showing the Effect of SuperPlasticiser at 0, 5, 10, & 15 % (wt of OPC).

Flexural Strength of Concrete

The flexural strength of the control and test concretes is in the range of 8% to 10% of the corresponding compressive strength for all tests Figure . The flexural strength shows an increase with age with 10% SCBA at 28 days showing the highest strength however also the lowest at 7 days. The flexural strength is a measure of the capacity of the concrete to bend before failure. Flexural strengths of concrete are usually about 10% of the compressive strengths. The results indicate that addition of SCBA achieves satisfactory flexural strengths but does not provide any significant increase in flexural strengths.

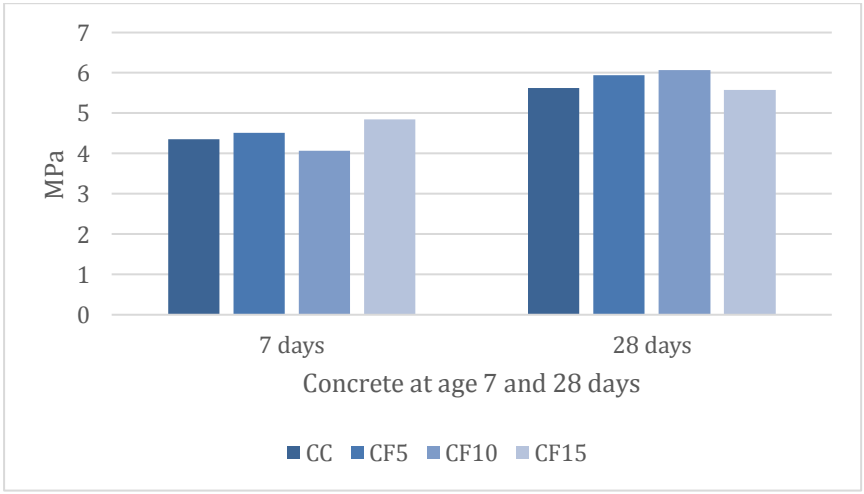

Figure 21 Early Age Flexural Strength of Concrete with SCBA at 0, 5, 10, & 15 % (wt of OPC).

The flexural strength of CF20 is not reported as the mix was too dry and the workability was too low to allow proper compaction into the mould. The flexural strength of concrete beams for all superplasticizer blends at 7 and 28 days is shown in Figure 22 Early age flexural strength of concrete beams with SCBA replacing sand (%wt OPC) with superplasticizer.. It can be seen that the flexural strengths did not greatly differ from the flexural strength of the control concrete. All superplasticizer concrete beams reported about 10% of the compressive strength of the corresponding blend in flexural strength. This is again in the typical range for flexural strengths of concrete.

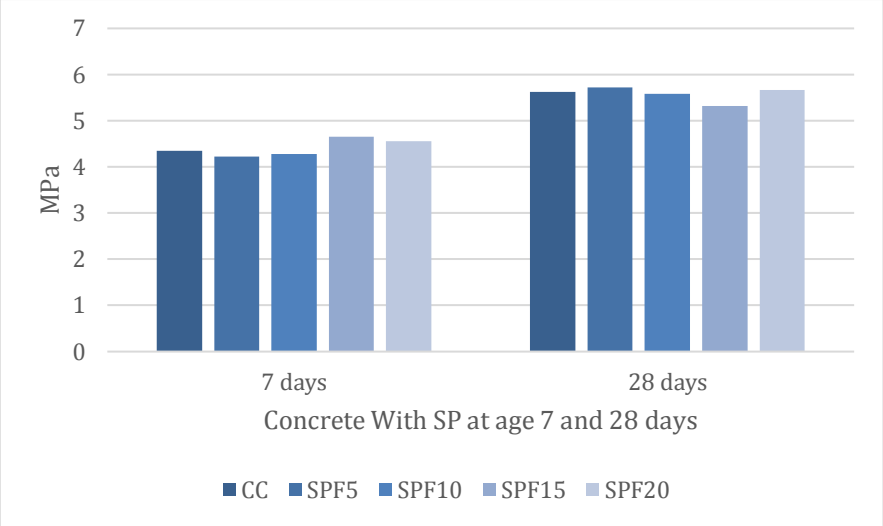

Figure 22 Early age flexural strength of concrete beams with SCBA replacing sand (%wt OPC) with superplasticizer.

Zeolite Results and Discussion

Optimisation, of the zeolitisation of the SCBA, indicate that characterising by X-ray diffraction (XRD) shows a maximum of about average yield 50% zeolite-X with silica. XRD also confirmed the presence of some Zeolite-A and smaller amounts of a variety of zeolitic crystals including small amounts of sodalite crystals, which are a by-product of the synthesis. Scanning Electron microscope (SEM) confirms the covering of the silica core of the very vast majority of particles by a layer by zeolite-X. A number of measurements of the thickness of the zeolite coverage were taken using SEM measurements tools demonstrating a thickness of 1-2 µm. The SCBA particle's size was determined qualitatively to be mostly 10 to 20 µm as observed under SEM (Figure 23).

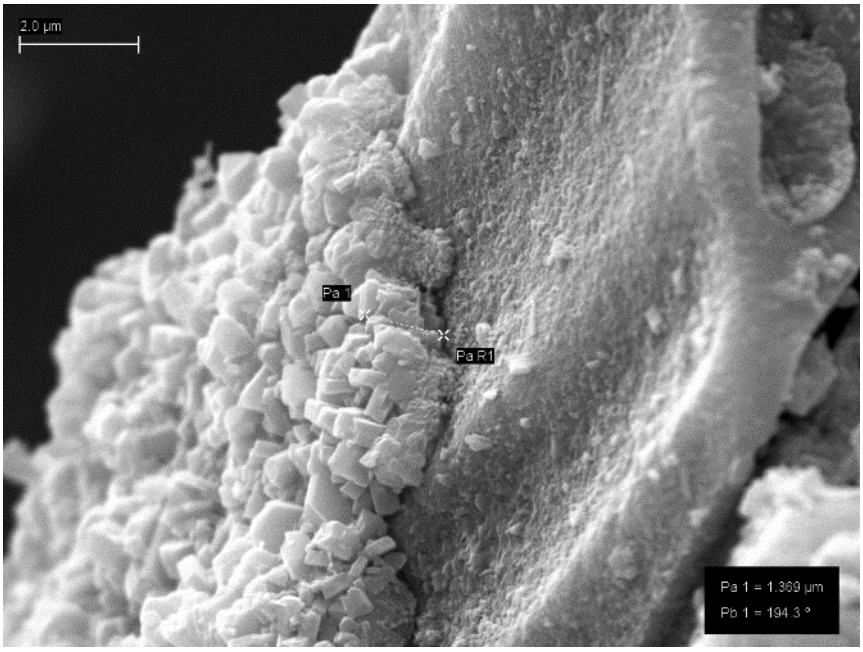

Figure 23. SEM image of the zeolite crystals adhering as a coating to the silica core to provide a self-supporting fine aggregate. Crystals are on average 0.5 µm in size attached to a 10 to 20 µm silica core. This zeolite over coating will therefore provide 3 distinct porosities during analyses; 1) the pore space between zeolite coated silica core, 2) the porosity between zeolite crystallites, and 3) internal porosity within the zeolite structure.

The Design-Expert™ factorial design software provided robust statistical analysis of the synthesis conditions from the 3-factor design (Table 13). These statistical out puts show a curved surface response to the 3 factors

and provide the optimal conditions to maximise the surfaces. When considering the optima temperature a plot of Molarity, Al:Si ratio, and the yield in the third axis (Figure 24) indicates that of 0.43 of the factor is an optimal temperature. Therefore as 1 factor is 5 °C and the 0 factor is 70°C the optimal temperature is (0.43*5)+70, which equals 72.5°C. Similarly, the optimisation curve for the optimal molarity a plot of Al:Si ratio, Temperature, and yield indicates that 0.03 or 5.02 M NaOH (Figure 25). Also a plot of Molarity, Temperature, and yield indicates that an optimum Al:Si ratio is -0.19, or 0.59 (Figure 26)

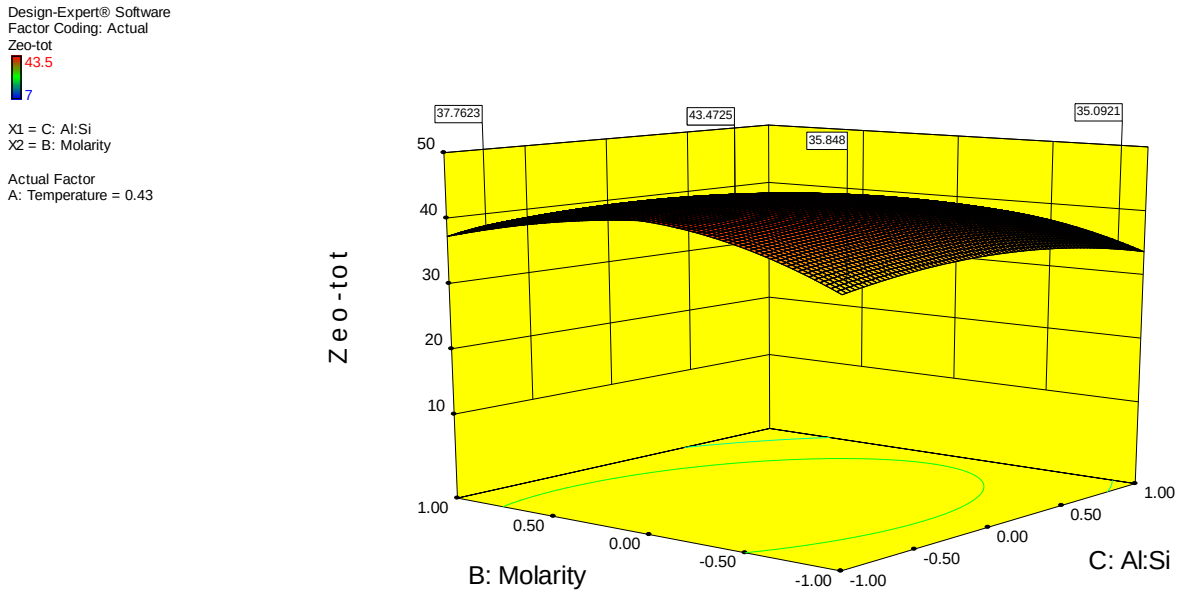

Figure 24 Surface response curve of zeolite yield at the optimum temperature of 71.1°C.

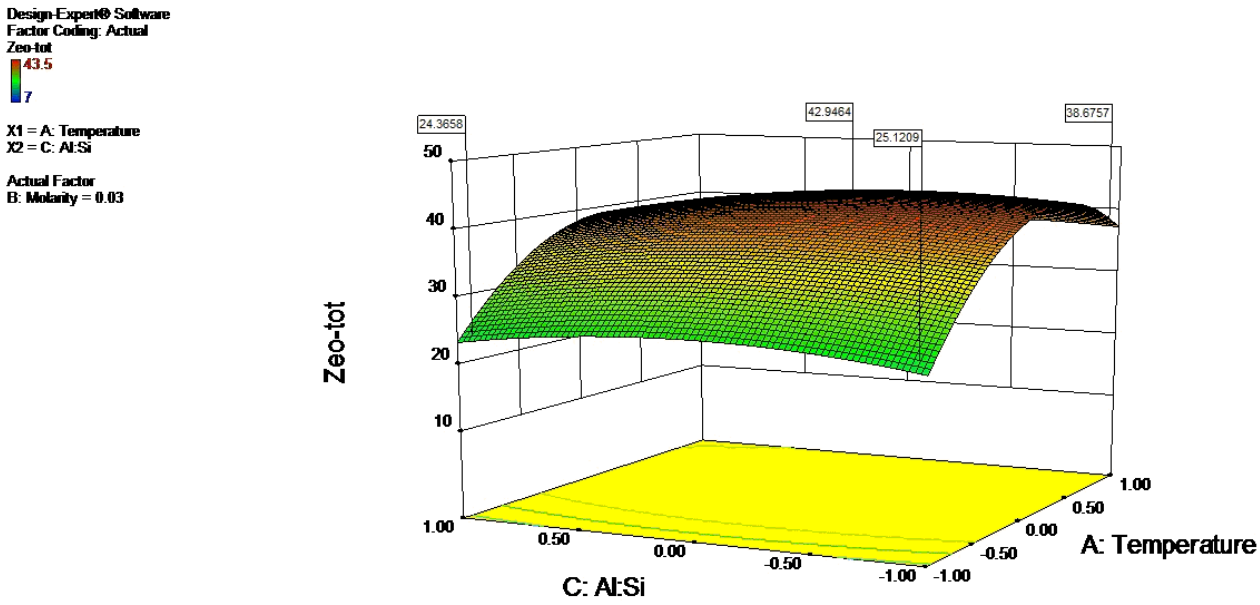

Figure 25 Surface response curve of zeolite yield at the optimum molarity of 5.02 M NaOH.

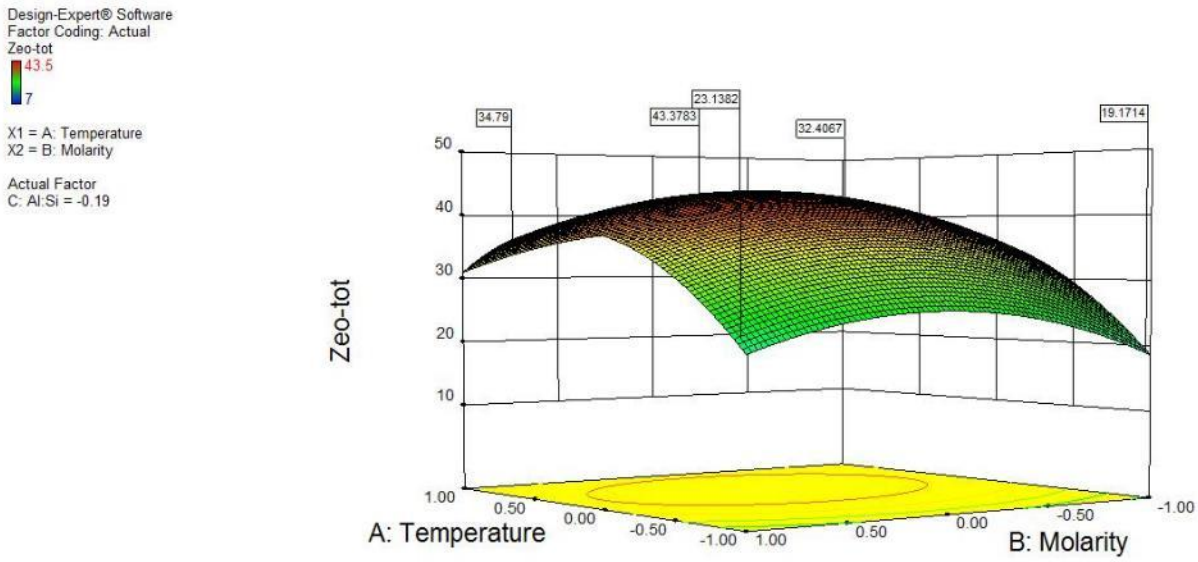

Figure 26 Surface response curve of zeolite yield at the optimum Al:Si ratio of 0.59.

These data on the condition of zeolite formation, particularly for the temperature 71-73°C, are ideal for the consumption of waste steam from the boilers at the sugar mills. However, in scale up experiments heat transfer through the larger containers delayed zeolitisation, but not yield. In addition, experimentation with open systems rather than closed systems indicated that yields were not substantially altered. Hence, it is likely that a zeolite plant established on a mill site could be established using waste steam, in an open and unpressurised system as a continuous feed system

Surface sorption

The very fine crystallites of the zeolite-x over the silica core (Fig. 23), should provide high surface areas because of the 0.5 µm crystallite size, and consequently should provide a very high cationic exchange. Analysis of the zeolite through argon porosimetry and BET surface are measurement at Particle and Surface Science's laboratories (Gosford, NSW), indicate that the zeolite-composite has a single point surface area at P/Po = 0.045 or 228 m^2/g and a Langmuir Surface Area of 251 m^2/g. These separate measures are in close agreement with each other, indicating that it is the surface area of crystallites on the surface that are being measured and that adsorption occurs through most of the zeolite layer (Figure 23).

The single point adsorption total pore volume of pores less than 1,300 Å diameter at P/Po = 0.98 is 0.13 cm^3/g (13% porosity), suggesting that the majority of pore space is between silica particles. Overall, the adsorption average pore width (4V/A by BET) is 22.3 Å. However on closer analysis of the data 0.065 cm^3/g (6.5% porosity, or ≈50% of the total porosity) is associated with pore sizes of 7 Å or less (which are the internal pore throat size for zeolite-X). Similarly, ≈90% (210 m^2/g of the surface area) is associated with pore sizes of 7 Å or less. Hence, the vast majority of surface area for sorption is provided by the internal porosity and lattice exchange of the zeolite-X. A second pore width peak, which accounts for about half of the residual surface area, occurs at ≈13 Å (0.005 cm^3/g or 0.5% porosity) and appears to be related to the pore-space between crystallites. The residual 0.06 cm^3/g of porosity is associated with pores >20 Å, but this only accounts for ≈5% of the total surface area measured, and by 500 Å no further surface area is provided for exchange processes by the pore space.

From the surface area it is possible to calculate a theoretical CEC capacity, which at 251 m^2/g, provides a surface site density of 964 µmol/g or 0.96 meq/g. This theoretical exchange capacity is about 20% of that reported for zeolite-X, of 4.73 meq/g. However given that the recovery of zeolite-X is estimated at 50%, and that 90% of all of the adsorption surface area is provided by the zeolite-X internal porosity (7 Å pores), then a readjustment must be made. Therefore, the zeolite-X is providing 1735 µmol/g of internal CEC, or 1.74 meq/g. This is about a third of the estimated CEC provided by zeolite-X, hence the remaining two thirds of the reported CEC must be to external surfaces ≈3 meq/g or 3000 µmol/g, but this will depend on pH because of the isoelectric point, and surface charge density. The isolectric point (IEP) of the system was measured using Malvern Zetasizer, dynamic light scattering/laser doppler electrophoresis instrument. This measure provided a bulk IEP for the system of 4.9 ± 0.1, which is the pH at which there is zero net surface charge and is in the typical range for alumino silicates (IEP 2.5-5.5). At pH >5 a net negative charge will dominate attracting cations, and at pH <4.8 a net positive surface charge is carried. However, although dominated by a particular surface charge does not mean that mineral surfaces carry no charge of the opposite sign. Hence at pH < 4.8 cations may well be attracted to and exchange for exchange cations, they will be inhibited, which is what is observed in (Figures 27 - 30).

A series of adsorption experiments were conducted on the zeolite-composite for 48 hours (the assumed equilibrium time) with copper and zinc concentrations ranging from about 4 to 182 mg/L at pH 3.5 to 8.5 (Figures 27 - 30). The concentrations of the copper, zinc concentrations were measured in each solution by inductively coupled plasma mass spectroscopy (ICP-MS). These figures show a typical loading behaviour where as concentration increases that the pH of maximum adsorption also increases. For example at 10 mg/L Zn maximum adsorption maximum occurs at pH 5 (the IEP) but at 182 mg/L maximum adsorption is delayed to pH 6. These data show the influence of the IEP on the sorption curve, and that surface loadings of metals tends to increase the IEP slightly, thereby delaying maximum sorption to higher pH (Figures 27 - 30).

The nature of the sorption can also be assessed and modelled using either Langmuir, of Freundlich plots. Langmuir plots indicate a homogeneous sorption site distribution assuming a single adsorption layer, which has a sorption/exchange maximum. Whereas, Freundlich fits imply a heterogeneous site distribution (i.e., more than one possible site description), where no theoretical maximum loading occurs, because precipitation continues the cation removal process. Data from adsorption experiments were analysed both using the Langmuir and Freundlich methods, where it was found that Langmuir provide the most consistent results.

In addition, Langmuir was also chosen because not only does it provide a linearization of the model, but a high degree of association between the sorption surface area and the internal pore openings of 7 Å is seen, indicating that a single adsorption layer is more likely. The Langmuir isotherm equation in its linear form can be expressed as follow:

$$1/q_e = (1/q_m.K_L) \,.\, (1/C_e) + (1/q_m)$$

Equation 12

where C_e is the equilibrium concentration (mg/L), q_e is the amount removed to the solid (mg/g), q_m is the maximum saturation capacity at the isotherm pH (mg/g).

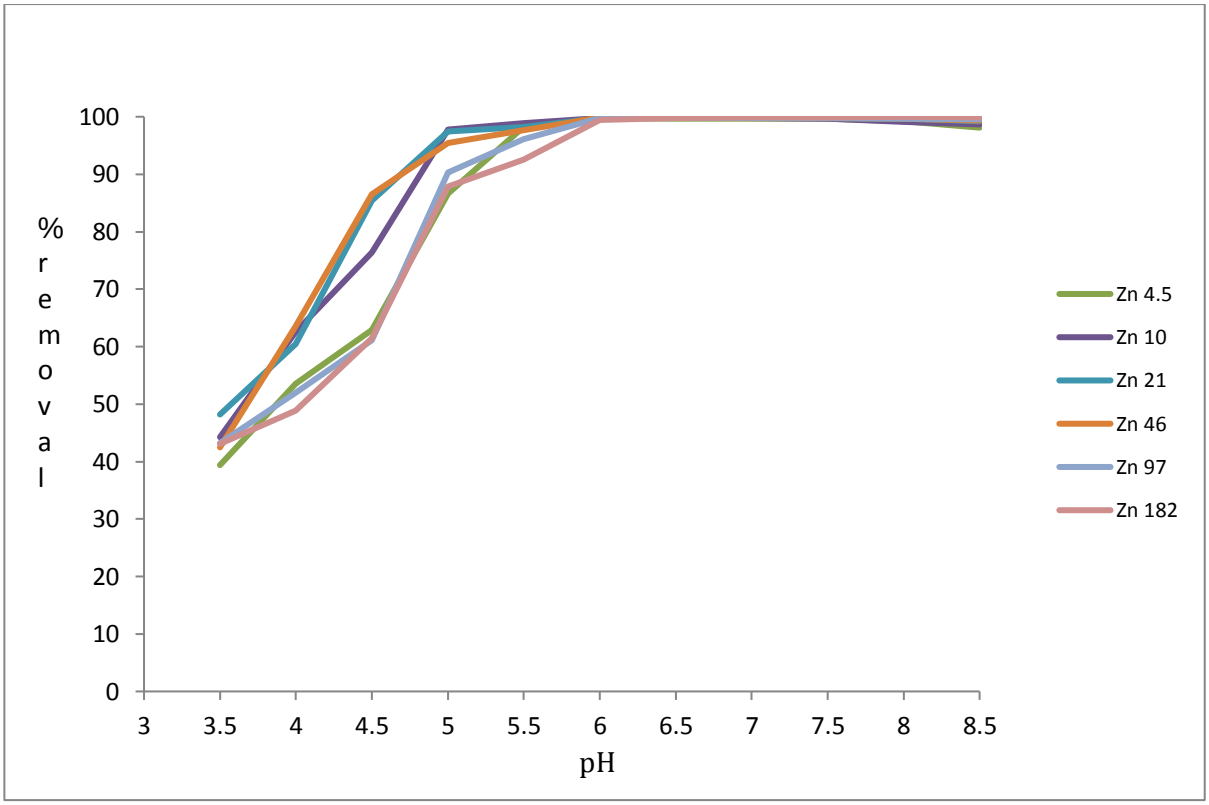

Figure 27 The removal efficiency of the zeolite against Zn concentrations from ≈5 mg/L to ≈180 mg/L at different pH's.

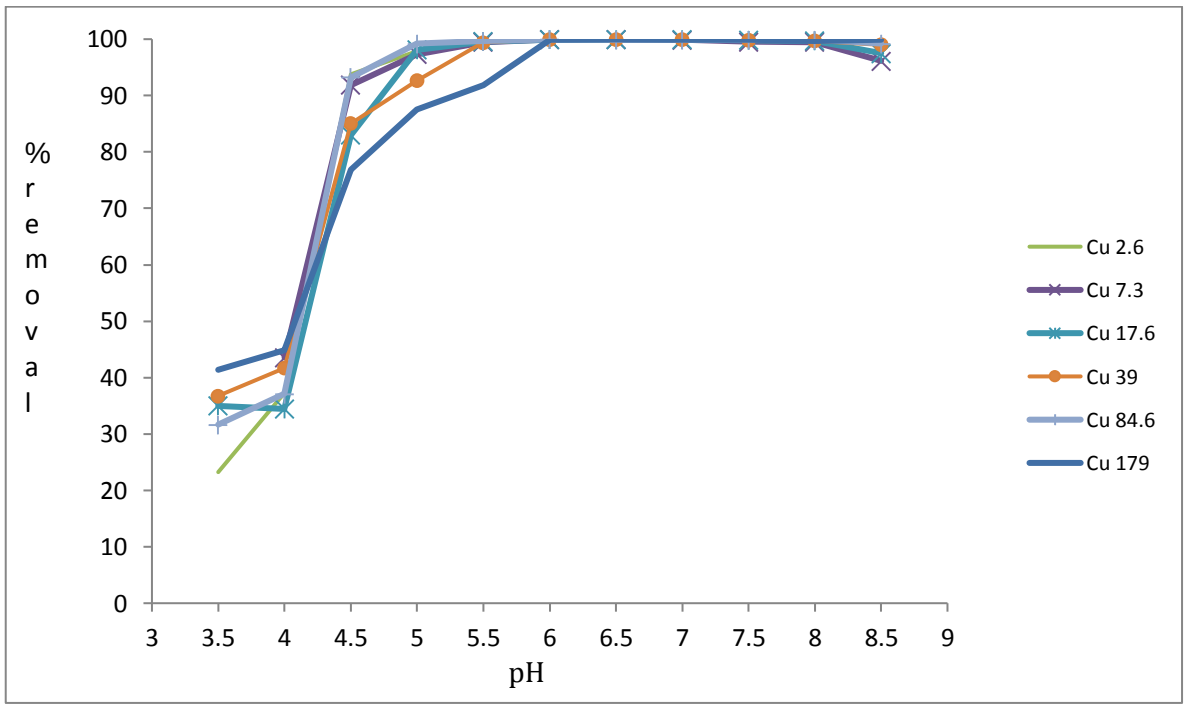

Figure 28 The removal efficiency of the zeolite against Cu concentrations from ≈3 mg/L to ≈180 mg/L at different pH's.

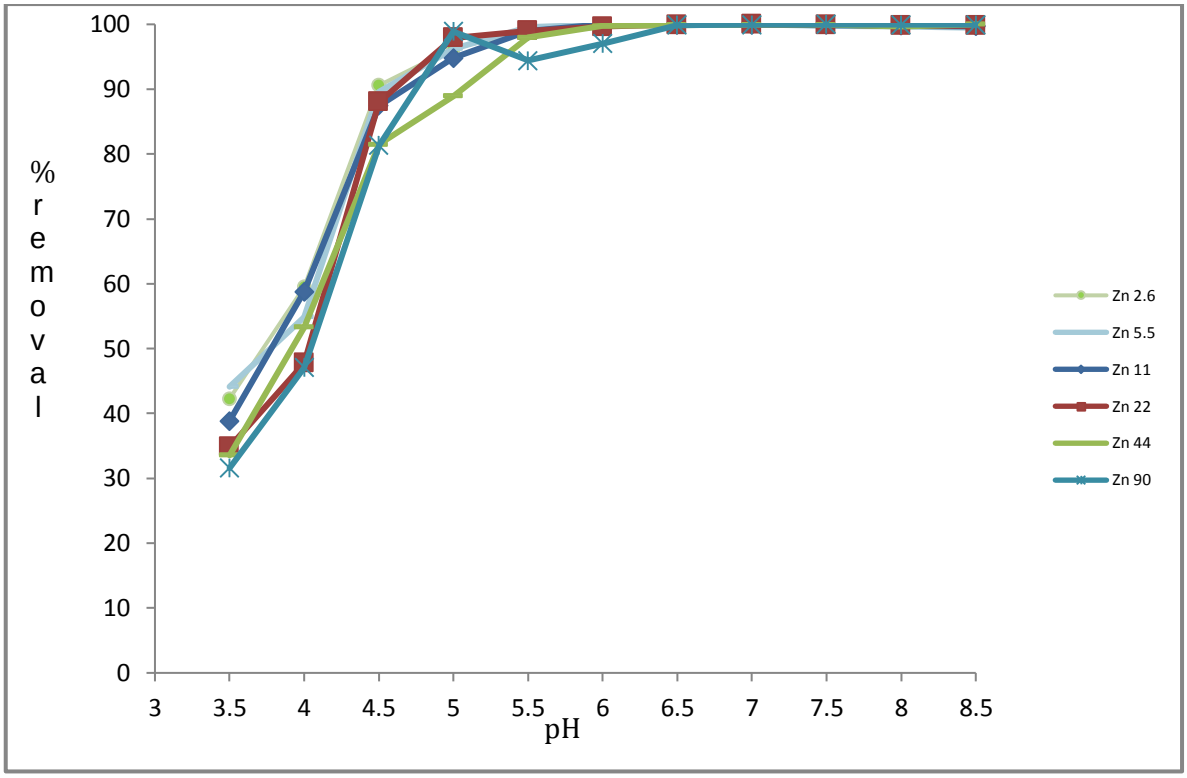

Figure 29 The removal efficiency of the zeolite against Zn concentrations from ≈3 mg/L to ≈90 mg/L at different pH's when in competition with Cu.

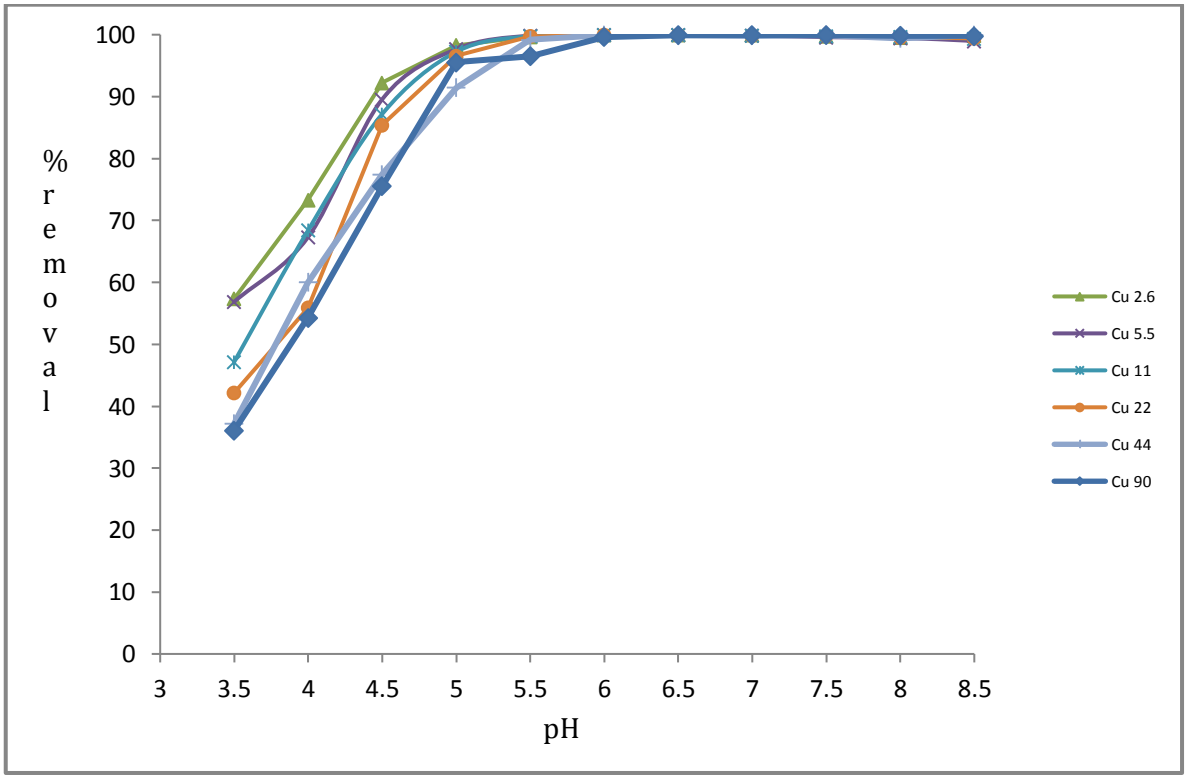

Figure 30 The removal efficiency of the zeolite against Cu concentrations from ≈3 mg/L to ≈90 mg/L at different pH's when in competition with Zn.

The line of best fit to the Langmuir adsorption model shows that 1 gram of zeolite-composite is able to adsorb 38 mg of copper from a solution at pH 6.5 containing copper only at very high correlation index $R^2 = 0.99$ (Fig. 31). However when copper is mixed with an equal amount of zinc the adsorption of copper and zinc increases respectively to 93 and 105 mg/g of solid while maintaining a high correlation index (Figs 32 and 33).

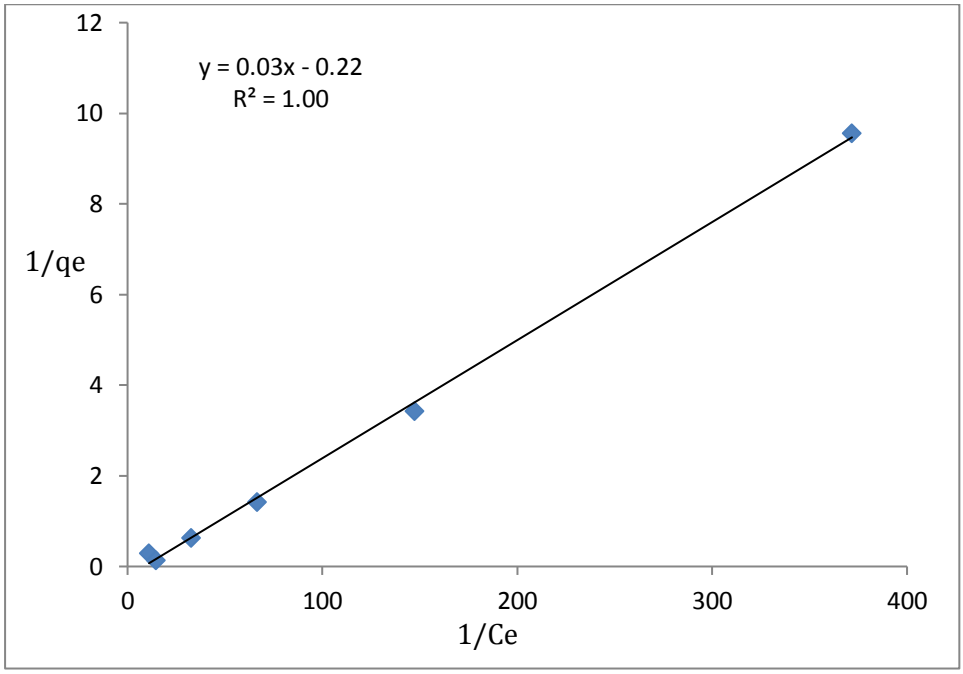

Figure 31. The linear regression of the Langmuir equation for copper only solution at pH 6.5 is plotted from the inverse of the equilibrium metal concentration (Ce) in mg/L on the X-axis and the inverse of the amount adsorbed (qe) by the zeolite-composite (mg/g) on the Y-axis. The amount of copper removed (38 mg/g) is calculated from the inverse of the value 0.0261 from the trend-line equation in the top left hand corner of the plot.

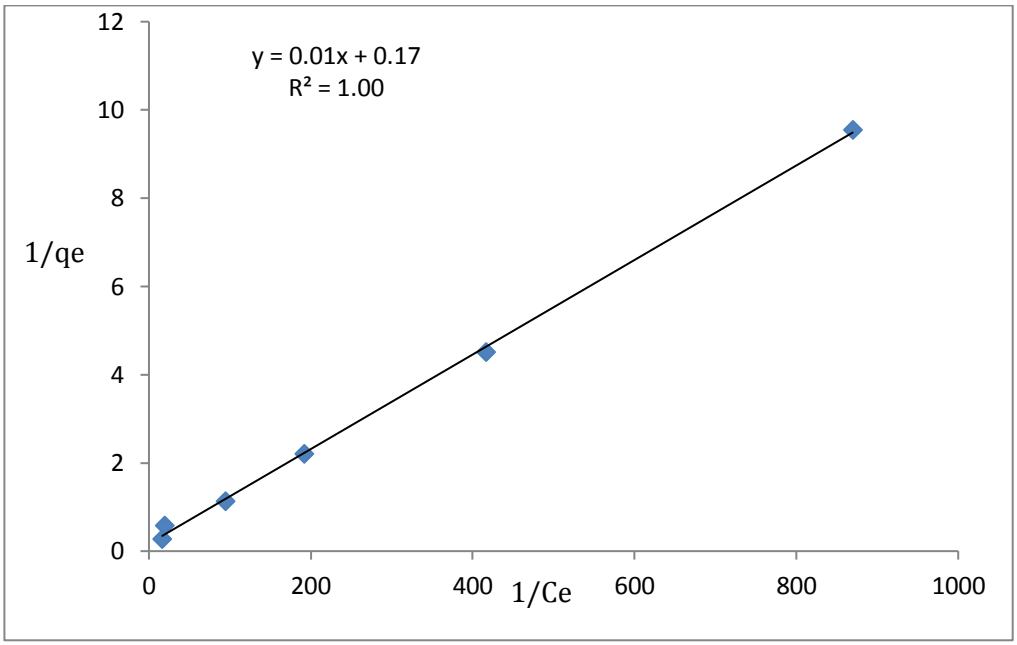

Figure 32. The linear regression of the Langmuir equation for copper in the copper/zinc solution at pH 6.5 is plotted from the inverse of the equilibrium metal concentration Ce in (mg/L) on the X-axis and the inverse of the amount adsorbed by the zeolite-composite (qe) (mg/g) on the Y-axis. The amount of copper removed (93 mg/g) is calculated from the inverse of the value 0.0107 from the trend-line equation in the top left hand corner of the plot.

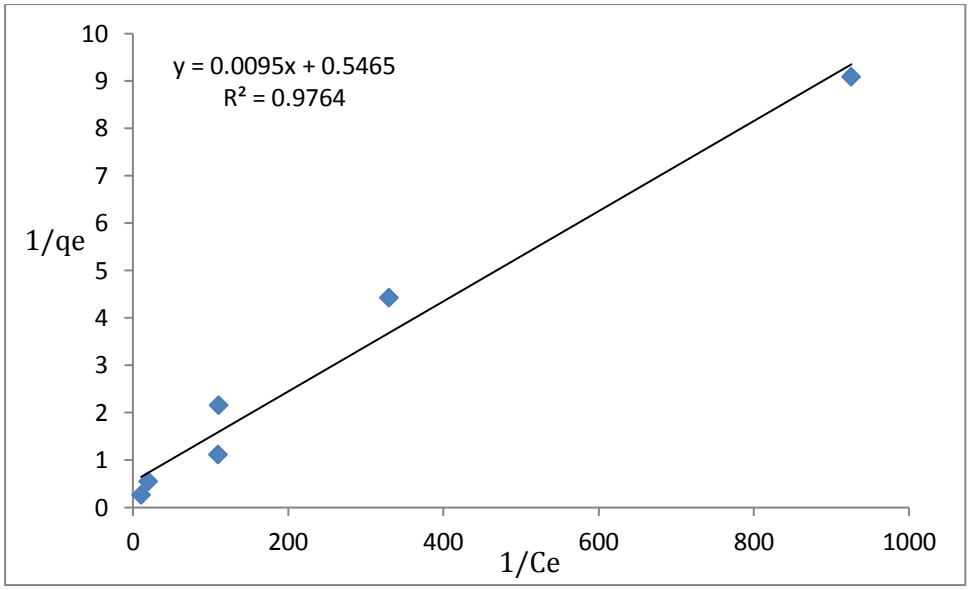

Figure 33. The linear regression of the Langmuir equation for zinc in the copper/zinc solution at pH 6.5 is plotted from the inverse of the equilibrium metal concentration (Ce) in (mg/L) on the X-axis and the inverse of the amount adsorbed by the zeolite-composite (mg/g) on the Y-axis. The amount of zinc removed (105 mg/g) is calculated from the inverse of the value 0.0095 from the trend-line equation in the top left hand corner of the plot.

The C_{max} of 105 mg/g of Zn, and 93mg/g Cu for the mixed metal sorption suggest that the CEC is 1.6 meq/g for Zn, and 1.5 meq/g for Cu (assuming the mode of removal is as MOH^+, i.e. above the pKa of hydration). Moreover because both cations are in competition with each other these values may be summed which gives a CEC of 3.1 meq/g. However, at pH 6.5 the pH of the experiment both Cu and Zn are both below their pKa of hydration, which suggest that Cu^{2+} and Zn^{2+} dominate. A PHREEQ speciation simulation of these metal concentrations suggests that 85% of the Cu and 99.8% of the Zn will be as Cu^{2+} and Zn^{2+} states without the solubility index exceeding 1 (i.e. metals do not precipitate). Hence, the CEC of the zeolite measure in the adsorption experiments will be 2.6 meq/g for Cu, and 3.2 meq/g for Zn giving a CEC of 5.8 meq/g, suggesting that the zeolite produced here has a higher CEC than those previously reported (4.7 meq/g) and is more in line with the CEC of zeolite-A (5.5 meq/g).

Kinetics of Removal

Processing of the kinetic data indicates that first order Lagergren, and Elovich models do not provide suitable correlations. However, pseudo-second order correlations (R^2) are very strong across all copper and zinc concentrations (Tables 19 & 20). Moreover, the equilibrium removal capacity calculated from the PSO model q_e(cal) for the longest contact time of 384 hours was close to the experimental data q_e (exp) (Tables 19 & 20). The pseudo second order model is a good fit for removal from solution of copper, zinc, copper in zinc and zinc in copper to the SCBA zeolite-composite. However, since the PSO model is based on the assumption of a chemically rate controlling removal {Cheng, 2010 #742} and includes precipitation, co-precipitation, external and intra-particle film diffusion as well as surface adsorption (Mohan, 1997). Hence to determine the controlling factors in the sorption process the following equation:

$$h = k_2.q_e^2$$

Equation 13

determines the initial sorption rate for the PSO model; the value of (h) (Tables 19 & 20) increases with increasing initial concentration (C_0) and the K_2 value of equation (3) that is equal to the square of the slope over the intercept q_e = 1/slope, K_2 = slope^2/intercept {Kumar, 2006 #770} decreases with increasing

concentrations (Figures 34 & 35). The K_2 of Pseudo second order of copper only, zinc only, copper in zinc and zinc in copper solution decreases with increased concentrations (C_0) but does not reach zero since the fitting trend or regression type is exponential (Figure 36).

Table 19. The copper only and zinc only solution parameters of the adsorption kinetics of the pseudo second order. The experimental q_e (exp) of contact time (384 hours) is the closest to the q_e (cal) calculated of the Pseudo second order for each initial concentration (C_0). The regression coefficients (R^2) of the pseudo second order are very high as well. The smaller K_2 value indicates a faster adsorption rate corresponding with higher initial concentration (C_0).

Pseudo second order kinetic model											
Copper only pseudo second order kinetic model						Zinc only pseudo second order kinetic model					
$C_{0\ mg/L}$	q_e (exp)	K_2	R^2	q_e(cal)	h	$C_{0\ mg/L}$	q_e (exp)	K_2	R^2	q_e(cal)	h
9.4	0.373	2.357	1	0.374	0.330	9.0	0.359	0.771	0.999	0.363	0.102
18.8	0.747	1.096	1	0.750	0.616	18.4	0.731	0.362	0.999	0.738	0.197
38.0	1.507	0.329	0.999	1.518	0.760	36.3	1.434	0.054	0.982	1.494	0.121
78.3	3.106	0.130	1	3.125	1.270	73.9	2.902	0.115	0.999	2.929	0.985
149.1	5.847	0.041	0.999	5.893	1.429	146.4	5.612	0.046	0.999	5.688	1.491
221.7	8.426	0.031	0.999	8.525	2.217	210.4	8.069	0.022	0.999	8.137	1.457
257.1	9.773	0.016	0.998	9.843	1.513	247.4	9.386	0.016	0.999	9.506	1.450
313.4	11.728	0.019	0.998	11.990	2.779	300.5	11.289	0.013	0.998	11.468	1.745
402.3	14.239	0.013	0.997	14.641	2.714	414.2	14.967	0.009	0.998	15.175	2.021

Table 20. The copper and zinc in mixed copper/zinc solutions parameters of the adsorption kinetics of the pseudo second order. The experimental q_e (exp) of contact time (384 hours) is the closest to the q_e (cal) calculated of the Pseudo second order for each initial concentration (C_0). The regression coefficients (R^2) of the pseudo second order are very high as well. The smaller K_2 value indicates a faster adsorption rate corresponding with higher initial concentration (C_0).

Pseudo second order kinetic model											
Copper in the mixed copper/zinc solution						Zinc in the mixed copper/zinc solution					
$C_{0\ mg/L}$	q_e (exp)	K_2	R^2	q_e(cal)	h	$C_{0\ mg/L}$	q_e (exp)	K_2	R^2	q_e(cal)	h
3.1	0.122	13.928	1	0.122	0.208	3.1	0.120	5.628	0.999	0.121	0.083
5.8	0.232	3.719	0.999	0.233	0.202	5.9	0.232	1.598	0.999	0.235	0.088
12.0	0.476	1.591	1	0.478	0.364	11.8	0.466	0.822	0.999	0.470	0.181
24.5	0.967	0.658	0.999	0.974	0.624	23.5	0.917	0.363	0.999	0.927	0.312
51.3	2.014	0.112	0.998	2.040	0.468	48.8	1.882	0.074	0.996	1.917	0.272
100.3	3.707	0.071	0.997	3.693	0.963	95.5	3.305	0.056	0.993	3.270	0.594
128.0	5.002	0.030	0.997	5.015	0.759	122.5	4.689	0.021	0.989	4.634	0.449
154.7	5.985	0.026	0.997	5.988	0.940	152.4	5.654	0.019	0.991	5.580	0.605
217.7	7.597	0.026	0.998	7.610	1.488	202.2	6.188	0.031	0.998	6.180	1.169

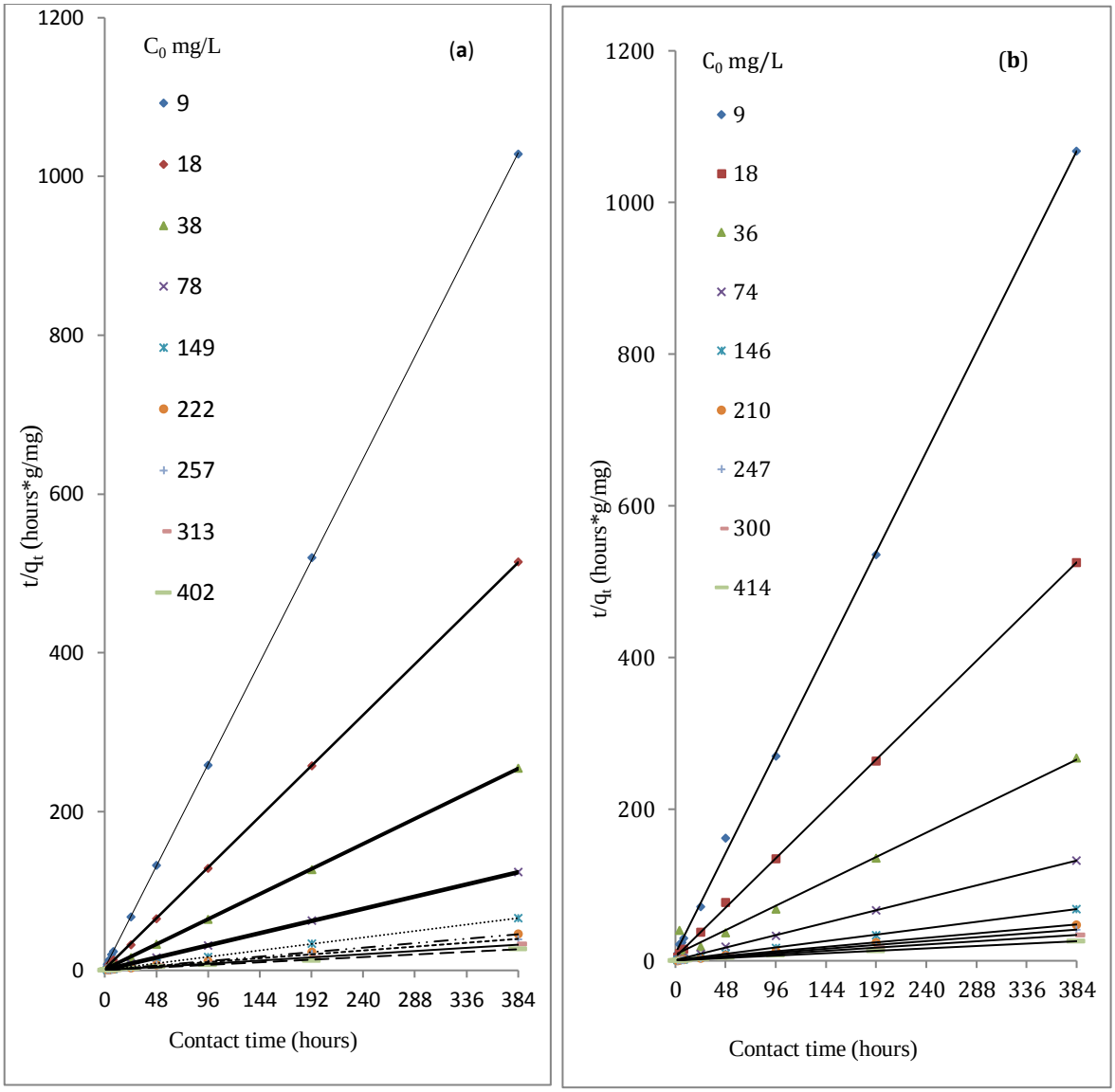

Figure 34. Plots of the pseudo-second order model for the removal of copper from copper only solution (a) and the removal of zinc from the zinc only solution (b) to the SCBA zeolite-composite. Strong correlations for data (Table 19) and agreement between experimental and calculated q_e data suggest that this model represents copper and zinc removal extremely well.

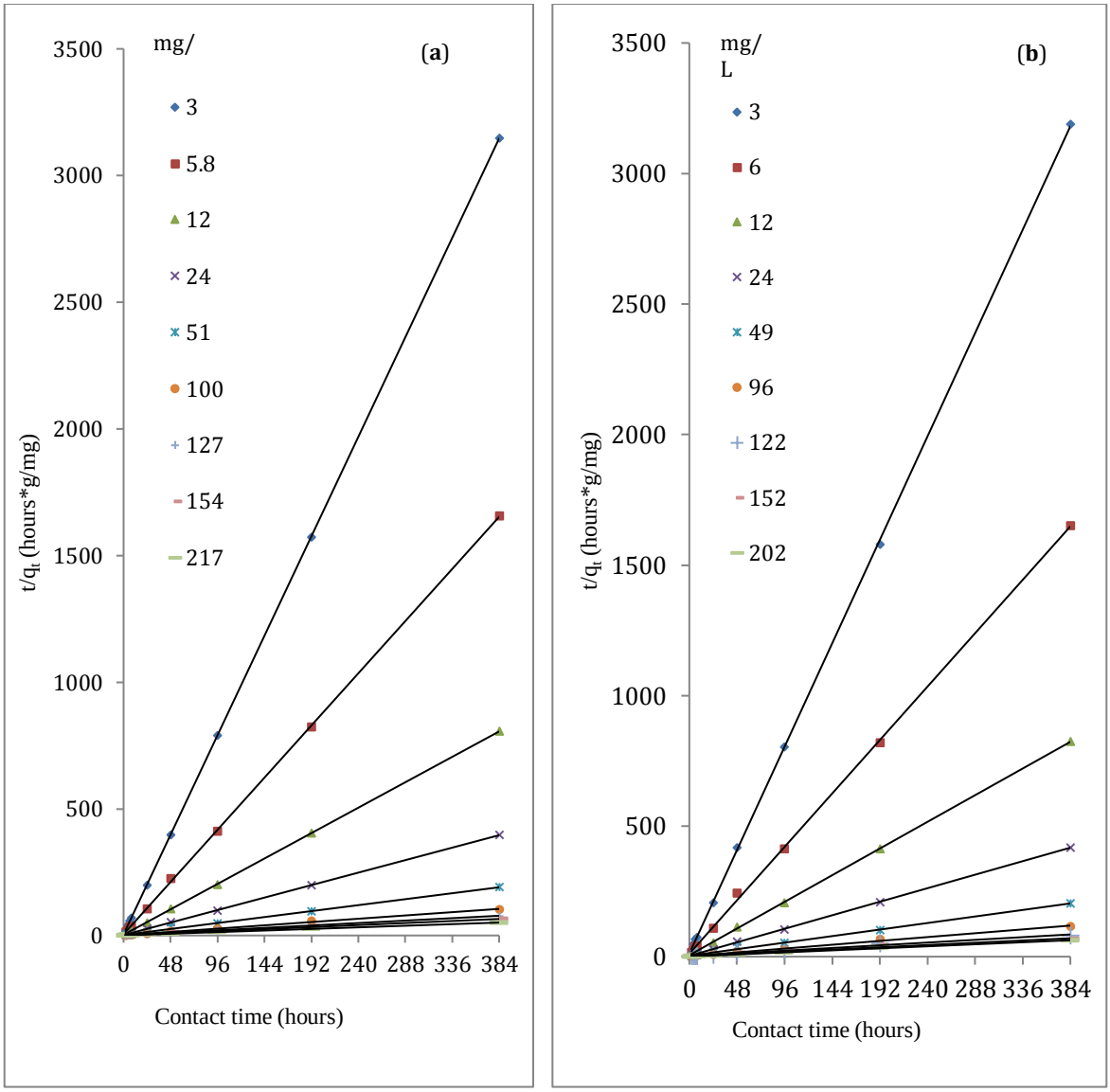

Figure 35. Plots of the pseudo-second order model for the removal of copper from the mixed copper/zinc solution (a) and the removal of zinc from the mixed copper/zinc solution to the SCBA zeolite-composite. Strong correlations for data (Table 20) and agreement between experimental and calculated q_e data suggest that this model represents copper and zinc removal extremely well.

3.4 The diffusion models

The PSO model does not account for diffusion separately therefore to determine the rate-controlling step for copper and zinc removal to the SCBA zeolite-composite we used the linear derivation of the Weber and Morris intra-particle diffusion model, Equation (13) to determine K_{id} (mg/g.min$^{1/2}$) the intra-particle diffusion constant and the intercept of the plot C (mg/g) that is an indication of the thickness of the boundary layer {Mall, 2005 #400}; large C value indicates significant external mass transfer in the sorption therefore considered as rate-controlling step at the longer periods of adsorption (Tables 19 & 20). External mass transfer and adsorption is represented by a steep slope in the linear trend of the Weber model plot of qt and the root square of time (Figures 37, 38, & 39). The K_{id} value clearly decreases when comparing similar concentrations of copper and zinc of the first six periods (Table 19) to the last three periods (Table 20) in single metal concentrations. The trend is similar in the mixed metal since the K_{id} values of each corresponding concentration decreases when comparing the first six adsorption periods (Table 19) to the last three periods (Table 20); the saturation of the exterior surface was followed by internal pores adsorption until saturation and consequently the diffusion rate was slowed particularly after the decrease in the copper and zinc concentrations in the solution however

equilibrium was not reached and an extended period beyond the 384 hours would have been needed to reach saturation (Figures 27 - 30).

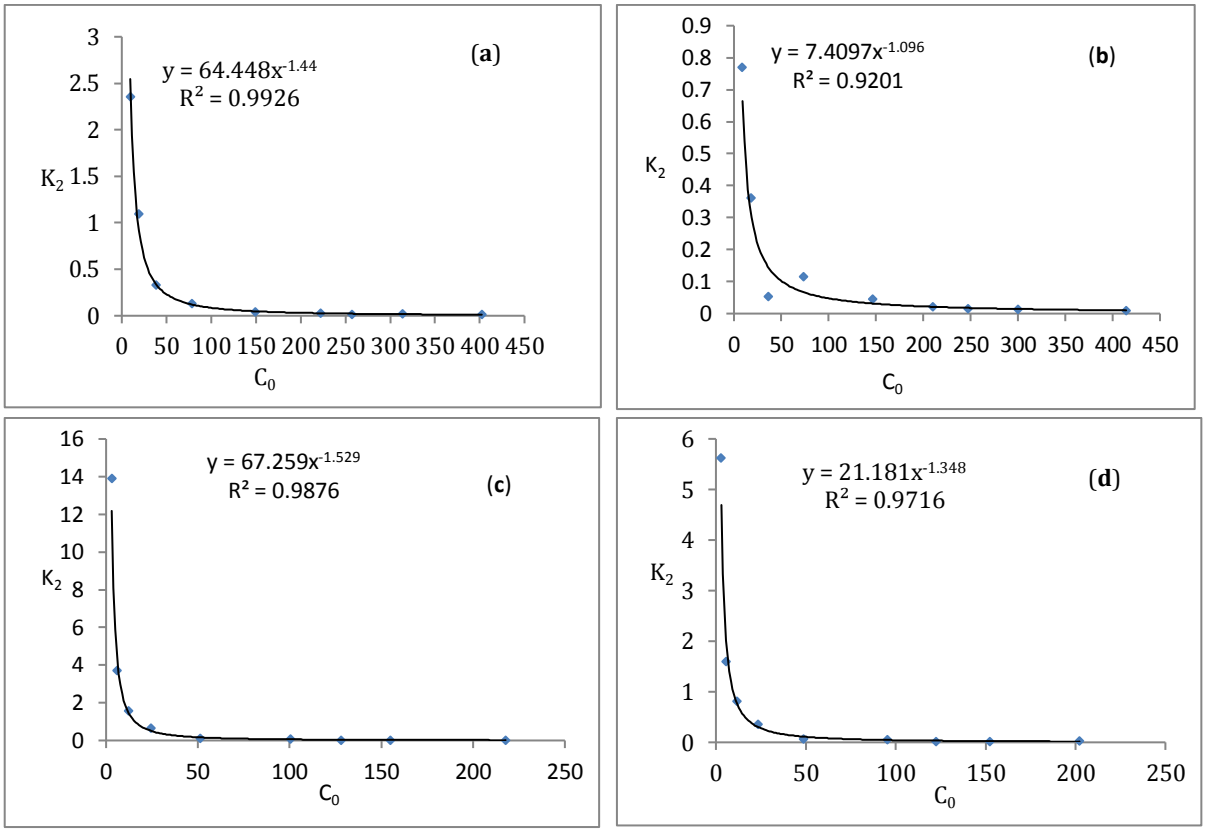

Figure 36. Pseudo second order K2 of copper only (a), zinc only (b), copper in copper/zinc (c) and zinc in copper/zinc solution (d) with initial concentrations C_0. K_2 decreases with increased concentrations but does not reach zero since the fitting trend or regression type is exponential in all four solutions.

The transfer of cations from the solution to the solid is partly dependent on the inter-particle space that is directly related to the particle's size with the majority of the SCBA zeolite-composite particles being mostly below 20 µm, the intra-particle diffusion resistance decreases along with the mass transfer resistance and consequently the solute reaches faster the internal pores of the SCBA zeolite-composite. The intra-particle diffusion is not the rate-limiting step because it does not fit the Weber model since the diffusion slope does not pass through the origin (C = 0) in any of the solution; furthermore the slope could be divided into multiple distinct trend lines (Figures 37 - 39). Figure 37 in particular shows that up to concentrations of 220 mg/L Cu in Cu only systems that the SCBA-zeolites become diffusion limited by $T^{1/2}$ minutes of 80, or a total of 6,400 minutes or about 107 hrs. As concentration decreases from there then the time to reach diffusion-limited conditions reduces to some 400 minutes at 10 mg/L. At concentrations above 220 mg/L Cu in Cu only systems the data appears more scattered and diffusion limited conditions do not necessarily appear to have established.

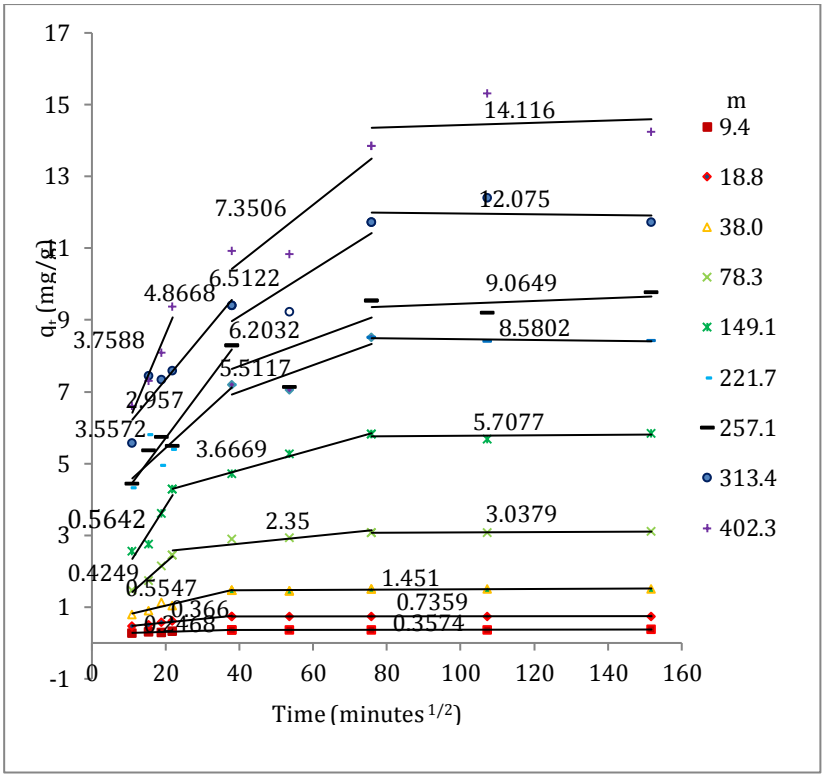

Figure 37. Copper only linear regressions diffusion trends with mass loading q_t (mg/g) versus the root square of time. The steeper slope of the first trend corresponds to the rapid external mass transfer. The decrease in slope indicates an increase in intra-particle diffusion; the value is indicated above each trend, the higher the value the higher the diffusion layer. No fits pass through the origin therefore intra-particle diffusion was not the sole rate-controlling step at any stage of adsorption.

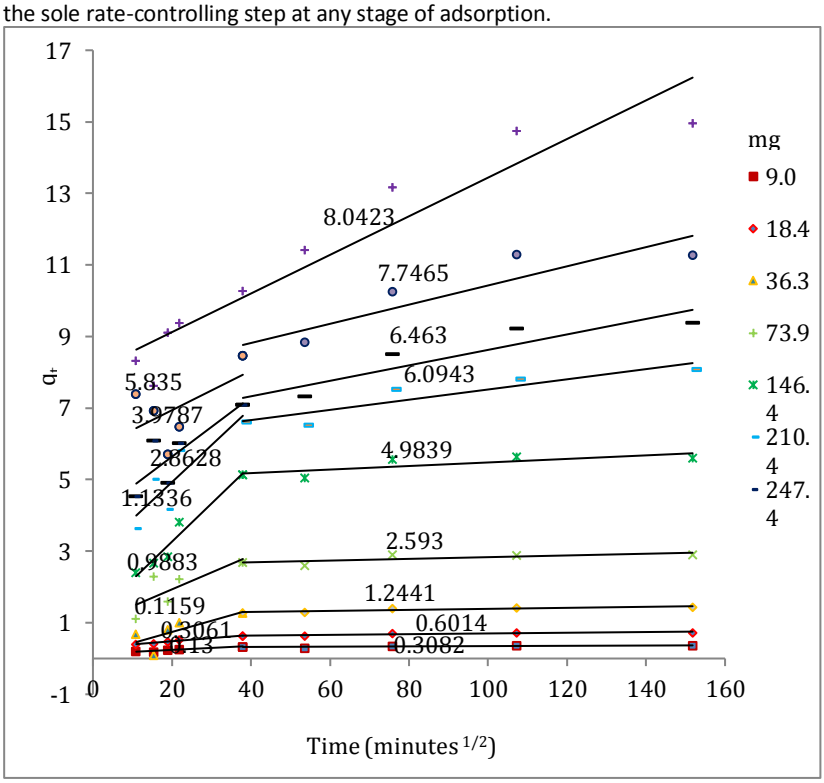

Figure 38. Zinc only linear regressions diffusion trends with mass loading q_t (mg/g) versus the root square of time. The steeper slope of the first trend corresponds to rapid external mass transfer. The decrease in slope indicates an increase in intra-particle diffusion; the value is indicated above each trend, the higher the value the higher the diffusion layer. No fits pass through the origin therefore intra-particle diffusion was not the sole rate-controlling step at any stage of adsorption.

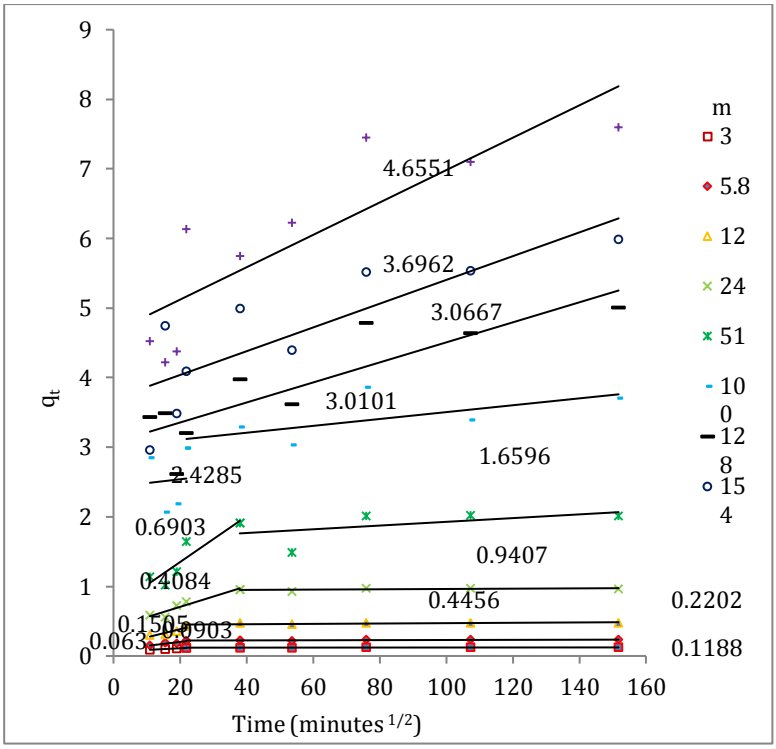

Figure 39. Diffusion trends of copper in mixed copper/zinc solution versus the root square of time. The steeper slope of the first trend corresponds to rapid external mass transfer. The decrease in slope indicates an increase in intra-particle diffusion; the value is indicated above each trend, the higher the value the higher the diffusion layer. No fits pass through the origin therefore intra-particle diffusion was not the sole rate-controlling step at any stage of adsorption.

Economic Summary

The two aspects of this project were initially to target the use of sugar cane bagasse flyash for conversion to a synthetic zeolite and for conversion to geopolymers.

Zeolites:

Synthetic zeolite conversion was a key target for value adding where potential products ranged from low value low functionality zeolites for water softening and simple waste treatment applications, through to high value but relatively lower volume zeolitic catalysts. Research outcomes indicated initially a high conversion to zeolites but not to products suitable for evaluation for catalytic applications, yield for water softening and waste treatment appears modest, and intrinsically too expensive for low value products.

Characteristics of the zeolitic product synthesized in the research include relatively large particle size; agglomerated zeolite on the surface of occluded residual particles (Figure 23) of the bagasse fly ash, and excellent cationic exchange capacity including for zinc removal from water (Figures 27 & 29). The feature of agglomerated zeolite on the surface of occluded residual fly ash particles offers potential for an active filtration media for removal of cations from water for environmental, waste and potable water treatment applications. While the production cost of the SCBA based zeolite is expected to be high and of the order of ~$1.10 per kg, the high exchange capacity of the product indicates a good potential for economic production and use.

The market for active filtration media is significant worldwide with major multinational companies creating and developing and producing media for many aspects of water treatment (Table 21). Additionally much research is carried out to identify and develop such media at low cost and high efficacy. Specific companies in this field include Dow Chemical; GE; Evoqua; Ashland Chemicals; 3M. Table 21 lists some of the major products used worldwide where the zeolitic product developed in this project will be competing. In addition to these developed products a wide range of industrial and agricultural wastes are often used for aspects of water treatment for removal of heavy metals, usually the low cost is accompanied by low removal capacity.

Table 21. Summary of active filtration media available for the treatment of waters. The table is by no means comprehensive, but provides an illustration of the range of systems available that the self supported zeolites woud be competing against.

Product	Activated Carbon	MetSorb HMRG	Isolux	ADSORBSIA	PUR	Bentonite Sorbent
Company	Various	MetSorb Division of Graver Techn	MEL	Dow Chemicals	Procter and Gamble	Ecochemicals
Type of product	Biomass based	Titanium media	Cartridge with zirconium media	Titanium adsorbent media	Ingredients - ferric sulphate calcium hypochlorite	Sorbent powder
Meets WHO standards	Yes	Yes	Yes	Yes	Yes	No data
Meets EPA standards	Yes	Yes	Yes	Yes	Yes	No Data
Hazardous waste issues	No	No	No	No	No	No
Cost of treatment	Moderate	High	High	High	Very low	Average
Patented Technology	No	Yes	Yes	Yes	Yes	Yes
Selling price	Low	Low	Low	High	Low	Average
Contaminants effectively removed from water	Arsenic, ammonia, mercury, selenium, thallium, cadmium	Uranium, lead, antimony, arsenic, cadmium, copper, selenium, mercury, zinc	Arsenic, cadmium, chromium, lead, fluoride, copper and non-metal contaminates	Arsenic, lead	Arsenic, chromium, lead, organic matter, micro-organisms	Paints, heavy metals, colloids
Country made in	Various	United States of America	Unites States of America	World-wide	Unites States of America	Latvia, Finland, Lithuania
Other issues	-	-	High pressure drop	Can be harmful to health	-	-

The synthetic zeolite produced through this project will still require significant development for commercialization – validation and approval for water treatment will need to be undertaken; significant engineering development will also need to be undertaken prior to market entry. With these constraints there still appears to be valuable and sensible market opportunities both within Australia and internationally. Focusing on zinc as an environmental contaminant – we have identified the galvanizing industry as a significant potential early market client for this product where a key need within the industry is the capture and removal of zinc from site runoff water from every rain event. This is driven by environmental regulation rather than recovery of zinc value, but has a reasonable market in Australia with every galvanizing operation required to continue to control and improve surface runoff water management where they are also liable for the costs associated with this and the costs defending any charges (fines) for non compliance. We have currently identified three galvanisers in Brisbane, five in Melbourne, two in Sydney, and one in Perth that as requiring improved zinc surface water management. These 11 businesses offer a potential minimum annual market of 200T of zeolite for zinc removal. In addition, there are clear other applications include mine site water treatment and specifically two sites in Tasmania are constrained by zinc surface water management and acid rock drainage; we have been in discussion regarding active filtration media in the past.

Economic Projections

With broad engineering and production assumptions the following table summarizes the opportunity to commercialise the process for SCBA zeolitisation developed during this project. However, significant risk still exists with respect to market entry, engineering costs, and operating costs. Typically the hurdle rate for this will be higher than a low risk project.

Capital Expenditure			
	Broadwater	$750,000	
Upfront Costs			
	Validation work	$120,000	
	Regulatory Approval	$35,000	
	Market Development	$150,000	
			$1,055,000
Revenue			
	Sale of SCBA zeolite@ $1.5/kg		
	1,000t @ $1,500/t	$1,500,000	
Operating Expenses			
	Transport		
	1,000t @ $20/t	$20,000	
	Labour	$120,000	
	Ongoing QA/QC	$20,000	
	Production Cost	$1,100,000	
	EBITDA		$240,000
	Return on Investment (ROI)		23%

Geopolymers:

The reuse of fly ash into cementitious products has a long history, where financial benefits are achieved by both waste generators (who can realises a value from a process by-product), and the re-user (who reduces raw material costs through sourcing low-value supplements). Significant, and substantial quantity of research and capital investment has been made by the broader cement industry in incorporating fly ash (mostly Class F) into various products, with significant cost-savings to the industries concerns, while also improving the recycled-content of the finished products.

The following is a preliminary feasibility assessment of the viability of reusing SCBA in standard concrete batching plants, based on:

- Raw material costs;
- Required investigative costs;
- Required capital investment;
- Transport and logistics.

Implementation scenario

To establish the financial viability of reusing the SCBA into blended cement products, the following scenario has been developed to enable a costed model of any reuse opportunity with existing 'ready-mix' plants. The following model parameters were used for the costs.

Product generation: 6,000 tonnes per year
Reuse: 15% replacement in OPC blends

Ordinary Portland Cement Price: $200/tonne
Transport costs: $20 per tonne per 100km

End-use market assessment

As the site of generation is the Broadwater sugar mill, it is desired that any reuse established is in close proximity to the site of generation thereby minimising associated transport costs, and maximising the local community benefits. Within the near vicinity of Broadwater Mill, the following potential reuse concrete plants exist: *Boral* at Evans Head, Ballina, Lismore, and Maclean; and *Holcim* at Astonville, Lismore, Casino, Brunswick Heads. Although the capacities of these plants are confidential, during an interview with the Technical Manager at Boral the volumes specified above would be a "drop in the ocean" from a production perspective, and capacity to take process the physical volume is easily met.

Capital requirements

Most ready-mix plants have a series of silos and/or hoppers installed to receive and handle volumes of OPC and CFA, which are automatically fed into the mixing units in ratios depending on the client requirements. If certified as CFA-C**, then there is the potential to dovetail the volumes with existing CFA feed-stock reducing the need for additional silos.

It is considered that as the SCBA under assessment has a higher LOI than the standard, pre-blending of the SCBA with existing CFA feed-stock may not be possible, and a new silo would need to be installed. An estimated 'installed' price for a standard 50t silo would be $50,000. In addition to on-site capital requirements for the ready-mix plant, it is anticipated that additional silos and pneumatic loading facilities would be required at the point of generation, to enable loading of powder-tankers for delivery to the reuse sites. While details of current infrastructure have not been evaluated, it is assumed that these loading facilities would be required 'as new', which are anticipated to be in the order of $200-300,000.

Raw material benefits to reusers

At a modeled price of $200/t, it would appear at first glance that the replacement of 15% of the OPC from standard concrete mixes could provide a $30/t cost-savings. The current practice however with most ready-mix plants is that CFA is already substituted for OPD in significant quantities, where between 40% and 70% substitution rates are the norm, depending on the end product specification.
Compared with OPC, CFA is a very cheap product, varying from $10/t to $50/t, and is largely controlled by the cement producers themselves. The inclusion of SCBA into the concrete mixture in lieu of the current CFA volumes, would therefore only attract a $7.5/t savings.

Acid resistance

While most of the testing performed to date has focused on maintaining compressive strengths of end-products, the most notable benefit of the SCBA addition is in acid-resistance, whereby SCBA-blends had superior acid-resistance than the control. Comments were sought on whether these acid-resistant products would attract a price-premium, and whether there was a market for this type of product.

The response from the industry representatives was that acid-resistant products are not highly sought-after, and generally purchased for project-specific works, on rare occasions. To meet this demand, Granulated Blast Furnace Slag is generally added into products, which provides significant improvement to acid-resistance. As a by-product from the steel industry, this slag is not an expensive raw material, in the order of $50-$80/t, is readily available, and generally provided to a pre-approved specification that can be readily incorporated into concrete blends.

Key technical concerns

From the interviews conducted, a number of issues were identified with the information provided, raising doubts of the suitability of SCBA reuse into concrete blends as follows:

- Specification and continuity of product

If the SCBA could be certified to CFA-standards, then ready incorporation into existing feedstocks could be technically possible. On being provided an overview of the results to date, questions were raised over the conformance of this material to existing standard, and then whether the production process was consistent enough to enable a strong continuity of supply.

- Product appearance and acceptability by end-users

On being provided select photos from the draft report, the interviewees noted the colour of the blended products, being particularly dark in colour due to presumed residual carbon content. This "above all" is a deterrent for most end-users, the concreting industry who lay these products for clients to walk on and 'admire' visually. Without concrete *laying* company willing to take of materials that did not meet normal colour definitions, then it is unlikely for any batching plant to want to produce an unsaleable product.

Cost of further testing, and scope of testing work.

Given the materials tested were outside the scope of the relevant standards, it was suggested that further validation test work would be required, prior to the final roll-out of SCBA-derived products. The scope of this is very hard to delineate, as 'pass' results from initial rounds of testing can cause a very short validation regime, while continued 'fails' and re-designs can (at times) lead to significant amounts of wasted time and money. Broad cost indications therefore for this kind of validation work ranges from $20,000 to $100,000.

Economic Projections

If technically viable, the following table is a broad assessment of the potential ROI for the proposed installation of plant and equipment at both the site of generation, and reuse facility. They key assumption in this calculation that the reuse of SCBA can be achieved in conjunction with existing CFA, and a rate of $30/t can be achieved if the product is suitable for end-users based on workability and colour.

Capital Expenditure			
	Broadwater	$250,000	
	Reuse facility	$50,000	
Upfront Costs			
	Validation work	$50,000	
			$350,000
Revenue			
	Sale of SCBA @ CFA rates		
	6,000t @ $30/t	$180,000	
Operating Expenses			
	Transport		
	6,000t @ $8/t	$48,000	
	Labour	$40,000	
	Ongoing QA/QC	$20,000	
	EBITDA		$72,000
	ROI		21%

Section 4: Outputs and Outcomes

List the Outputs (manuals, processes, technology, equipment, workshops) or knowledge (scientific or other - including skills) that was derived from this project.

The following conclusions/out puts can be drawn based on the investigation into the use of oven dried sugarcane bagasse ash in blended cement systems.

- The SCBA as received from the Broadwater Co-Generation Plant does not contain significant amorphous silica but does contain significant crystalline silica as quartz.
- Mortar containing up to 15% sugarcane bagasse ash as OPC replacement has a pozzolanic index above the required 75%.
- Concrete made with sugarcane bagasse ash replacing sand up to 20%, achieved 28-day strengths higher than the control 28 day strength.
- Workability of fresh concrete was significantly reduced as SCBA content increased and no replacement level was found to comply with the target workability.
- Superplasticizer addition to the blended cement concretes resulted in compressive strengths above the 28-day target strength but below the reference concrete 28-day strength.
- The incorporation of SCBA has a positive effect on the acid resistance of concrete and mortars at all SCBA replacement levels.
- Zeolites are readily produced at 71°C, which can utilise waste steam from sugar mills.
- Zeloites produced are desirable forms with high cation exchange capacities that have applications in wastewater treatment.
- Zeolites are self-supported so have a much greater hydraulic conductivity that crystallite size indicates.
- Zeolites have pseudo-second order kinetics in removal of Cu and Zn.
- Kinetics are sufficiently rapid that metal removal becomes diffusion limited within ≈6,400 minutes of initial contact, even at very high concentrations > 200 mg/L.

These out comes indicate, that sugar can bagasse fly ash should not be viewed by the industry as a waste material, but should be considered as a resource, which can be value added to produce products. The concretes developed have significant acid resistance making it ideal for use within the sugar mills, where cane juice spills often generate acidity and concrete attack with conventional concretes. However, colour is a concern for the concrete industry, and requires further product development. However, based on some conservative estimates a potential return on investment, has been calculated at about 21%.

The zeolites developed in the project have interesting exchange capacities that make them ideal for water treatment. The inability to remove the unburnt carbon (only locking it within the matric) does preclude the higher-end uses of the materials (e.g., detergents). However, the self-supporting nature of the material makes it unusual, and provides addition benefits in treating water in flow through systems. Hence, the use of these zeolites in water filters is a distinct possibility. The economic assessment of these materials and in establishing a production plant suggest (given the assumptions used) that about a 23% return on investment is possible.

Section 5: Intellectual Property (IP) and Confidentiality

Detail any intellectual property considerations or discoveries made and if these are to be protected and how. Outline any publications produced. State what information, if any, is to be treated as confidential, to whom and for how long.

The intellectual property & confidentiality situation remains as previously reported: Because of the industry partner (Australian Biorefining) involvement with the project the whole project is subject to a commercial in confidence agreement. Consequently, information regarding the cationic properties of the zeolites, sorption capacities and kinetics are subject to that agreement. Hence, until the industry partner agrees that there is no new IP worth protecting via patents in the methods developed, yields, and compositional outputs or potential applications of the materials information cannot be released to members. We estimate that data will remain

in confidence at least until the end of 2015, to allow the commercial partner the option of deciding which if any aspects of the data will be commercially protected; at this stage commercial protection appears unlikely, although some novelty may be forth coming in the purification/surface sorption work.

Similarly, with the cements, mortars and concretes work Australian Biorefining involvement with the project the project data subject to a commercial in confidence agreement. This work including the mixes, strengths, acid resistance data are subject to that confidential agreement. However, we estimate that data will remain in confidence at least until the end of 2015, to allow the commercial partner the option of deciding which if any aspects of the data will be commercially protected; at this stage commercial protection appears unlikely as the data and applications appear to lack novelty.

Section 6: Industry Communication and Adoption of Outputs

a) *What key messages have come from the project to date, when and how they have been communicated and to whom? Has there been any communication with the relevant SRA Professional Extension and Communication (PEC) officer or unit?*

We have communicated the key findings of the zeolite optimisation, the zeolite metal uptake and kinetic models with the industry partner (Australian Biorefining). We have also communicated the results of the cement and concrete work with Australian Biorefining as well, high lighting with the acid resistance, and improved strengths.

The SRA representatives Michael O'Shea and Peter Samson (presentations and meeting at SCU, April 4th, 2014) were the last communications held with them.

b) *What new information, if any, is available on the adoption of project outputs?*

None to date, but once the IP issues have been sorted through, we intend to make appropriate information announcements, mostly via the

c) *List any newsletters, fact sheets or any other media coverage*.

None have been made to date, but once the IP issues have been sorted through, we intend to make appropriate announcements through SCU's media office.

d) *Identify any further opportunities to disseminate and promote project outputs at seminars, field days etc.*

Once the IP issues are determined, we intend to present the core findings of the project as a seminar series to the industry.

Section 7: Environmental Impact

Outline any new information on adverse/beneficial environmental impacts of conducting the project and/or implementing its findings.

The environmental impact for zeolites remains as previously reported: No new adverse/beneficial environmental aspects, zeolites are well known, and a self-supported colloid matrix on phytolith surfaces allows potential development of filters for water treatment. Filter and water treatment systems were envisaged in the proposal as a potential output stream, are highly likely given the exchange capacity of the zeolite system developed.

The cements, mortars and concretes developed have particular acid resistance, and we have applied for funding from AINSE and the Bragg Institute to do some neutron tomography work, and determine if the acid resistance is because of pore filling or development of additions C3S or similar phases. The successful use of SCBA in concretes is a high volume low cost consumption of the SCBA, and should reduce the requirements for stock piling of the material, or submission to landfill. Finding alternative uses for the material such as in concretes as a sand replacement may not necessarily generate any additional incomes, it will reduce management costs for the storage or dumping of the material.

Section 8: Recommendations and Future Industry Needs

Include activities or other steps to further develop, disseminate, commercialise or exploit the Project Outputs and realise the industry benefits.

There, is still quite a bit of work to be conducted on both aspects of the project, to more fully determine the full potential uses of both the zeolites and the concretes. Consequently the team has sought other funding to do this work, and have been successful in getting some neutron beam work at ANSTO to determine if the acid resistance of the concretes is because of pore filling, or geochemical in regards that more Ca-silicates are produced (which are acid resisting) rather than Ca-aluminates. On going sulphate expansion testing, and sulphate resistance of the concretes are being conducted, to determine if the developed concretes have applications in marine, or acid sulphate systems, to provide increased service life.

Similarly, with the zeolite work, greater understanding of the metal binding capacity, and anion-binding (e.g., phosphate) are required to determine how and where such metals are bound; such investigations require access to synchrotron XAFS, and XANES techniques. Similarly the reversibility of bound trace metals will be made using isotopic exchange techniques. Consequently because of the specialist nature of these techniques further funding to conduct these experiments will be made from The Australian Synchrotron, and AINSE. Although such data are interesting from a scientific point of view, they are not necessarily important, in regards to future industry needs.

Section 9: Publications

At present no publications have been forthcoming from the project for several reasons. Firstly, and most importantly we have deliberately held off any publication to allow the industry partner sufficient time to fully explore an IP position for the 2 aspects of the work. Secondly, the students have been sufficiently busy collecting and processing data that they have only now been able to pull together the data into a publication format.

Currently, the zeolites student Philip Doumit, has completed initial drafts of 2 papers that his supervisory team have edited and provided direction on. These 2 papers detail the full nature of the sorption of Cu and Zn to the zeolite materials, and the kinetic controls on metal removal. Mr Doumit also has a third paper on the optimization of zeolite formation in first draft form, however the supervisory team are yet to see the full draft of the paper yet; he is also planning a 4th paper on the up-scaling of the zeolite formation process. From his literature review of zeolites and zeolite manufacture Mr Doumit will also be able to publish a review paper.

The cements and concretes work currently completed by Ms Elisabeth Arif, will be written up as 2 papers, however both papers are in the early stages of drafting as the student continues to collect data. The first of these papers will detail the addition of the SCBA in to cements and mortars either as a cement replacement, or as a sand replacement, and the second will detail the addition of SCBA to concretes. We intend to examine further the acid resistance post project, into the concrete resistance to sugar cane juice. Ms Arif has also

conducted extensive literature review on the use of waste materials and this review is also likely to be produced as a publication.

The acid resistance of the concretes and mortars developed by Ms Arif, was noted and an additional student Mrs Rumia Tamsin was offered a scholarship to develop additional tests to determine the acid-sulfate resistance of concretes. Acid-sulfate-resistance test development have not previously been made by the engineering fraternity and her work may well establish a new standards test for concretes in acid sulfate soils, and will be a very novel publication. In addition, she has also conducted an extensive review of acid resistance and sulfate resistance in concretes and cements; this will make an additional paper to the current body of work.

In addition to the student work, we have collected over the course of this project substantial data on the nature of bagasse ashes, which will make a suitable publication as well. Hence from the work we are planning on producing some 7 to 8 data publications, and 3 review papers.